ISTANBUL TECHNICAL UNIVERSITY ★ GRADUATE SCHOOL OF SCIENCE ENGINEERING AND TECHNOLOGY

CONCEPT AND CONSTRUCTION DESIGN OF A FREIGHT WAGON BOGIE FRAME WITH VARIABLE AXLE DISTANCE

M.Sc. THESIS

Volkan İGDE

Department of Mechanical Engineering

Solid Mechanics Programme

DECEMBER 2018

ISTANBUL TECHNICAL UNIVERSITY ★ GRADUATE SCHOOL OF SCIENCE ENGINEERING AND TECHNOLOGY

CONCEPT AND CONSTRUCTION DESIGN OF A FREIGHT WAGON BOGIE FRAME WITH VARIABLE AXLE DISTANCE

M.Sc. THESIS

Volkan İGDE
503151522

Department of Mechanical Engineering

Solid Mechanics Programme

Thesis Advisor: Assoc.Prof. Dr. Emin SÜNBÜLOĞLU

DECEMBER 2018

<u>ISTANBUL TEKNİK ÜNİVERSİTESİ ★ FEN BİLİMLERİ ENSTİTÜSÜ</u>

DEĞİŞTİRİLEBİLİR AKS AÇIKLIĞI OLAN BİR YÜK VAGONU BOJİ KARKASI KONSEPT VE TAŞIYICI KONSTRÜKSİYON TASARIMI

YÜKSEK LİSANS TEZİ

Volkan İGDE
503151522

Makine Mühendisliği Anabilim Dalı

Katı Cisimlerin Mekaniği Programı

Tez Danışmanı: Doç. Dr. Emin SÜNBÜLOĞLU

ARALIK 2018

Volkan İGDE, a **M.Sc.** student of **İTU Graduate School of Science Engineering and Technology** student ID **503151522**, successfully defended the thesis entitled **"CONCEPT AND CONSTRUCTION DESIGN OF A FREIGHT WAGON BOGIE FRAME WITH VARIABLE AXLE DISTANCE"**, which he prepared after fulfilling the requirements specified in the associated legislations, before the jury whose signatures are below.

Thesis Advisor : **Assoc.Prof. Dr. Emin SÜNBÜLOĞLU** ....
İstanbul Technical University

Jury Members : **Prof. Dr. Mustafa Kelami ŞEŞEN** ....
Istanbul Technical University

Prof. Dr. Mehmet DEMİRKOL ....
Işık University

Date of Submission : 14 November 2018
Date of Defense : 14 December 2018

To my family,

FOREWORD

I would especially like to thank Assoc.Prof.Dr. Emin SÜNBÜLOĞLU for being supervisor of this study and great scientific support.

I would also like to thank Alper DENİZ, Sarven YARDIM and Deniz Ege EDİLGE for their helpings in this project.

Finally, infinite thanks to my family for their understanding and encouragement and great support through my life.

December 2018

Volkan İGDE
Mechanical Engineer

TABLE OF CONTENTS

Page

ABBREVIATIONS

BS EN **:** British Standart

UIC **:** Union Internationale Des Chemins De Fer

DVS **:** Deutscher Verband Für Schweissen Und Verwandte Verfahren E.V.

SYMBOLS

F_z	: Vertical Load Applied to the Bogie
F_{z1}	: Vertical Force on Sideframe 1
F_{z2}	: Vertical Force on Sideframe 2
F_{zp}	: Vertical Force on Center Pivot
F_{y1}	: Transverse Force on Axle 1
F_{y2}	: Transverse Force on Axle 2
F_{x1}	: Longitudinal Force at Each Wheel
M_y	: Vehicle Mass in Running Order
m^+	: Bogie Mass
α	: Roll Coefficient
b_g	: Half of the Distance between Sidebearers
β	: Bounce Coefficient
d_1	: Diameter of the Journal
d_2	: Diameter of the Collar Bearing Surface
F_0	: Reference Vertical Force for
j	: Number of Wheelsets per Vehicle
m_{max}	: Vehicle Design Mass according to EN 15663
F_{rn}	: Nominal Radial Test Force
F_{an}	: Nominal Axial Test Force
F_r	: Radial Force
P	: Equivalent dynamic bearing load
L	: Basic Rating Life in million revolutions
C	: Basic Dynamic Load Rating
L_{10s}	: Basic Rating Life in million km
D_W	: Mean Diameter of the Wheel
n	: Exponent of the Life Equation
$\sigma_{z\,max}$	: Maximum Stress

$\boldsymbol{M_x}$	: Moment about the x - Axis
$\boldsymbol{I_x}$	: Area Moment of Inertia with Respect to the x - Axis
$\boldsymbol{y_{max}}$	: Farthest Distance from Neutral Axis
$\boldsymbol{F_1}$	: Vertical Force on Axle 1
$\boldsymbol{F_2}$	: Vertical Force on Axle 2
$\boldsymbol{P_1}$	: Radial Force on Bearing 1
$\boldsymbol{P_2}$	: Radial Force on Bearing 2
$\boldsymbol{Q_1}$	: Vertical Reaction Force from the Rail
$\boldsymbol{Y_1}$	: Transverse Reaction Force from the Rail
$\boldsymbol{m_2}$	: Mass of the Wheelset
$\boldsymbol{MR}$	: Resultant Moment
$\boldsymbol{K}$	: Stress Concentration Factor

LIST OF TABLES

LIST OF FIGURES

Page

CONCEPT AND CONSTRUCTION DESIGN OF A FREIGHT WAGON BOGIE FRAME WITH VARIABLE AXLE DISTANCE

SUMMARY

In the world, the importance of the human transportation and the cargo is arising. The railway systems are safe, economic and sustanaible right along with being the most energy efficient way of transportation.

The vehicles in the railway systems are the locomotive, the cargo or human transportation wagon and the bogie which is the wheeled part.

During the usage of railway systems which is efficient in long haul, some problems are encountered. While the track gauge can be same inside most of the countries but it may change between country to country. Railway vehicles have ability to move along the country but if the track gauge changes in the other country during the transportation, the bogies must be changed to adopt to the the different wheel distances. At the boundaries of the countries, this process requires to seperate each wagon and locomotive one by one from their bogies with cranes and to place them to the new bogies of the other railway.

Within the study in this thesis, it is aimed to eliminate the time and energy loss with the design of a bogie which has variable gauge between its wheels, which is appropriate for the working and manufacturing conditions of our country and which is also conforming to the railway system standards.

With the help of the proposed design, the change stations will be established at the junction points of the railways with variable gauge dimensions. Thus the railway tracks will move in a continuous manner, without any hesitance, the transition to the other railway will be completed. While the wheels and the bogies positioning is kept constant en route by the lock system of the the inner axle boxes in the bogie, the locks are opened in the change stations, and the positions of a guide rail and the wheels are changed there.

During the switching process, the load is carried by the side structures of the bogie, the frames. When the replament of the wheels are completed the lock will be closed again to disable the movement of the wheel.

The concept design of bogie is created with CATIA V5, in accordance with the railway systems standards and operating conditions. The design is based on the three-piece bogie concept.The finite element model of the bogie was created with Altair Hypermesh pre-process program, and solved with ABAQUS. Fatigue analysis solved with LIMIT-CAE.

DEĞİŞTİRİLEBİLİR AKS AÇIKLIĞI OLAN BİR YÜK VAGONU BOJİ KARKASI KONSEPT VE TAŞIYICI KONSTRÜKSİYON TASARIMI

ÖZET

Gelişmekte olan dünyamızda, insan ve yük taşımacılığının önemi sürekli artmaktadır. Raylı sistemler, güvenli, ekonomik ve sürdürülebilir olmakla birlikte, özellikle enerji verimliliği açısından taşımacılık alanında en uygun ulaşım yolu olarak kabul görmektedir.

Raylı sistemlerde kullanılan araçlar; lokomotif, yük ve yolcu taşıyan vagon, lokomotif ve vagonların raylar üzerindeki hareketini sağlayan tekerlekli aksam olan boji, olarak sınıflandırılabilir.

Uzun mesafe taşımacılığında etkin olarak kullanılan raylı sistemler ile ülkeler arasında yol alırken birtakım engeller karşımıza çıkmaktadır. Ülkelerin sınırları içerisindeki demiryollarının hat açıklığı, kendi içinde çok büyük oranda aynı olmasına rağmen, bu açıklık mesafesi ülkeden ülkeye farklılık gösterebilmektedir. Bu nedenle, demiryolu araçları, ülke sınırları içinde sürekli hareket kabiliyetine sahip iken, hat açıklığı farklı olan ülkeye geçiş durumunda, var olan bojilerini teker açıklığı farklı olan bojiler ile değiştirmek zorunda kalmaktadır. Demiryolu hat açıklığı 1435mm olan ülkemiz ile 1520mm hat açıklığına sahip doğudaki komşu ülkeler arasında da böyle bir değişim sistemi uygulanmaktadır.

Bu değişim vagonların ve lokomotifin tek tek, vinçler ile kendi bojilerinden ayırıp, diğer demiryolundaki bojiler üzerine konulması işlemi ile yapılmaktadır. Kullanılan bu sistemin, iş gücü ve zaman kaybı açısından düşünülürse çok büyük dezavantajı söz konusudur.

Bu tez kapsamında yapılan çalışmada; raylı sistem standartlarını sağlayan, ülkemiz çalışma ve üretim şartlarına uygun, tekerlekleri arasındaki mesafesi değiştirilebilir bir boji tasarımı ile bahsedilen zaman ve enerji kaybının ortadan kaldırılması amaçlanmıştır. Çalışmalar sayesinde günler mertebesinde olan değişim işlemi saatler mertebesine inecektir.

Yapılan tasarım sayesinde, farklı mesafe ölçülerine sahip demiryollarının birleşme noktalarında kurulacak olan değişim istasyonlarında; trenlerin yavaşlayarak, herhangi bir duraksama olmadan, sürekli bir şekilde diğer demiryoluna geçişi tamamlanacaktır. Bojideki iç aks kutularında uygulanan kilit sistemi ile, seyir halinde tekerleklerin bojiye göre konumu sabit tutulmakta iken, bahsedilen değişim istasyonlarında kilitler açılmakta, ve bir kılavuz ray ile tekerleklerin konumları değiştirilmektedir. Bu süre zarfında, vagonu taşıma işlemini bojinin yan yapıları üstlenecektir. Tekerleklerin yer değişiminin tamamlanmasının ardından; kilit tekrar kapanarak, tekerleklerin hareketini önlemeye devam edecektir. Bu sayede sürekli vagonlar sürekli bir şekilde ilerleyebilecektir.

Boji tasarlanırken öncelikle raylı sistem standartlarında yer alan tasarım kriterleri incelenmiştir. Yapılan konsept tasarıma; maksimum aks yükü, maksimum hız, izin verilen geometrik uzunluklar, standart parçaların birbirine göre konumları ve gibi bu standartlardan edinilen bilgiler yardımıyla başlanmıştır.

Tasarım, CATIA V5 yazılımı kullanılarak oluşturulmuştur. Yapılan konsept tasarım, üç parçalı boji olarak adlandırılan boji tipi esas alınarak yapılmıştır. Fakat değişebilir aks açıklığına sahip olabilmesi için diğer boji tiplerinden daha farklı bir tasarım yapılmıştır.

İlk olarak ana taşıyıcı oluşturulmuş, ardından yan taşıyıcılar tasarlanmıştır. Standart bojilerde sağ ve sol olmak üzere iki yan taşıyıcı bulunur iken, yapılan konsept tasarımda dört adet yan taşıyıcı kullanılmıştır. Aynı zamanda standart bojiler iki aksa sahip iken yeni tasarımda her tekerlekte bir adet olmak üzere toplamda dört adet aks kullanılmıştır.

Kullanılan dört adet aks için toplamda sekiz adet olmak üzere, dört adet iç ve dört adet dış aks kutusu tasarlanmıştır.

İç aks kutusu, yatay yönde hareketi kısıtlayan kilit mekanizmasını içermektedir. Yapılacak olan değişim istasyonlarında, kılavuz rayın yardımı ile kilit açılarak, tekerleklerin iç veya dış tarafa hareketi tamamlamasının ardından yine kılavuz ray yardımı ile kilitlenerek yatay hareketi kısıtlamaya devam edecektir. İç aks kutusu ile dış aks kutusu aynı tip standart rulman kullanmakta olup üst taraflarında kauçuk parçalar bulundurmaktadır.

Konsept tasarıma devam edilirken; raylı sistem standartları incelenerek, bojinin maruz kaldığı yükleme durumları ve sürüş koşulları incelenmiştir. Bu koşullara uygun standart parçalar (boji yayları, mil, rulman) gerekli hesaplamalar yapılarak seçilmiştir. Bojinin tasarımı, belirlenen parçaların ölçülerine uygun olacak şekilde oluşturulmuştur.

Standartlarda yer alan yükleme durumlarının incelenmesi ve yapılan hesaplamaların ardından, yükleme koşulları tablosu oluşturulmuştur. Bu tabloda yer alan yük senaryoları, standartlardaki tüm yüklem durumlarını ve bu yüklemelerin gerekli kombinasyonlarını içermektedir. Sonlu elemanlar metodu ile yapılan analizde bu yükleme durumları kullanılmıştır.

Yapılan tasarımın tamamlanmasının ardından bojinin, sonlu elemanlar metodu kullanılarak analiz edilmesi amacı ile sonlu elemanlar modeli oluşturulmuştur. Bojinin karkası ve iç aks kutusu yükleme koşullarına göre ayrı ayrı analiz edilmiştir.

Sonlu elemanlar analizi modeli oluşturulurken Altair Hypermesh yazılımı kullanılmıştır. Boji karkası uygun eleman tipleri ile modellenmiş, standart parçalar rijit elemanlar ile modellenmiştir. Her yükleme koşulu için, duruma uygun sınır koşulları verilmiştir.

Oluşturulan model ABAQUS yazılımı ile çözülmüştür. Boji karkası toplamda standartlara göre hazılananmış yirmi yedi farklı yük senaryosu ile analiz edilmiş, sonuçlar incelenmiştir. Yüksek gerilmeye maruz kalan bölgelerde çeşitli iyileştirilmeler yapılmış, tüm yük senaryoları ile tekrar analiz edilmiştir. Bu iyileştirme iterasyonları, boji karkasındaki gerilme değerleri güvenli mertebeye ulaşıncaya kadar tekrar edilerek tasarım optimize edilmiştir.

Boji karkasının analizinden alınan, iç aks kutusuna gelen kuvvet değerleri tüm senaryolar için incelenmiş, en tehlikeli durumlar için oluşan kuvvetler belirlenmiş, ardından aks kutusu modeli hazırlanmıştır.

İç aks kutusu ve içerdiği kilit mekanizmasının modeli, boji karkasından ayrı olarak oluşturulmuştur. Modelleme işlemi için Altair Hypermesh yazılımı kullanılarak oluşturulan modelde bağlantı elemanları ve aks rijit olarak modellenmiştir. Boji karkasının analizinden alınan kuvvet değerleri girilmiş ve sisteme uygun olarak sınır koşulları tanımlanmıştır. Yüksek miktarda temas elemanı içeren iç aks kutusu modeli ABAQUS kullanılarak çözülmüştür.

Uygulanan kuvvetler ile yapılan analizde aks kutusunda oluşan gerilme değerlerinin sınır değerlere yakın olmadığı, güvenli bölgede olduğu gözlemlenmiştir ve üzerinde bir iyileştirme işlemi yapılmamıştır.

Yapılan tüm analizlerin sonuçlanmasının ardından LIMIT CAE yazılımı kullanılarak boji için kaynak yorulma analizi yapılmıştır.

Yorulma analizi için, oluşturulan sonlu elemanlar modeli ve analiz sonuçlarından elde edilen gerilme değerleri yazılıma bilgi olarak girilmiştir. Bojideki tüm kaynaklar için, kaynak tipi, kaynak kalitesi bilgileri girilmiştir. Yapılan analiz, standartlarda yer alan yorulma koşullarına uygun olarak yapılmıştır. Bu yükleme durumlarındaki değerler tablo haline getirilerek programa giriş yapılmıştır. Yorulma için kullanılacak çevrim sayıları ve gerilme değerlerinin uygun hale getirilmesi için gerilme değerleri ölçeklenerek yazılıma girilmiştir.

Yapılan yorulma analizinin ardından, sonuçlar incelenmiş, bazı kaynak bölgelerinde yüksek gerilme değerlerinden kaynaklanan tehlikeli bölgeler saptanmıştır. Bu bölgelerde kaynak kalitesini iyileştirme ve kaynak yapılan sacların kalınlık değerlerini arttırma işlemleri ile tekrar analizler yapılmış olup, sonuç olarak tüm kaynakların uygun değerlere sahip olması sağlanmıştır.

Analizler ve iyileştirme işlemleri sonunda; tasarlanan bojinin tüm yükleme ve yorulma koşullarında güvenli sonuçlar verdiği görülmüştür.

Yeni boji tasarımı ile, farklı demiryolu hat açıklığına sahip işletmeler arasında, uzun iş gücü ve zaman kaybı elimine edilerek, demiryolu araçlarının sürekli hareket halinde geçişinin sağlanması amaçlanmıştır. Elde edilen sonuçların ışığında, tasarımın bu amaca yönelik, güvenli bir tasarım olduğu ve tüm raylı sistem standartlarını karşıladığı görülmektedir.

Yapılan bu tasarım bir konsept tasarımdır. Standart parçalar kullanılmış olup, tasarım yapılırken ülkemizin üretim şartları göz önünde bulundurulmuştur. Gelecekte yapılacak projelerde yapılan tasarımın bir prototip imalatı yapılarak, gerçek yükleme koşullarında test edilmesi ve bu testler ile uygunluğunun değerlendirilmesi düşünülmektedir.

Prototip imalatı ve prototip üzerinde yapılan testlerin başarılı olması durumunda, tasarımın üretime geçirilerek, ülkemizdeki demiryolu ticaretine büyük katkı yapması planlanmaktadır.

1. INTRODUCTION

Track gauge is the spacing of the rails on a railway track in rail transport. It is measured between the inner faces of rails (Figure 1.1). Usually, this gauge is the same within the country boundaries. Railway system vehicles are designed or imported according to these dimensions.

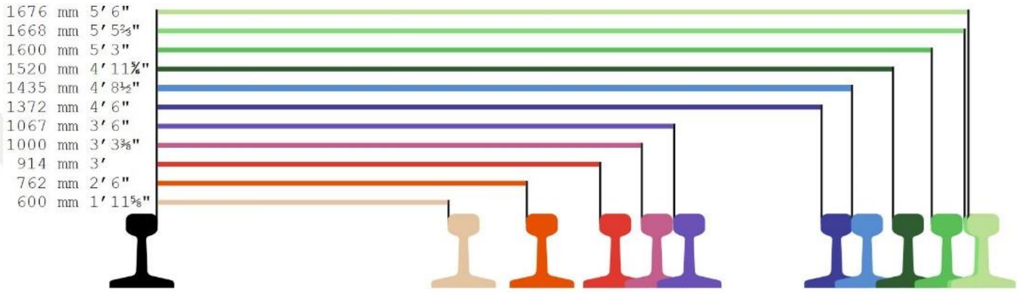

Figure 1.1 :Different railway track Gauges [1]

There are 11 different track gauges in the world (Figure 1.2). Approximately 60% of the countries have 1435 mm gauge, include most of Europe and Turkey. East neighboring countries of Turkey and former Soviet Republics have 1520 mm gauge. This situation makes it difficult for the railway transportation between Turkey and Post-Soviet states, and this negatively affects trade.

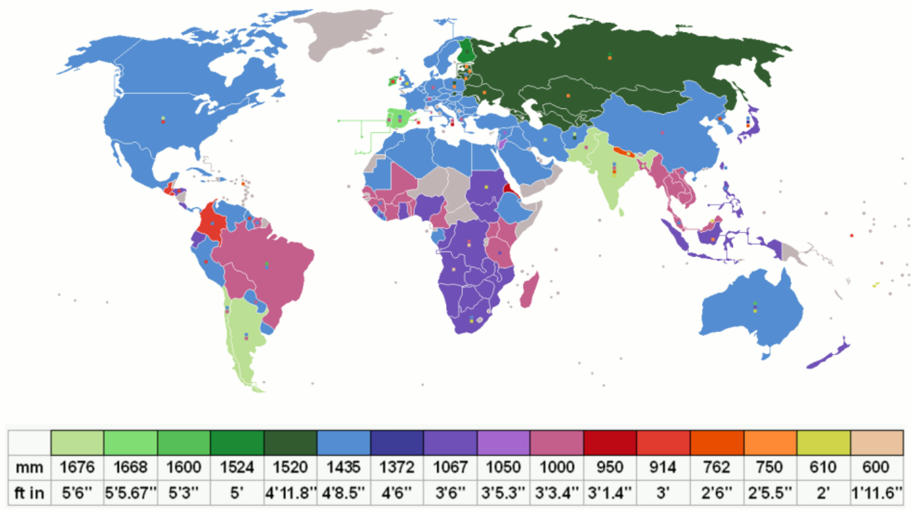

Figure 1.2 : Track gauges map of the world.[1]

In usual conditions in junction point of railway tracks, bogie switching method is time consuming process. Initially the bogies are decoupled from the wagons, wagons are lifted upwards with cranes, new bogies are placed under the wagons (Figure 1.3). This process is as time consuming as costly related to the manpower needed.

The railway track between the eastern neighboring countries and Turkey has the same system. [1]

Figure 1.3 : A bogie change station in China/Mongolia border.

The purpose of this thesis, is eliminating the time and energy loss with the design of a bogie which has adaptable distance between its wheels, which is appropriate for the working and manufacturing conditions of our country and which is also conforming to the railway system standards.

With the help of the new design, this change process time will be reduced from days range to hours.

The change stations that provide the change process will be established at the junction points of the railways with variable gauge dimensions. Thus the railway tracks will move in a continuous manner, without any layover, the transition to the other railway will be completed. While the wheels and the bogies positioning is kept constant en route by the lock system of the the inner axle boxes in the bogie, the locks are opened in change stations, and the positions of a guide rail and the wheels are changed there.

During the switching process, the carriage is loaded on the side structures of the bogie, the frames. When the replacement of the wheels are completed the lock will be closed again to disable the wheel movement.

2. DESIGN

Bogie systems are the parts of the railway system which carries the other parts of the vehicle and also which enables the movement in the railway systems.[3]

Bogie systems allow the long railway trucks to pass along the curved rails, disable the vibrations by damping with springs and provide the riding comfort. Also bogies ensures a comfortable ride and helps the wagons to pass along the curves without derailing.

First structured bogie (Figure 2.1) was developed in 1893 by Samson Fox for Victorian Railways in Canada[4]. From that day, bogie systems improved to fullfill the needs of the new technology developments.

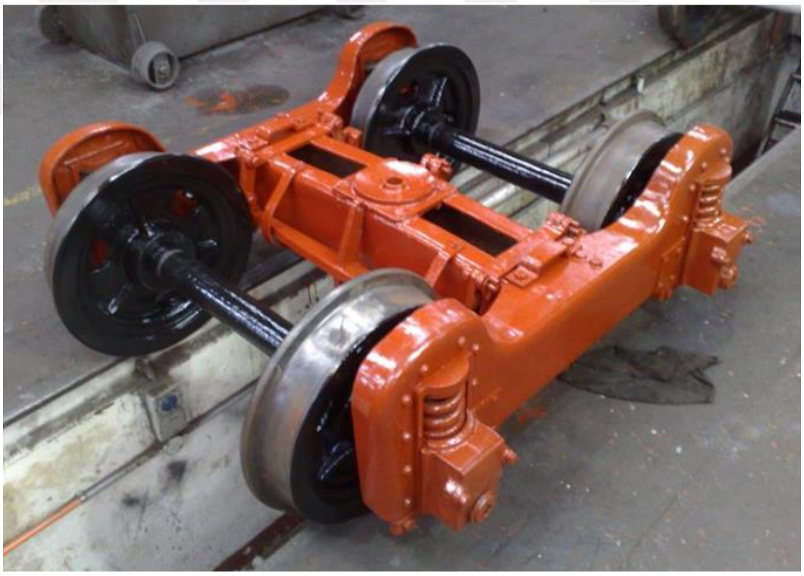

Figure 2.1 : The Fox type bogie developed in 1893 by Samson Fox

According to the European Standard EN 13749 bogies are divided to 7 different classes[5]. In general even the bogies are defined according to the type of the truck, structural conditions of the bogies differ so the definitions should be made according to the working conditions.

Bogie classifications according to the EN 13749;

- **Category B-I** bogies for main line and inter-city passenger carrying rolling stock including high speed and

very high speed vehicles, powered and un-powered;

- **Category B-II** bogies for inner and outer suburban passenger carrying vehicles, powered and un-powered;
- **Category B-III** bogies for metro and rapid transit rolling stock, powered and un-powered;
- **Category B-IV** bogies for light rail vehicles and trams;
- **Category B-V** bogies for freight rolling stock with single-stage suspensions;
- **Category B-VI** bogies for freight rolling stock with two-stage suspensions;
- **Category B-VII** bogies for locomotives.

In this thesis, in regard to the needs of the railway systems a **B-V** category bogie (Figure 2.2) is designed. The forces applied in the analysis are calculated according to the standards of this category.

Figure 2.2 : Widely used today B-V category, Y25 type bogie

2.1 Technical Requirements

The bogie should be designed in accordance with the rail system standards, and must compatible with other standard parts dimensions. Major standart dimension of **B-V** category freigth bogies are;

- Maximum axle-load is 22.5 tons
- Maximum speed is 120km/h

- Minimum non-stop distance covered at 120 km/h; 300km
- Wheels centre point distance on rail axis (Figure 2.3)

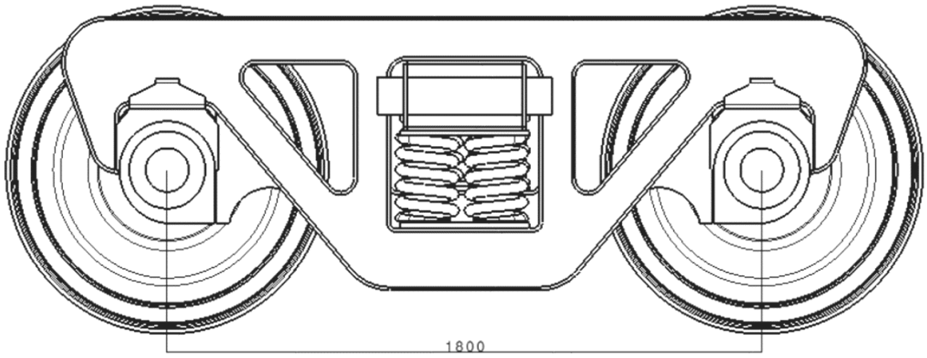

Figure 2.3 : Wheel distance dimension on rail axis

- Wheel inner surface distance on transverse axis (Figure 2.4)
- Distance covered per year under full load; 40000 km.
- Suspension (single stage)

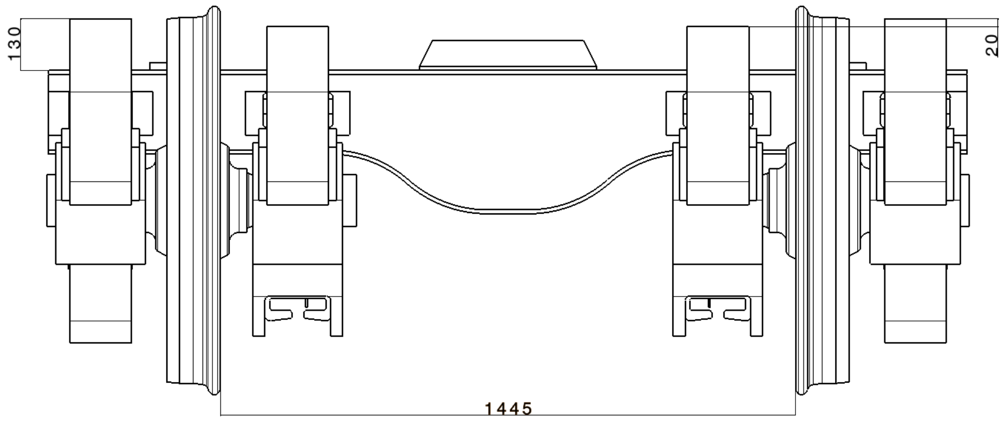

Figure 2.4 : Wheel inner surface distance on transverse axis (on 1520mm track gauge)

- Bolster distance on transverse axis
- Side frames height on vertical direction (Figure 2.5)
- Minimum temperature; 20°C
- Wheel dimensions (Figure 2.6)

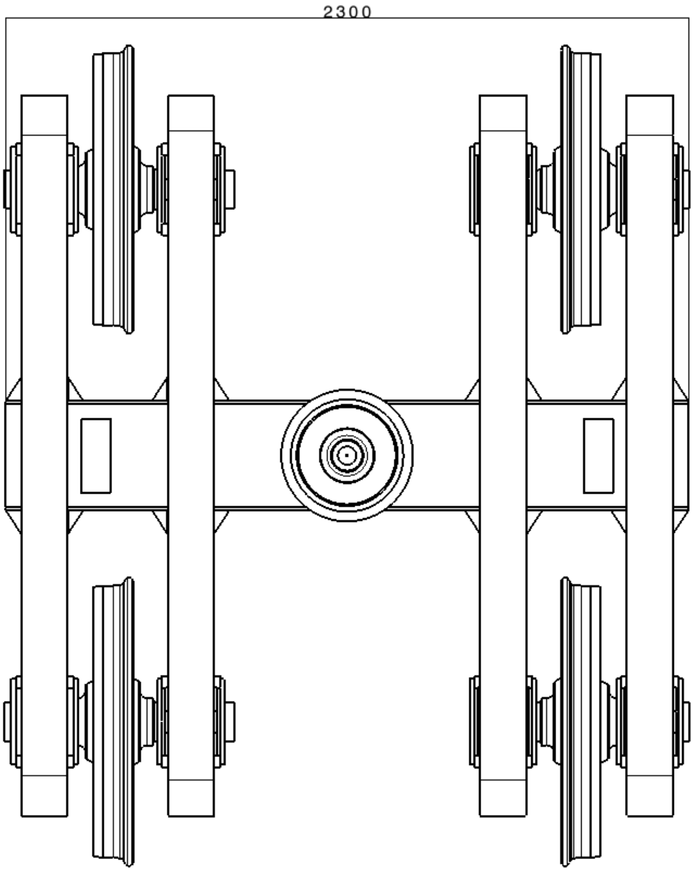

Figure 2.5 : Bolster distance on transverse axis

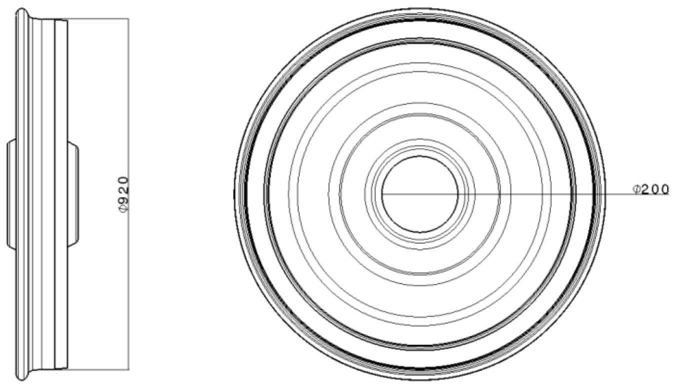

Figure 2.6 : Railway standart wheel

2.2 Engineering Design Criteria

2.2.1 Summary of Applicable Standards and Patents

Many design parameters and criteria must be taken into account when designing a complex system such as a bogie. It is aimed to satisfy all of these required conditions which can be found in the European railway standards.

In this thesis, the bogie has been designed in accordance with the requirements of technical data specified mainly in **EN 15827**, **EN 13749**, **EN 13103**, **UIC 501**, **EN 12080**, **EN 12082**, **EN 13775-4**.

The objective of **EN 15827** is to provide a general information about the design criteria described in the above-mentioned standards.

EN 13749 standard is used for calculating the exceptional and normal loads and assessing the strength requirements of bogie. This European Standard, mentions structural specifications of the bogie frames consist of both bolsters and axlebox housing and design procedures, assessment methods, verification and manufacturing quality requirements are also covered in this standard.
EN 13103 has been used to define geometrical parameters of the axle and to calculate maximum stresses at the different regions of the axle such as transition areas.

This standard:

- Identifies the braking forces and moments and their relation with the masses.
- Identifies the diameters and fillet radiuses for the various parts of the axle and suggests the favoured shapes and transitions to provide required strength characteristics.
- Determines stresses for the various parts of the axle by using fatigue stress concentration factor (K) to identify geometric characteristics of the axle.

The information required about axle box is found from the standards **EN 12080** and **EN 12082**. For determining the rolling bearing life calculations and bearing loads made based on those aforementioned European standards. The main scope of this standard is to describe the requirements for the performance test of the axlebox rolling bearings, housing, seals and grease.

The design of the external and internal frame is based on the requirements of **EN 13775-4**. This standard includes the geometrical parameters that has been used in the design of bogie frames.

The design life of the bearings must also be considered according to the **UIC 510-1** which, comprises of the contents such as wheels, axles, wheelsets, axle boxes fitted their bearing, wheelsets fitted with their axle boxes, 2-axle bogies, 3-axle bogies.

Numerous patents have been also analyzed in detail in the design of the project to make a valid design. The axle structures used in the existing bogie patents have been changed due to concerns about the cost of the bogie. Instead of 2 axles per bogie, it was tried to concentrate on a shorter axle design for each wheel. patents were used in the consideration of the mechanism of changing gauge. The patent of **EP 2 351 679 A1**, which is used in the studies on redesigning and developing of the housing structure and lock mechanism to be used, clarified the subject in many respects.

2.2.2 General Loads Due to Bogie Running

As stated in Annex C of EN 13749, in service conditions, bogies are subject to, and should withstand, loads (Table 2.1) caused by the following:

- the weight of the supported vehicle, including any payload;
- changes in the payload;
- track irregularities;
- running on curves;
- acceleration and braking;
- abrupt application of payload (freight wagons);
- minor derailments (e.g., low-speed drop on to ballast, if required by the specification);
- buffing impacts;
- extreme environmental conditions;
- fault conditions (e.g., motor short circuit torque);
- maintenance/recovery situations (e.g., lifting and jacking).

Table 2.1 : Types of Forces

Static Forces (N)	Position	Symbol
Vertical	Load applied to bogie	F_z
	Force on sideframe 1 or sidebearer 1	F_{z1}
	Force on sideframe 2 or sidebearer 2	F_{z2}
	Force on center pivot	F_{zp}
Transverse	Load applied to bogie	F_y
	Force on axle 1	F_{y1}
	Force on axle 2	F_{y2}
Longitudinal	Force at each wheel	F_{x1}

2.2.3 Loads for Freight Bogies with a Central Pivot and Two Sidebearers

This load cases limited to the two axle bogies which are described as in this senior design project.

2.2.3.1 Exceptional Loads

Vertical Forces

F_z is the total vertical load supported by the bogie;

F_{zp} is the vertical force applied to the pivot;

F_{z1}, F_{z2} are the vertical forces applied to each sidebearer

$$F_z = \left(\frac{M_v - 2m^+}{2}\right)g \tag{2.1}$$

M_v is the vehicle mass in running order;

m^+ is the bogie mass;

Case 1 – The case where the force is applied only to the pivot:

$$F_{zp\,max} = 2F_z \tag{2.2}$$

Case 2 – The case where the force is applied to both the pivot and one sidebearer:

$$F_{z1\,max}(or\ F_{z2\,max}) = 1{,}5 \times F_z \alpha \tag{2.1}$$

$$F_{zp\,max} = 1{,}5 \times F_z\ (1 - \alpha) \tag{2.4}$$

For 1,7 m distance between the sidebearers, α is taken as 0,3. If the distance between the sidebearers ($2b_g$) is different from 1,7m then

$$\alpha = 0{,}3 \times \left(\frac{1{,}7}{2b_g}\right) \tag{2.5}$$

Transverse Forces (applied to each axle)

$$F_{y1\,max} = F_{y2\,max} = \frac{F_{y\,max}}{2} = 10^4 + \frac{F_z + m^+g}{6} \tag{2.6}$$

Longitudinal Lozenging Forces

$$F_{x1\,max} = 0{,}1 \times (F_z + m^+g) \tag{2.7}$$

Longitudinal Shunt Loads

A static longitudinal shunt load should be applied, in which the force is equal to bogie mass times maximum vehicle acceleration or 5g.

Twist Loading

The bogie frame should resist resulting loads due to track twist of 1 % under exceptional loading conditions.

2.2.3.2 Normal in-Service Loads

Case 1 – The case where the force is applied only to the pivot:

$$F_{zp} = F_z \tag{2.8}$$

Case 2 – The case where the force is applied to both the pivot and one sidebearer:

$$F_{z1}\ (or\ F_{z2}) = F_z\,\alpha \tag{2.9}$$

$$F_{zp} = F_z\,(1-\alpha) \tag{2.10}$$

According to the UIC, for 1,7 m distance between the sidebearers, α is taken as 0,2. If the distance between the sidebearers ($2b_g$) is different from 1,7m then

$$\alpha = 0{,}2 \times \left(\frac{1{,}7}{2b_g}\right) \tag{2.11}$$

Transverse Forces (applied to each axle)

$$F_{y1} = F_{y2} = \frac{F_y}{2} = 0{,}1 \times (F_z + m^+g) \tag{2.12}$$

Longitudinal Lozenging Forces

$$F_{x1} = 0{,}05 \times (F_z + m^+g) \tag{2.13}$$

Track Loading

Resulting loads due to track twist of 0,5 %

2.2.4 Static Test Programs

Load cases for static test programs can be adapted to the computer environment via using FEM. The purposes of static test programs are as follows:

- Determination of stress/strain values at critical points;
- Verification of general specifications that are stated in the standards;
- Design life estimation of rolling bearings;
- Consideration of static load conditions to choose an effective cross-sectional area of the components.
- Selection of the proper welded joints.
- Determination of the potential risk of fatigue cracks by the superposition of the in-service dynamic loads.

2.2.4.1 Static Test Program for Bogies with Central Pivot and Two Sidebearers

The stresses which have been calculated using exceptional load (loads due to bogie running) equations, has to be compared to the yield strength of the material.

Loads Resulting from Bogie Running

The Table 2.2 represents different loading conditions which can be applied to the bogie. The loads ($F_{zp}, F_{z1}, F_{z2}, F_{y1}, F_{x1}$) are shown in Figure 2.7 and can be calculated from normal loads stated in section **2.3.3.2**. Roll coefficient α is generally taken as 0,2 according to EN 13749 and the coefficient β, indicates the bouncing effect, is generally taken as 0,3 according to EN 13749.

Table 2.2 : Load cases for tests under normal loads resulting from bogie running

	Force on Sidebearer 1 F_{z1}	Force on Pivot F_{zp}	Force on Sidebearer 2 F_{z2}	Transverse Force F_y
1	0	F_z	0	0
2	0	$(1+\beta)\ F_z$	0	0
3	0	$(1-\beta)\ F_z$	0	0
4	0	$(1-\alpha)(1+\beta)\ F_z$	$\alpha\,(1+\beta)\ F_z$	F_y
5	0	$(1-\alpha)(1+\beta)\ F_z$	0	$-F_y$
6	0	$(1-\alpha)(1-\beta)\ F_z$	$\alpha\,(1-\beta)\ F_z$	F_y
7	0	$(1-\alpha)(1-\beta)\ F_z$	0	$-F_y$

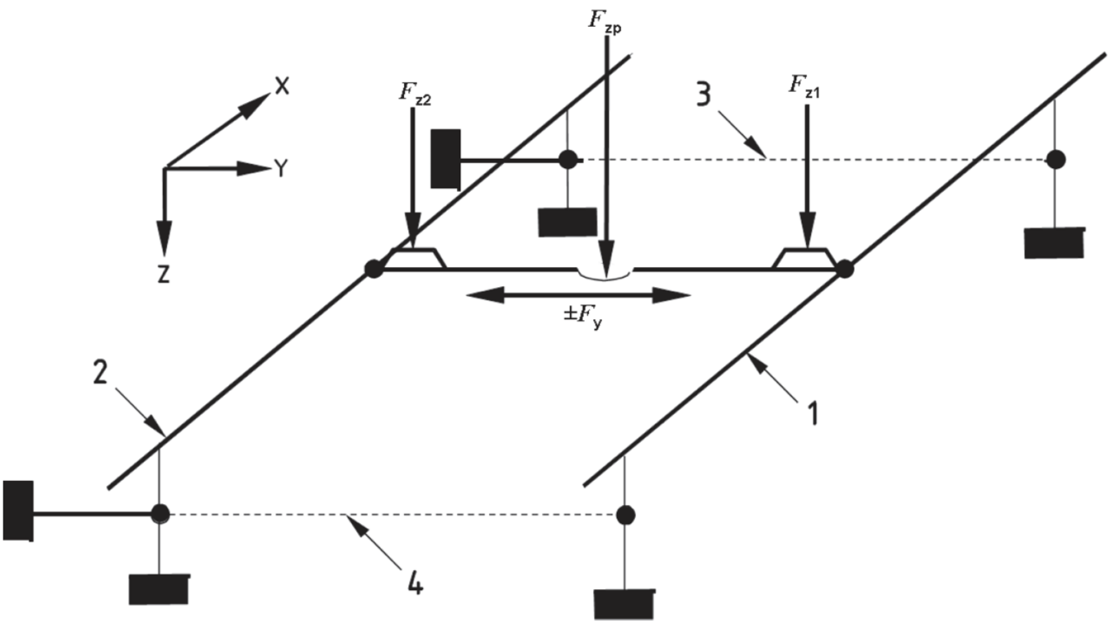

Key
1 side 1
2 side 2
3 axle 1
4 axle 2

Figure 2.7 : Centre pivot bogie loading arrangement

2.2.4.2 Determination of the Diameter of the Various Parts from the Diameter of the Axle Body or from the Journals

The diameter of the collar bearing surface (d2) should be 30 mm larger than that of the journal (d1) for standardizing the dimensions when it is achievable. Indeed, the transition between the journal and the collar bearing surface is arranged as stated as Figure 2.8, Figure 2.9 and Figure 2.10.

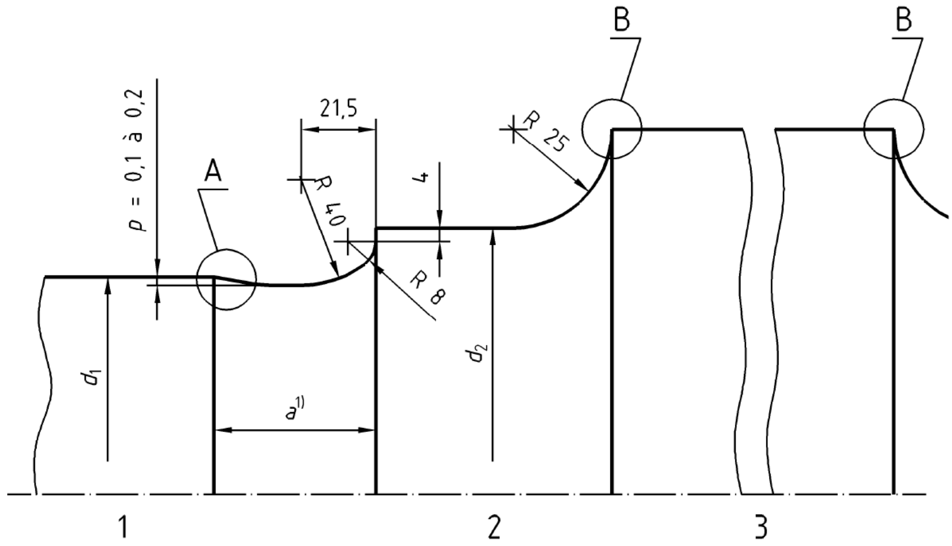

Key

1 journal
2 collar bearing surface
3 wheel seat

Figure 2.8 : Transition areas between journal and collar bearing surface – collar bearing surface and wheelset [12]

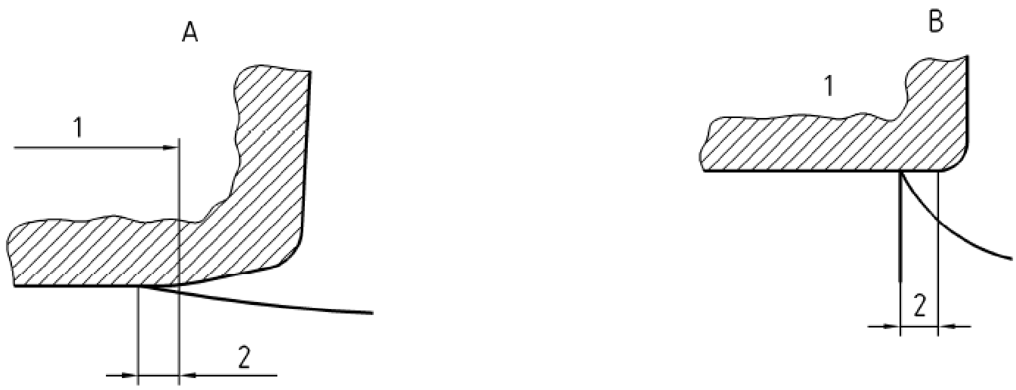

Key

1 cylindrical part of the bearing ring bore
2 ≥ 2 to ≤ 3: overlap

Key

1 wheel hub
2 ≥ 0 to ≤ 5 overlap

Figure 2.9 : Detail A and B [12]

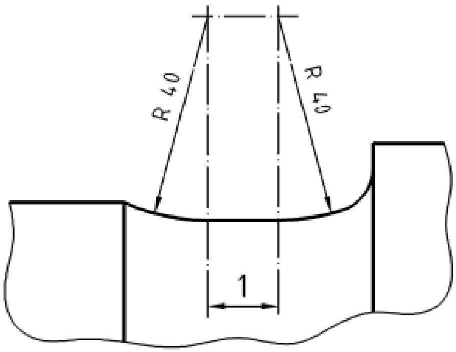

Key
1 bottom of cylindrical groove

Figure 2.10 : Transition between journal and collar bearing surface

2.2.5 Design Life of the Bearings

The design life of the bearings will be considered according to Table 2.3.

Table 2.3 : Specifications for axle boxes fitted with their bearings

Characteristics	Units	Values
Maximum axle-load	t	22.5
Maximum speed	km/h	120
Minimum non-stop distance covered at 120 km/h	km	300
Distance covered per year under full load	km	40000
Minimum temperature	°C	-20
Service life for 75 % of the bearings and for 90 % of the bearings	year	40 20

From **Table 2.3**, the design life (in km) of the bearings can be calculated as follows:

Design Life (in km) = Distance covered per year (in km) × Service life (in year)

Design Life (in km) = 40000 km × 20 years (75 %) = 800000 km = 0,8 million km

Design Life (in km) = 40000 km × 40 years (90 %) = 1600000 km = 1,6 million km

So, it can be stated that the design life of the bearing must be more than 1,6 million km.

2.2.6 Definition of the Forces

Test forces can be calculated as follows:

Reference Vertical Force: F_0

$$F_0 = \frac{1}{j} \times m_{max} \times g \tag{2.14}$$

j is the number of wheelsets per vehicle which is equal to 4

m_{max} is vehicle design mass according to EN 15663 which is equal to 90 ton

(90×10^3 kg)

Nominal Radial Test Force: F_{rn}, in N

$$F_{rn} = \frac{1,2}{2} \times (F_0 - m_2 \times g) = 0,6 \times (F_0 - m_2 \times g) \tag{2.15}$$

m_2 is the wheelset mass and masses on the wheelset between rolling circles, like brake disc, etc. (nearly 1,5 ton)

Nominal Axial Test Force: F_{an}, in N

$$F_{x1} = 0,05 \times (F_z + m^+ g) \tag{2.16}$$

Where; 1,2 applies to 20 % safety margin in addition to the vertical reference force;

2.3 Concept Design

2.3.1 Bojie Concept Design

Bogies of the same category might have different structural designs. This thesis is based on the 3 piece bogie concept. The structure and the number of the components are changes in order to meet the goal of variable gauge design.

Standard 3 piece bogie consists of a pivot, a bolster, 4 side frames, 2 side bearers, 4 axle boxes, 2 to 4 springs between the bolsters and side frames and a wheelset consisting of 2 wheels and a shaft (Figure 2.11).

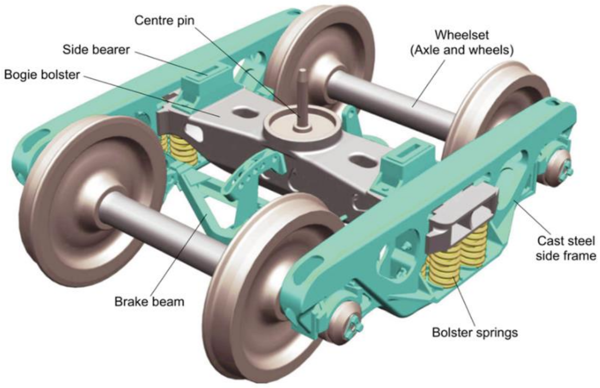

Figure 2.11 : 3 piece bogie main components [7]

Components are designed according to the standards. These components are 2 inner and 2 outer side frames, 4 shafts, 4 axle boxes which enables the connection of the shafts and the side frames and a locking mechanism under the inner axle box for the changeability of the axle distance (Figure 2.12). The working principle of the locking mechanism is described in the section 2.1.3.2

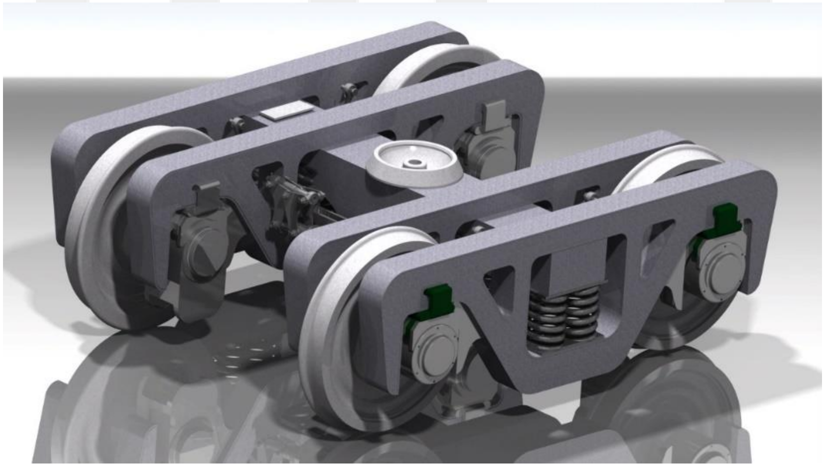

Figure 2.12 : The concept design of the new bogie

The parts designed for the Bogie are listed below.

2.3.2 Bolster

Bolster (Figure 2.13) is the steel part connected from the sides to the side frames and from the center to the pivot. It transfers the load from the wagon to the side frames with the help of the springs.

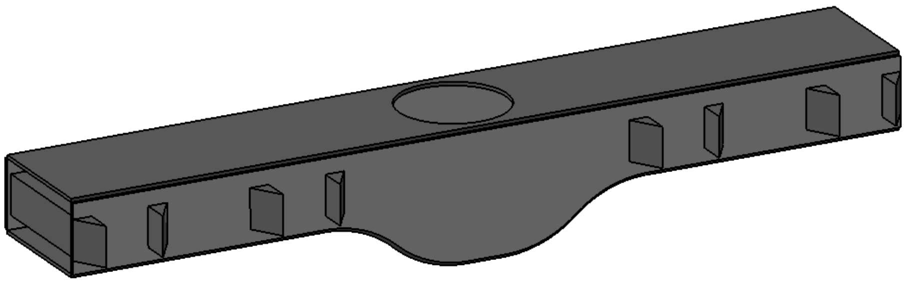

Figure 2.13 : Bolster

Designed bolsters main body consist of 4 sheet metals welded together. There are 16 nail part to transfer the transverse loads to the side frames and inside reinforcements are added to increase the strength (Figure 2.14).

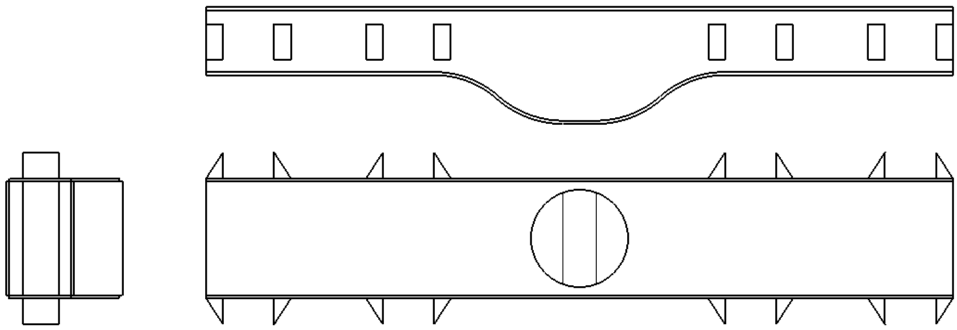

Figure 2.14 : Bolster

2.3.3 Side Frames

There are 2 outer and 2 inner, in total 4 side frames in the design (Figure 2.15). The pressed sheet metals are welded together to form the frames. Frames transfer the load from bolster and springs to the wheelsets.

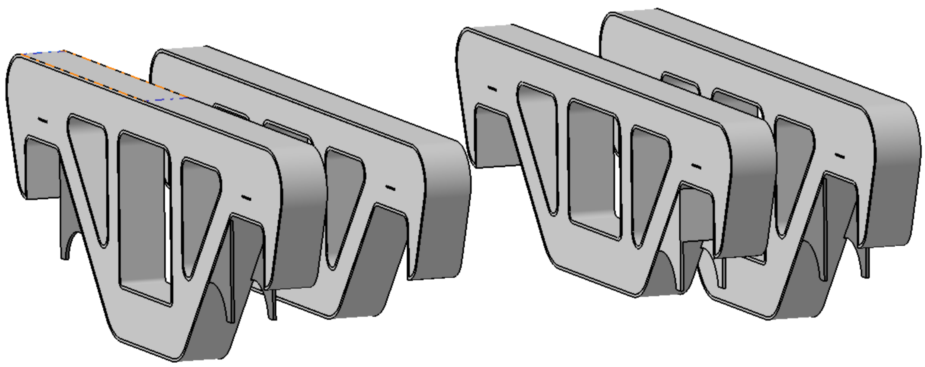

Figure 2.15 : Inner and outer side frames

The main difference of the Inner side frame is shorter than outer frame in vertical direction because of the guide rail used in the changing operation. This allows the guide rail to pass under the inner frames (Figure 2.16). There is a sheet metal structure between the side frames and the axle boxes for load transfer.

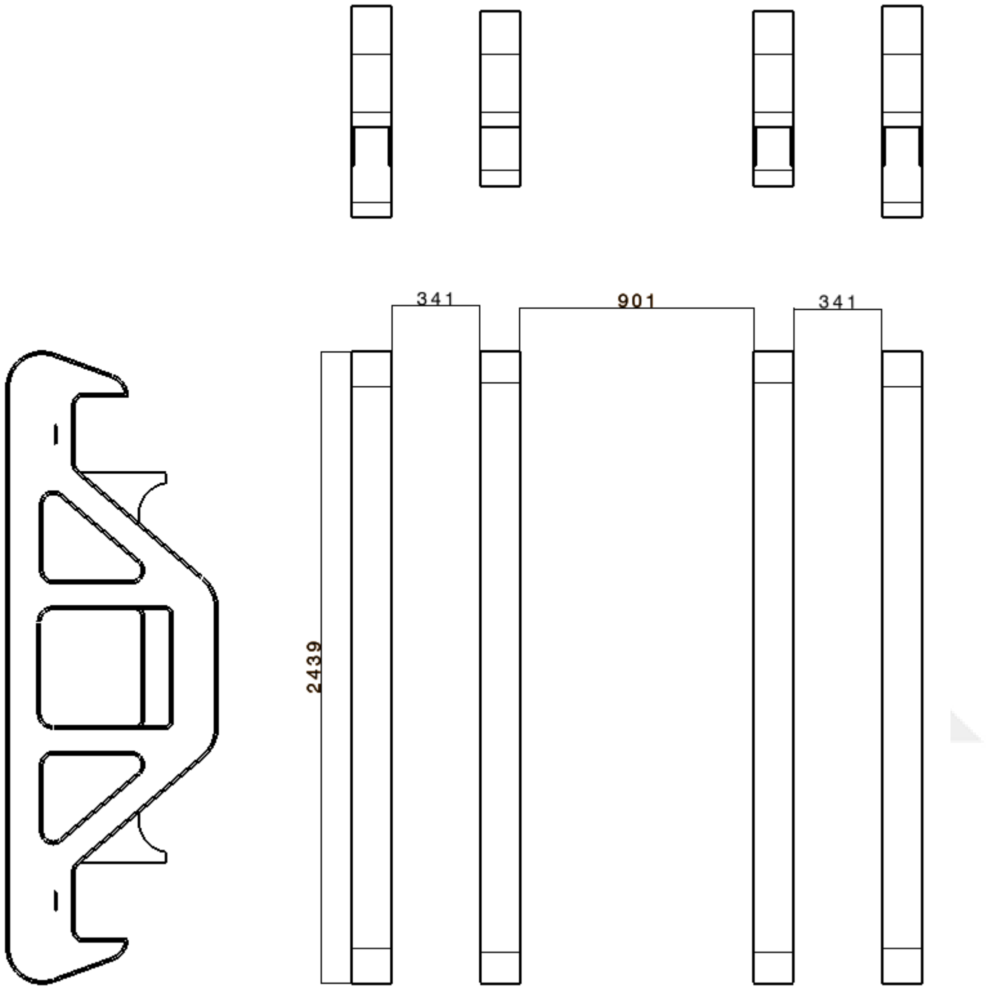

Figure 2.16 : Side frames

2.3.4 Axle Boxes

Axle boxes transfer the load from side frames to the shaft while they are connected to each other by a shaft. Because of the working principle of the system two different axle boxes are used in the design (Figure 2.17).

On the axle boxes, there is a sliding plaque allowing the connection with the side frames and a rubber part enabling the equal distribution of the load.

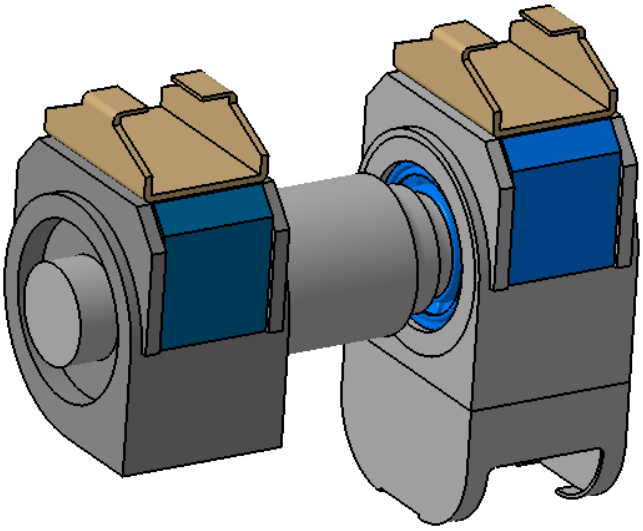

Figure 2.17 : Outer axle box(left) (right) and inner axle box(right)

2.3.5 Outer axle box

Outer axle box consists of a bearing, housing, sliding plaque and a rubber part (Figure 2.18).

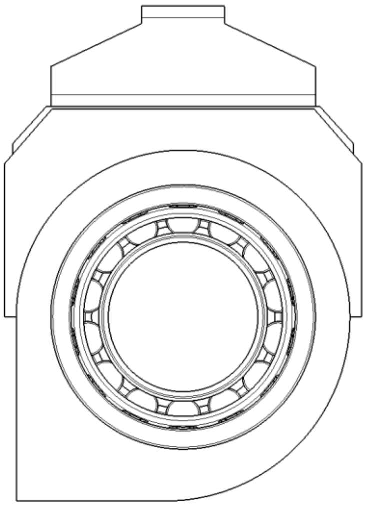

Figure 2.18 : Outer axle box

2.3.6 Inner Axle Box

Inner axle box consist of sliding plate, rubber part, inner and outer housing, outer housings lid and a bearing. Also there is a locking mechanism under the inner axle box. The locking mechanism is covered by a lid to protect it from the outer effects (Figure 2.19).

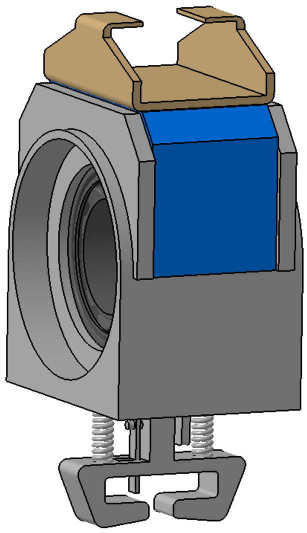

Figure 2.19 : Inner axle box and locking mechanizm

The locking mechanism (Figure 2.20), blocks the movement in transverse axis during normal on-track operation of the train. In the change stations with the help of a guide rail, mechanism is unlocked and moves along the transverse axis of the shaft to enable the change of the distance between the wheels. After the change, mechanism locks again and disables the shaft movement.

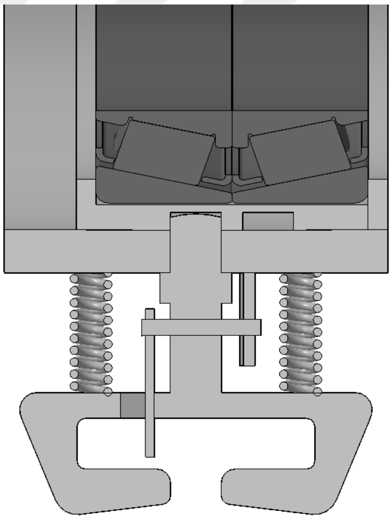

Figure 2.20 : Locking mechanizm (section)

The working principle is respectively:

As the bogie enters to the change station by decelerating, with the help of 2 supporting structures by left and right side, bogie continues to movement unloaded. After the unloading of the bogie, guideline starts to enter to the inside of the lock. By pulling the spring bolt down, it enables the vertical movement (Figure 2.21).

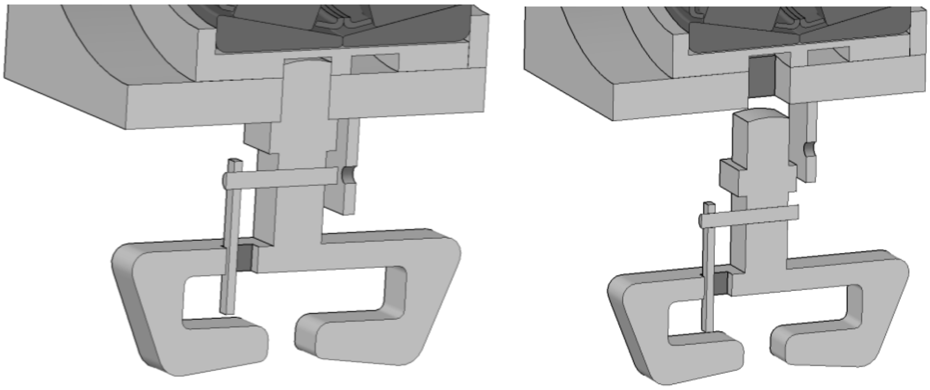

Figure 2.21 : Delocking system and pulling the lock down

Afterwards the inclined structure of the guideline pulls the lock down towards the ground so the horizontal movement is enabled between the housings. During the change process, guideline disables the vertical movement and prevents return of the lock to its previous place.

After the unlock, the wheel and the shaft are able to move horizontally. The auxilary rail set under the wheel which helps the locating of the wheel bidirectionally, augments the distance between the wheels to 1520 mm from 1435 mm. these auxiliary rail set entering before the unlock, helps to fix the location of the wheels until the locking (Figure 2.22).

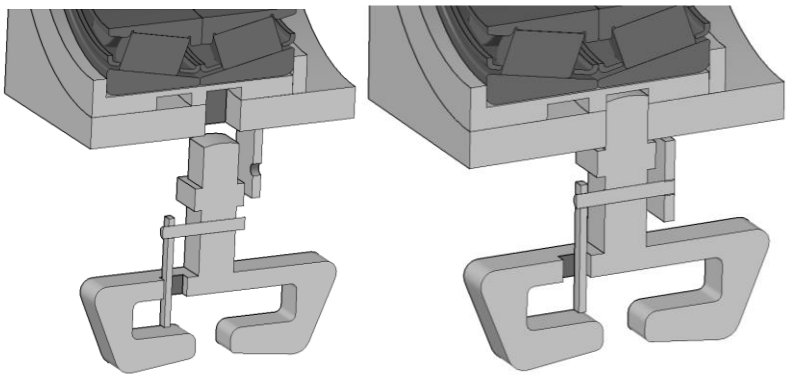

Figure 2.22 : Transverse movement of inner axle box and locking the mechanizm

Guideline with an inclined upwards enables the locking after the wheel distance becomes 1520 mm which is suitable for the eastern block countries. The guideline is redundant after this step.

With the locking, horizontal movement is disabled again so the auxiliary rail sets. The railway tracking continues Supporting structures declines vertically so the wagon is loaded on the bogie again. At the end of the change station, transferring between 1435 mm rail gauge to 1520 mm rail gauge is completed.

2.3.7 Axles

The bogie has 4 axles that are mounted to each wheel as a shrink fit. Section dimensions are designed according to standards (Figure 2.23).

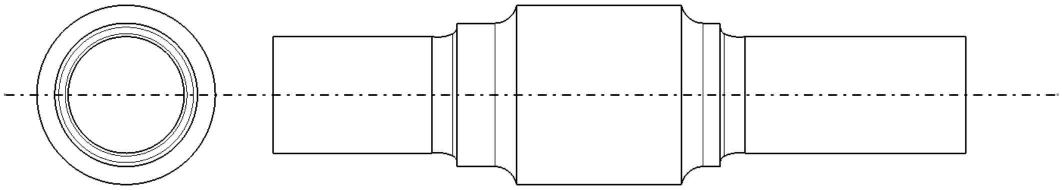

Figure 2.23 : Axle

2.3.8 Standart Parts

A total of 8 standard bogie spring sets are used between the bogie, side frames and bolsters (Figure 2.24).

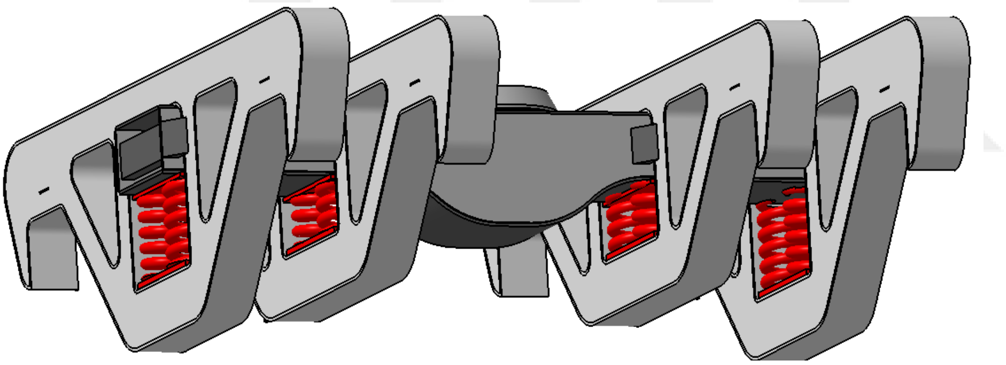

Figure 2.24 : Bojie spring sets (red)

Pivot, side bearers and wheels are parts used in standard bogies and will be supplied externally (Figure 2.25).

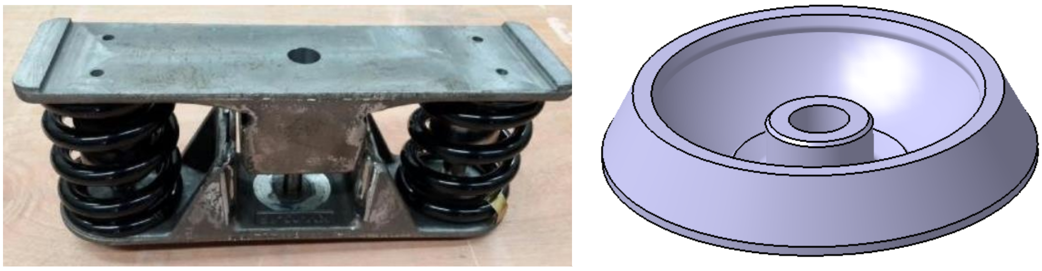

Figure 2.25 : Side bearer(left) [8] and hemi-spherical pivot housing (right)

Figure 2.26 : Railway wheel [9]

2.3.9 Design of Change Station

To let the railway vehicles adopt to the different railway tracks, change stations must be reconstructed according to the system proposed. The railway track design in the change station will connect the gauge distances of 1435 mm on one side and 1520 mm on the other side while the train moves continuously. The station will provide the railway vehicles to cross the borders seamlessly.

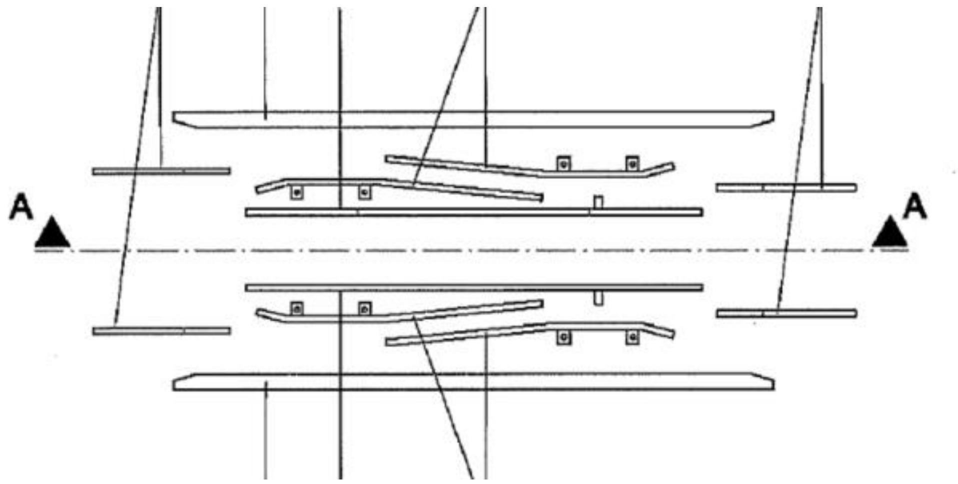

Figure 2.27 : Change station design [10]

At first a carrier guideline will be presented to the system to let the load be carried by the frames rather than the wheelsets. This guideline will be mounted under the frames to carry the load so the wheels will be load free while their locations change.

In the station also with the railway tracks, a guideline which allows the unlocking of the system that makes the wheels stay stable. The guide line will be mounted to the lock system of the inner axle box then it will pull the locking system down. During the process guideline will be bounded to the locking mechanism and after the gauge distance between the wheels changes, it will enable the lock in the axle box by moving upwards.

After the guideline unlock the system, wheels will enter to a two way rail and adopt to the new gauge distance by depending on the direction of travel through the station track.

3. ENGINEERING CALCULATION METHODS APPLIED

3.1 Finite Element Method

Finite element method (Figure 3.1), is a numerical method for solving engineering problems. The analysis of stress, heat transfer, electromagnetism and fluid mechanics problems can be solved as linear or nonlinear depending to time or not. Advantage of finite element method is; solving the problems which are difficult to calculate analytically.

The first step in this method, seperate the problem as small sub-structures. This process called meshing. Mesh consists of nodes and elements that connecting nodes. These elements are the sub-structures of problem. The desired magnitude to be calculated in the solution is obtained by interpolation using the values at the nodes.

There are some commercial programs for solving FEM problems. The FEM model is created in Hypermesh for the analysis conducted in this thesis and solved by using ABAQUS.

Basic steps in finite element method are;

1. Creating and discretizing the solution domain into finite elements; that is, subdivide the problem into nodes and elements.

2. Assume a shape function to represent the physical behavior of an element; that is, a continuous function is assumed to represent the approximate behavior (solution) of an element.

$$\Psi^{(e)} = [S_i \quad S_j \quad S_m \quad S_n]\begin{Bmatrix} \Psi_i \\ \Psi_j \\ \Psi_m \\ \Psi_n \end{Bmatrix} \tag{3.1}$$

3. Develop equations for an element.

4. Assemble the elements to present the entire problem. Construct the global stiffness matrix.

$$
[K]=\begin{bmatrix} k_{11}^1 & k_{12}^1 & k_{13}^1 & 0 & 0 \\ k_{21}^1 & k_{22}^1+k_{22}^2 & k_{23}^1+k_{23}^2 & k_{24}^2 & 0 \\ k_{31}^1 & k_{32}^1+k_{32}^2 & k_{33}^1+k_{33}^2+k_{33}^3 & k_{32}^2+k_{34}^2 & k_{35}^3 \\ 0 & k_{42}^2 & k_{43}^2+k_{43}^3 & k_{44}^2+k_{44}^3 & k_{45}^3 \\ 0 & 0 & k_{53}^3 & k_{54}^3 & k_{55}^3 \end{bmatrix} \tag{3.2}
$$

5. Apply boundary conditions, initial conditions, and loading.

6. Solve a set of linear or nonlinear algebraic equations simultaneously to obtain nodal results, such as displacement values at different nodes or temperature values at different nodes in a heat transfer problem.

7. Obtain other important information. At this point, you may be interested in values of principal stresses, heat fluxes, and so on.

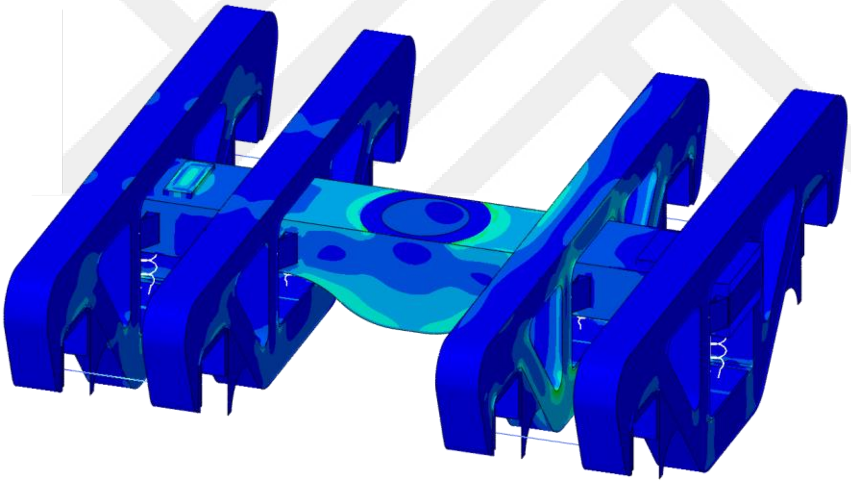

Figure 3.1 : Finite element analysis of the bogie

3.2 Fatigue Analysis Method

3.2.1 Introduction to Fatigue Mechanics

Fatigue strength is the highest stress that a material can resist for a given number of cycles without breaking. Fatigue strength depends on the properties of the material, the magnitude and the state of stress and number of cycles.

When the highest stress limit exceeds under the static loading, fracture occurs. With cyclic loading, even if the occurred stress is under the maximum tensile strenght, fractures or damages will occur.

The steps of the effect of fatigue consists of the crack initiation, crack propogation and the fracture.

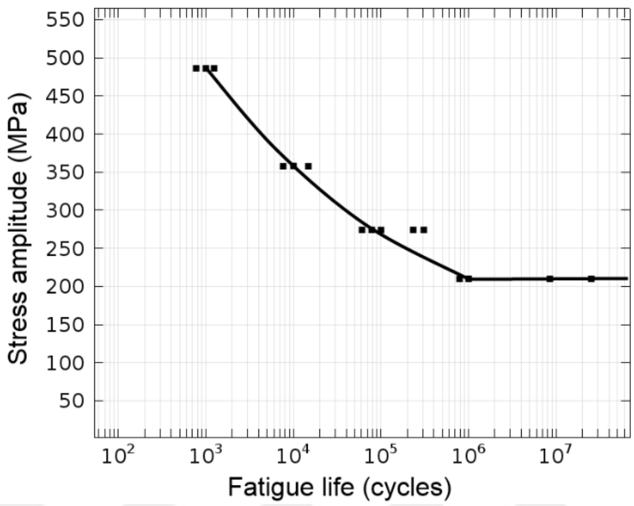

Figure 3.2 : Wohler curve

First tests about fatigue strength is made by August Wöhler(1819-1914).the wagon axes were tested. According to the results of the test, for an average stress, the curve between the number of load cycles to fatigue is called Wöhler curve (Figure 3.2).

Factors effecting fatigue strength are;

- Properties of the material
- State of stress
- Geometry
- Internal defects
- Residual stress
- Grain size
- Environment
- Temperature

The life of the material in the finite life area is due to the number of cycles. If the curve is under a defined β, the life of the material is accepted as infinite. Wöhler diagram ease the calculations by showing the experimental datas together in a diagram.

3.2.2 Fatigue of Weld Joints

Major effect of fatigue consists on weld joints in steel structures, due to welds located on hot spots. Hot spots are points in a structure where a fatigue crack may initiate due to the combined effect of structural stress fluctuation and weld geometry or a similar notch. The stress on that points called notch stress and contain nominal stress which are resolved using general theories, residual stresses due to welding action, and hot spot stresses due to geometric joint style (Figure 3.3).

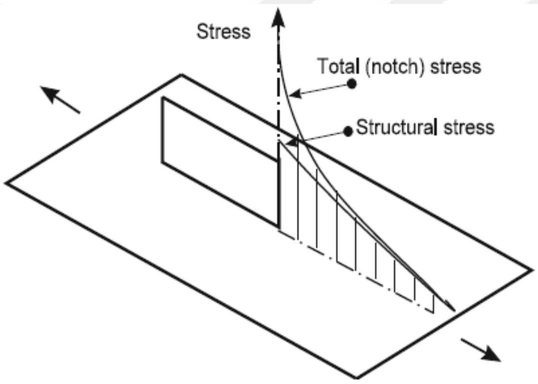

Figure 3.3 : Structural stress and notch stress[18]

Notch stress on a hot spot can be calculated with, sum of nominal stress and nonlinear stress peak (Figure 3.4).

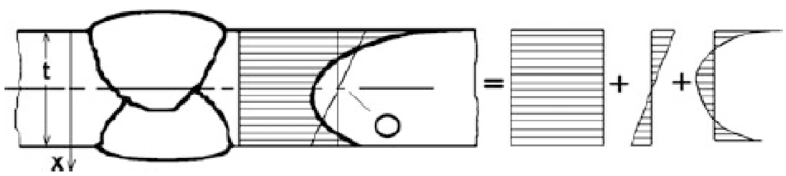

Figure 3.4 : Notch stress[18]

The maximum stress value is on the root of the weld on hot spot, and can be determined with extrapolation by using reference points from weld toe.

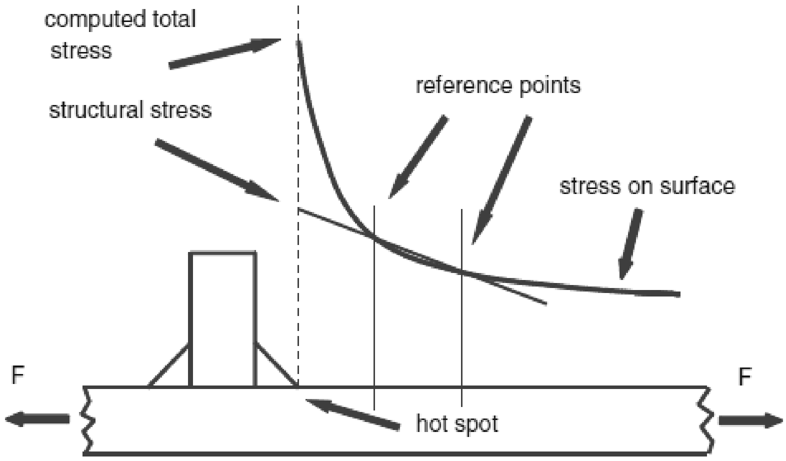

Figure 3.5 : Stress calculation on the root of weld[18]

3.2.3 Welding Design Criteria of Bogie

Bogie has been designed in accordance with the requirements of technical data specified in DVS 1612 standart. This standart contains the information of design and endurance strength of welded joints in rail vehicle construction. Fatigue model of bogie created and analyzed with LIMIT-CAE software, according to DVS 1612.

This standarts calculation method is based on; comparing notch stress on the hot spot with a permissible maximum normal stress σzul and permissible maximum shear stress τzul .Permissible maximum normal stress can be calculated with normal stress ratio Rσ, permissible endurance strength value x. Permissible maximum shear stress ratio τzul can be calculated with shear stress ratio Rτ and τmax,R=-1 value.

$$R_{\sigma} = \sigma_{min}/\sigma_{max} \tag{3.3}$$

$$R_{\tau} = \tau_{min}/\tau_{max} \tag{3.4}$$

$$\sigma_{zul}(R\sigma) = 150MPa * 1.04^{x} \frac{2 * (1 - 0.3 * R\sigma)}{1.3 * (1 - R\sigma)} \tag{3.5}$$

$$\tau_{zul}(R_{\tau}) = \frac{2 * (1 - 0.17 * R_{\tau})}{1.17 * (1 - R_{\tau})} * \tau_{zul,R=-1} \tag{3.6}$$

In the formula 7.1 and 7.2, σ_{max} and σ_{min} are existing maximum and minimum normal stresses, and τ_{max} and τ_{min} are existing maximum and minimum shear stresses

The permissible endurance strength values depend on the weld type and weld quality. This value can be determined with notch case line of weld type.

Joint and weld type					Type and scope of inspection	Weld performance class according to DIN EN 15085-3	Notch case line
Structural detail	Description	Weld type	Weld No. according to DIN EN 15085-3	Post-weld treatment of weld surface			
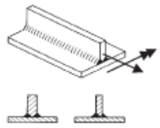	Full penetration weld on both sides with backing run	Double-bevel weld Single-bevel weld with fillet weld as backing run Single-bevel weld with backing run	7 10b 10d	Yes	100% NDT-V	CP A	B+
					10% NDT-V	CP B and CP C1	B
					Visual inspection	CP C2	B-
				No	100% NDT-V	CP A	C+
					10% NDT-V	CP B and CP C1	C
					Visual inspection	CP C2	C-

Figure 3.6 : Notch case line values of a full penetration weld on both sides[19]

Notch case lines are specified for weld types, in **DVS 1612** (Figure 3.6), and depend on post-weld treatment and Non-Destructive-Controlling of the Welds (either volumetri or surface methods, depending on weld type). By selecting the appropriate value, the endurance strength values can be calculated.

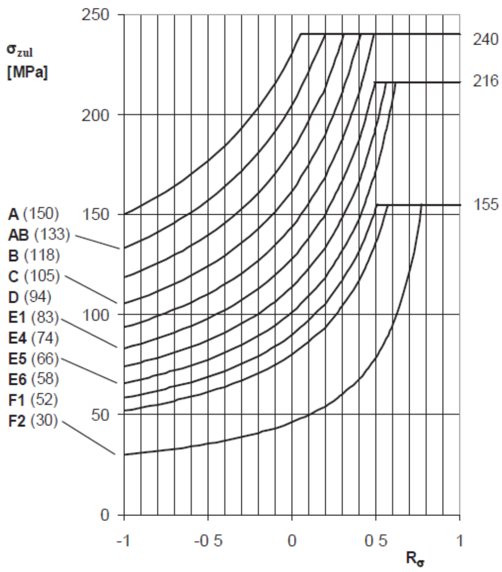

Figure 3.7 : Permissible maximum normal stress - normal stress ratio graph for different notch case line values. [19]

4. ENGINEERING CALCULATIONS

4.1 Loads

4.1.1 Exceptional Loads

Vertical Forces

Vertical forces can be calculated using Eq. **(2.1)**.

$M_v = 90\ ton = 90 \times 10^3\ kg$

$m^+ = 4{,}5\ ton = 4{,}5 \times 10^3\ kg$

So, from here F_z can be calculated as follows

$$F_z = \left(\frac{M_v - 2m^+}{2}\right) g = \left(\frac{90 \times\ 10^3 - 2 \times 4{,}5 \times\ 10^3}{2}\right) \times 9{,}8 \cong 400\ kN$$

Case 1 – The case where the force is applied only to the pivot:

$F_{zp\ max} = 2F_z = 2 \times 400\ kN = 800\ kN$

Case 2 – The case where the force is applied to both the pivot and one sidebearer:

For 1,7 m distance between the sidebearers, α is taken as 0,3. In this scenario, it is also 0,3.

$F_{z1\ max}$ (or $F_{z2\ max}$) $= 1{,}5 \times F_z \alpha\ = 1{,}5 \times 400 \times 0{,}3 \cong 180\ kN$

$F_{zp\ max} = 1{,}5 \times F_z\ (1 - \alpha) \cong 420\ kN$

Transverse Forces (applied to each axle)

$$F_{y1\ max} = \frac{F_{y\ max}}{2} = 10^4 + \frac{F_z +\ m^+ g}{6} = 10^4 + \frac{400 \times 10^3 +\ 4{,}5 \times 10^3 \times 9{,}81}{6}$$

$F_{y1\ max} = F_{y2\ max} = 84\ kN$

Longitudinal Lozenging Forces

$F_{x1\ max} = 0{,}1 \times (F_z +\ m^+ g) = 0{,}1 \times (400\ \times 10^3 +\ 4{,}5 \times 10^3 \times 9{,}81) = 44\ k$

4.1.2 Normal Loads

Vertical Forces

Case 1 – The case where the force is applied only to the pivot:

$F_{zp} = F_z = 400\ kN$

Case 2 – The case where the force is applied to both the pivot and one sidebearer:

For 1,7 m distance between the sidebearers, α is taken as 0,2. In this scenario, it is also 0,2.

F_{z1} (or F_{z2}) = $F_z \alpha = 400 \times 0{,}2 = 800\ kN$

$F_{zp} = F_z\,(1-\alpha)$ = $400 \times (1-0{,}2) = 320\ kN$

Transverse Forces (applied to each axle)

$$F_{y1} = F_{y2} = \frac{F_y}{2} = 0{,}1 \times (F_z + m^+ g) = 0{,}1 \times (400 \times 10^3 + 4{,}5 \times 10^3 \times 9{,}81)$$

$F_{y1} = F_{y2} = 44\ kN$

Longitudinal Lozenging Forces

$F_{x1} = 0{,}05 \times (F_z + m^+ g) = 0{,}05 \times (400 \times 10^3 + 4{,}5 \times 10^3 \times 9{,}81) = 22\ kN$

If all these numerical values are filled in a table, the following table will occur. Using normal loads shown in Table 4.1.

Table 4.1 : Exceptional and normal load cases

	Exceptional Loads	Normal Loads
Vertical Forces Case 1	$F_{zp\,max} \cong 800\ kN$	$F_{zp} = 400\ kN$
Vertical Forces Case 2	$F_{z1} \cong 180\ kN$ $F_{z1} \cong 180\ kN$	$F_{z1} = 800\ kN$ $F_{zp} = 320\ kN$
Transverse Forces	$F_{y1\,max} = F_{y2\,max} = 84\ kN$	$F_{y1} = F_{y2} = 44\ kN$
Longitudinal Forces	$F_{x1\,max} = 44\ kN$	$F_{x1} = 22\ kN$

Using these numerical values Table **4.2** which will be used in the static test program, can be filled as follows:

Table 4.2 : Numerical values of load cases for tests under normal loads resulting from bogie running

	Force on Sidebearer 1 F_{z1}	Force on Pivot F_{zp}	Force on Sidebearer 2 F_{z2}	Transverse Force F_y
1	0	400 kN	0	0
2	0	520 kN	0	0
3	0	280 kN	0	0
4	0	416 kN	104 kN	88 kN
5	0	416 kN	0	-88 kN
6	0	224 kN	56 kN	88 kN
7	0	224 kN	0	-88 kN

Loading actions can be seen in Figure 4.1 and all load case values using in static analysis are shown in Table 4.3.

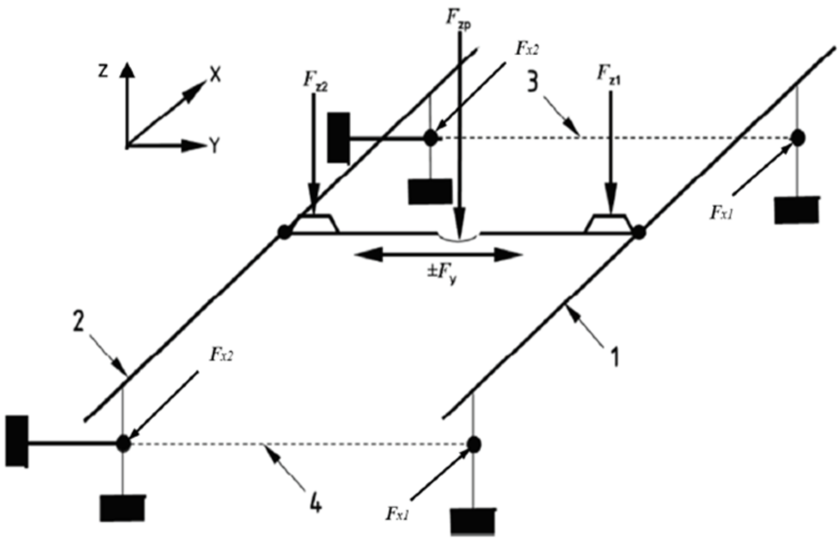

Figure 4.1 : All loads acting on the bogie frame

Table 4.3 : Loading Conditions [LC]

LC	Load (kN)							Reference to Standards
	Vertical			Transverse	Longitudinal		Twist	
	sidebearer 2	central pivot	sidebearer 1					
	F_{z2}	F_{zc}	F_{z1}	F_y	F_{x1}	F_{x2}	g^+	
1		800.00						EN 13749 (C.7)
2		420.00	180.00				$+10\ ^{o}/_{oo}$	EN 13749 (C.8; C.9; C2.1)
3		420.00	180.00				$-10\ ^{o}/_{oo}$	EN 13749 (C.8; C.9; C2.1)
4	180.00	420.00					$+10\ ^{o}/_{oo}$	EN 13749 (C.8; C.9; C2.1)
5	180.00	420.00					$-10\ ^{o}/_{oo}$	EN 13749 (C.8; C.9; C2.1)
6		420.00	180.00	168.05				EN 13749 (C.8; C.9; C10)
7	180.00	420.00		-168.05				EN 13749 (C.8; C.9; C10)
8		600.00			44.41	-44.41		EN 13749 (C11)
9		600.00			-44.41	44.41		EN 13749 (C11)
10		400.00			220.73			EN 13749 (Longitudinal loads)
11		400.00			-220.73			EN 13749 (Longitudinal loads)
12		400.00						EN 13749 (table F.3)
13		520.00						EN 13749 (table F.3)
14		280.00						EN 13749 (table F.3)
15	104.00	416.00		88.83				EN 13749 (table F.3)
16		416.00	104.00	-88.83				EN 13749 (table F.3)
17	56.00	224.00		88.83				EN 13749 (table F.3)
18		224.00	56.00	-88.83				EN 13749 (table F.3)
19		400.00						EN 13749 (C12)
20		320.00	80.00				$+10\ ^{o}/_{oo}$	EN 13749 (C.13; C.14; C2.1)
21		320.00	80.00				$-10\ ^{o}/_{oo}$	EN 13749 (C.13; C.14; C2.1)
22	80.00	320.00					$+10\ ^{o}/_{oo}$	EN 13749 (C.13; C.14; C2.1)
23	80.00	320.00					$-10\ ^{o}/_{oo}$	EN 13749 (C.13; C.14; C2.1)
24		320.00	80.00	88.83				EN 13749 (C.13; C.14; C15)
25	80.00	320.00		-88.83				EN 13749 (C.13; C.14; C15)
26		600.00			22.21	-22.21		EN 13749 (C16)
27		600.00			-22.21	22.21		EN 13749 (C16)

4.2 Calculation of Bearing

4.2.1 Bearing Test Forces and Selection of Suitable Bearing

Test forces can be calculated as follows:

Reference Vertical Force: F_0

$$F_0 = \frac{1}{j} \times m_{max} \times g$$

$$F_0 = \frac{1}{4} \times 90 \times 10^3 \times 9{,}81 \cong 220\ kN$$

Nominal Radial Test Force: F_{rn}

$$m_2 \cong 1{,}5\ ton \cong 1{,}5 \times 10^3\ kg$$

$$F_{rn} = \frac{1{,}2}{2} \times (F_0 - m_2 \times g) = 0{,}6 \times (220 \times 10^3 - 1{,}5 \times 10^3 \times 9{,}81) = 123{,}71\ kN$$

Nominal Axial Test Force: F_{an}

$$F_{an} = \frac{1{,}2}{2} \times 0{,}5 \times 0{,}85 \times \left(10^4 + \frac{F_0}{3}\right) = 0{,}225 \times \left(10^4 + \frac{220 \times 10^3}{3}\right) = 18{,}75\ kN$$

CRU 130x240 Cylindrical Roller Bearing (Standard Y25 Bogie Bearing) has been selected as a suitable bearing. Principal dimensions of this bearing are shown in the figures below.

Advantages of this bearing:

- The factory pre-lubricated design of this bearing unit provides ease of assembly for bogie manufacturers.
- The labyrinth seal provides zero friction during operational conditions.

Short CRU design – Type 1

The small width of the Short CRU design provides smaller axlebox design and a shorter axle journal. This design reduces axle bending and makes the bearing in-service life longer.

CRU cylindrical roller bearing units

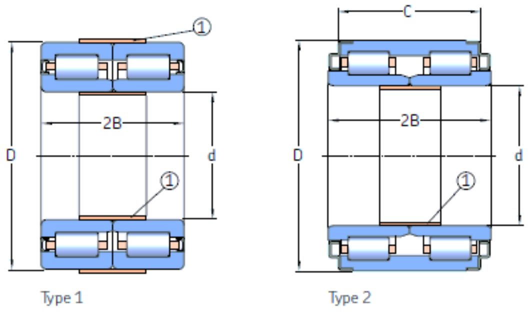

Size	Principal dimensions				Type
	d	D	C	2B	
–	mm				–
CRU 100 x 180	100	180	–	120,6	1
CRU 120 x 200	120	200	–	112	1
CRU 120 x 215	120	215	–	146	1
CRU 130 x 220	130	220	–	160	1
CRU 130 x 240	130	240	–	160	1
CRU 130 x 240	130	240	164	160	2

Figure 4.2 : Principal dimensions of CRU 130 x 240 bearing unit

According to the SKF Railway Handbook, for the calculation of equivalent dynamic bearing load which will be used for the bearing life calculation the following

$$P = F_r \tag{4.1}$$

Equation must be used. Here;

P is the equivalent dynamic bearing load. F_r is the radial force

$P = F_r \approx 124\ kN$

4.2.2 Bearing Life Calculation

For bearing life calculation, the following equation can be used.

$$L = \left(\frac{C}{P}\right)^n \tag{4.2}$$

$$L_{10s} = \frac{\pi \times L \times D_W}{1000} \tag{4.3}$$

L is the basic rating life [in million revolutions]

L_{10s} is the basic rating life [in million km]

C is the basic dynamic load rating [in kN]

D_W is the mean diameter [in m] (in this scenario it is equal to 0,95 m)

n is equal to 10/3 for roller bearings

If, the numerical values are inserted into **Eq. (4.2)** and **(4.3)**, bearing life can be calculated as follows:

According to the SKF Railway Handbook, the value of C is equal to 1010 kN.

The value of C can be found in **Figure 4.3**, which is equal to 1010 kN. So;

$$L = \left(\frac{C}{P}\right)^{10/3} = \left(\frac{1010}{124}\right)^{10/3} \approx 1087\ million\ revolutions$$

$$L_{10s} = \frac{\pi \times L \times D_W}{1000} = \frac{\pi \times 1087 \times 0{,}95}{1000} \approx 3{,}2\ million\ km$$

As it is mentioned earlier, according to **Table 2.3**, the design life of the bearing must be more than 1,6 million km. 3,2 million km is more than 1,6 million km. Therefore, selected bearing is suitable for the design.

4.3 Stress Calculations of the Axle

4.3.1 Stress Calculations under Exceptional Load Conditions – LC1

Case 1 – The case where the force is applied only to the pivot (Figure 4.3):

$F_{zp\ max} = 2F_z = 2 \times 400\ kN = 800\ kN$

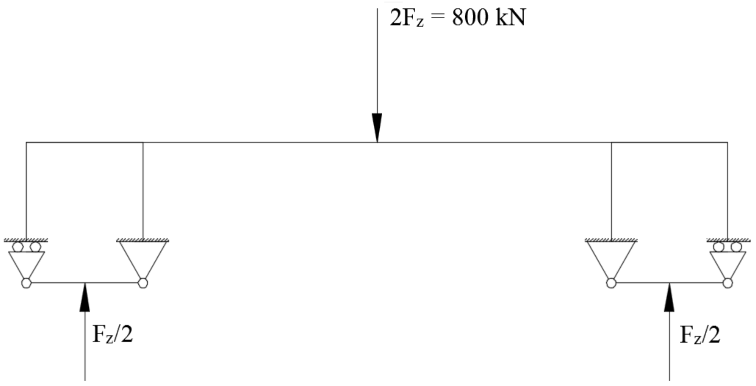

Figure 4.3 : Free body diagram of the bogie under exceptional load conditions – LC1

4.3.1.1 Stress Calculations of the Axle – LC1

There are four shafts. So, each shaft will experience a force of magnitude $\frac{F_z}{2} = 200\ kN$ (Figure 4.4).

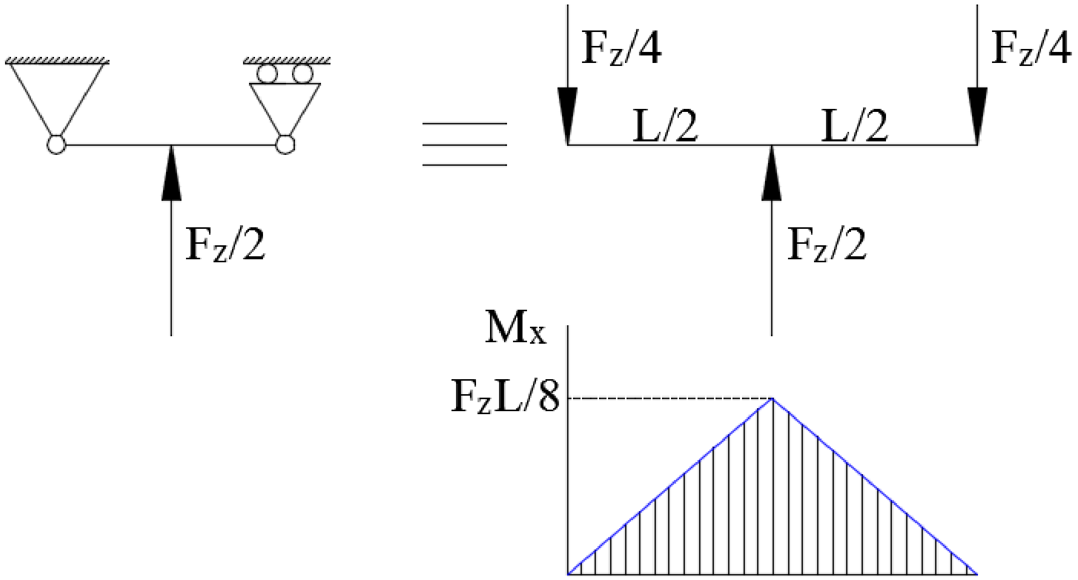

Figure 4.4 : Free body and moment diagram of the right-hand side shaft under exceptional load conditions

For the most critical section;

$$\sigma_{z\,max} = \frac{M_x}{I_x} y_{max} \tag{4.4}$$

$$M_{x\,max} = \frac{F_z L}{8}\ ;\ y_{max} = \frac{D}{2}\ ;\ I_x = \frac{\pi D^4}{64}$$

$$\sigma_{z\,max} = \frac{\frac{F_z L}{8} \times D/2}{\frac{\pi D^4}{64}} = \frac{\frac{F_z L D}{16}}{\frac{\pi D^4}{64}} = \frac{4 F_z L}{\pi D^3}$$

$$F_z = 400\ kN\ ;\ L = 800\ mm\ ;\ D = 200\ mm$$

$$\sigma_{z\,max} = \frac{4 \times 400 \times 10^3 \times 800}{\pi \times (200)^3} \approx 51\ MPa$$

From the result above (51 MPa) it is understood that this result does not exceed the limit values of steel grade EA1N material which is 200 MPa.

4.3.2 Stress Calculations under Exceptional Load Conditions – LC2

Exceptional load conditions on bogie are shown in Figure 4.5.

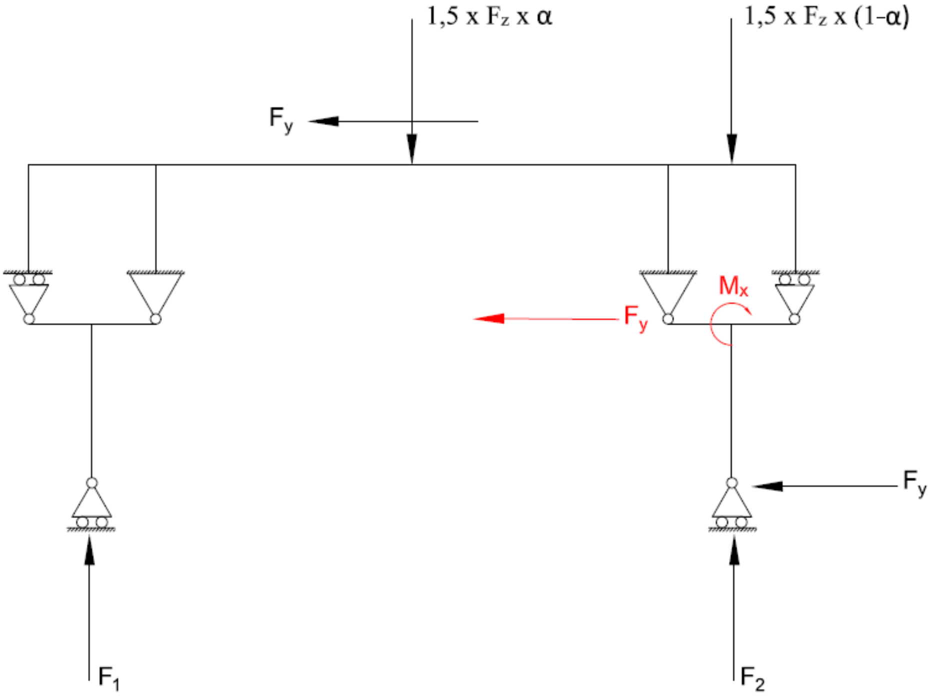

Figure 4.5 : Free body diagram of the bogie under exceptional load conditions – LC2

4.3.2.1 Stress Calculations of the Axle –LC2

Free body diagram of bolster is can be seen in Figure 4.6.

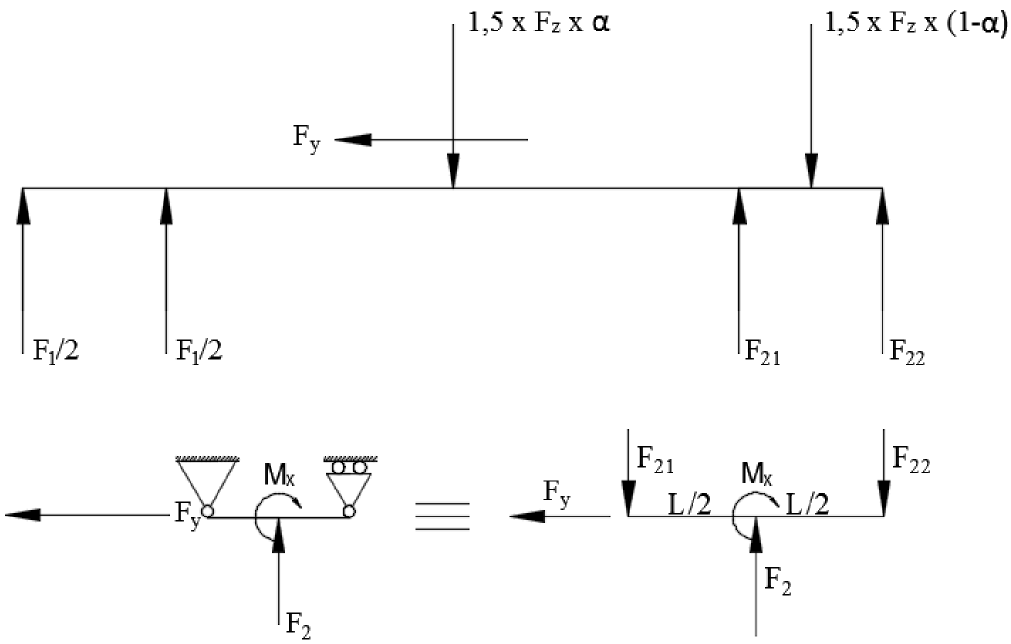

Figure 4.6 : Free body diagram of the bolster and right hand side shaft

Shaft Force Calculation:

$$F_2 \times \frac{L}{2} - F_{21} \times L + M_x = 0 \quad (L = 480\ mm)$$

$$F_{21} = \frac{F_2}{2} + \frac{M_x}{L}$$

$$F_{21} + F_{22} = F_2$$

$$\frac{F_2}{2} + \frac{M_x}{L} + F_{22} = F_2$$

$$F_{22} = \frac{F_2}{2} - \frac{M_x}{L}$$

Bolster Force Calculation:

$$F_1 + F_{21} + F_{22} = F_1 + F_2 = \frac{(420\ kN + 180\ kN)}{2} = 300\ kN$$

$$\frac{F_1}{2} \times (1034{,}5\ mm) + \frac{F_1}{2} \times (527{,}5\ mm) + 180 \times (861\ mm)$$
$$= F_{21} \times (527{,}5\ mm) + F_{22} \times (1034{,}5\ mm)$$

$$M_x = F_y \times R_{wheel} \approx \left(\frac{168}{2}\ kN\right) \times (460\ mm) = 38640\ kNmm$$

$$F_2 \approx 276\ kN$$

$$F_1 \approx 24\ kN$$

$$F_{21} = \frac{F_2}{2} + \frac{M_x}{L} = \frac{276\ kN}{2} + \frac{38640\ kNmm}{480\ mm} \approx 219\ kN$$

$$F_{21} = \frac{F_2}{2} - \frac{M_x}{L} = \frac{276\ kN}{2} - \frac{38640\ kNmm}{480\ mm} \approx 58\ kN$$

According the calculations, shear and moment diagram of right hand side axle is shown in Figure 4.7.

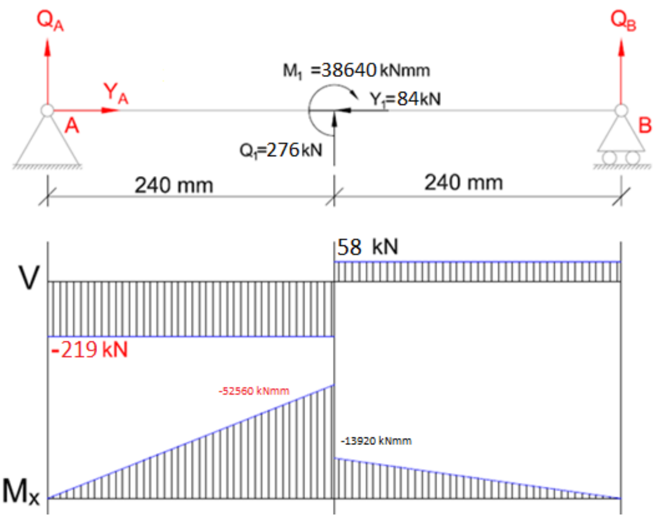

Figure 4.7 : Shear and moment diagram of right hand side axle

For the most critical section;

$$F_{x1} = 0{,}05 \times (F_z + m^{+}g) \tag{4.5}$$

$M_{x\,max} = 52560\ kNmm$; $y_{max} = D/2$; $I_x = \frac{\pi D^4}{64}$

$$\sigma_{z\,max} = \frac{(52560\ kNmm) \times D/2}{\frac{\pi D^4}{64}} = \frac{32 \times 52560 \times 10^3\ Nmm}{\pi (200)^3} = 67\ MPa$$

$S = \frac{200\ MPa}{67\ MPa} = 3$

From the result above (67 MPa) it is understood that this result does not exceed the limit values of steel grade EA1N material which is 200 MPa.

4.3.3 Stress Calculations of the Axle under Normal Loading Conditions

Free body diagram of bolster is can be seen in Figure 4.8.

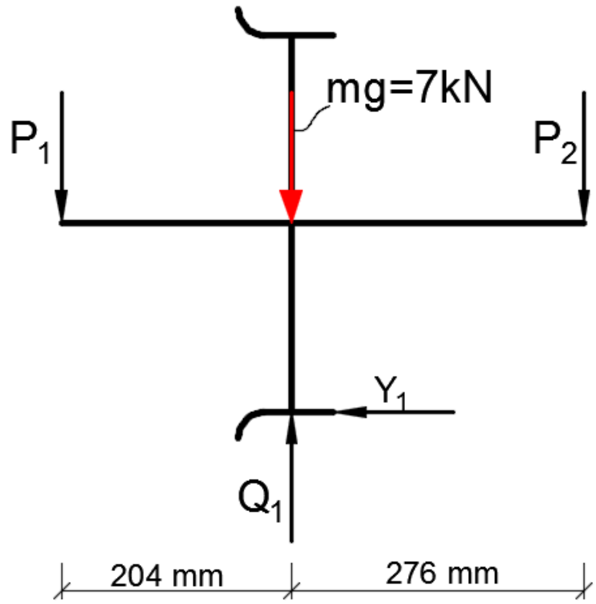

Figure 4.8 : Free body diagram of the right hand side axle

$P_1 \times (204\ mm) = P_2 \times (276\ mm) + Y_1 \times (460\ mm)$

$P_1 \cong 1{,}36 \times P_2 + 2{,}25 \times Y_1 \qquad (\mathbf{1})$

$P_1 + P_2 + m_2 g = Q_1$

$m_2 g = 7\ kN$

$P_1 + P_2 + 7\ kN = Q_1$

$P_1 + P_2 = Q_1 - 7\ kN \qquad (\mathbf{2})$

Free body diagram of bolster under normal loading conditions is can be seen in Figure 4.9.

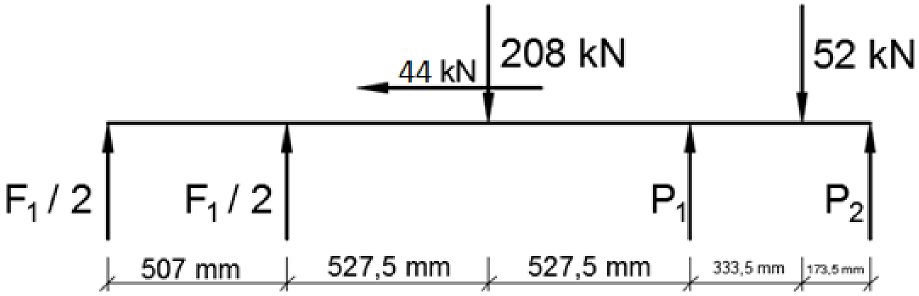

Figure 4.9 : Free body diagram of bolster under normal loading conditions

$F_1 + P_1 + P_2 = 260\ kN \implies F_1 + Q_1 - 7 = 260\ kN \implies F_1 + Q_1 = 267\ kN$

$$\frac{F_1}{2} \times (1034{,}5\ mm) + \frac{F_1}{2} \times (527{,}5\ mm) + 52 \times (861\ mm)$$
$$= P_1 \times (527{,}5\ mm) + P_2 \times (1034{,}5\ mm)$$

$P_2 = 33\ kN$

$P_1 \cong 144\ kN$

$Q_1 = P_1 + P_2 = 144\ kN + 33\ kN = 177\ kN$

According the calculations, shear and moment diagram of right hand side axle is shown in Figure 4.10.

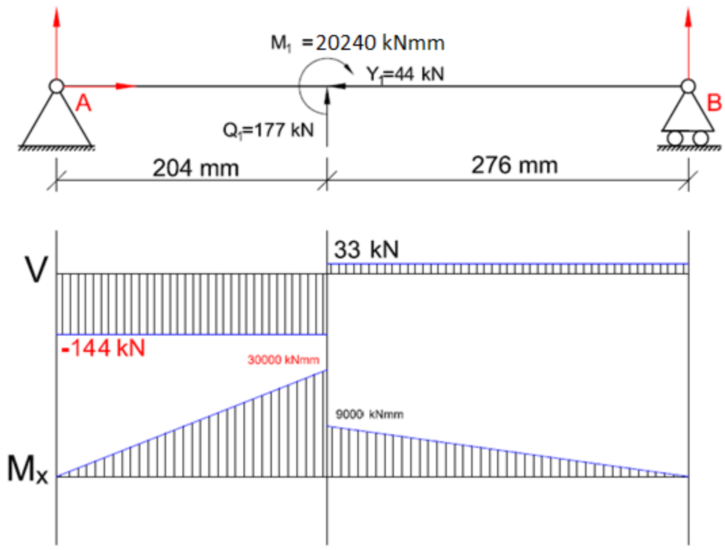

Figure 4.10 : Shear and moment diagram of right hand side axle

$MR \longrightarrow Resultant\ Moment$

$MR\ at\ 108\ mm = 15552\ kNmm$

$MR\ at\ 152\ mm = 21888\ kNmm$

$$\sigma = \frac{K \times 32 \times MR}{\pi d^3}$$

K ⟶ Stress Concentration Factor. It is calculated using Figure 4.15 and 4.16.

$$K_1 = 1{,}25 \left(\frac{D}{d} = \frac{d_2}{d_1} = \frac{160}{130} = 1{,}23, \qquad \frac{r}{d_1} = \frac{8}{130}\right) \approx 0{,}06$$

$$K_2 = 1{,}90 \left(\frac{D}{d} = \frac{d_3}{d_2} = \frac{200}{160} = 1{,}25, \qquad \frac{r}{d_2} = \frac{25}{160}\right) \approx 0{,}15625$$

$$\sigma_1 = \frac{K_1 \times 32 \times MR}{\pi d^3} = \frac{1{,}25 \times 32 \times (15552\ kNmm)}{\pi \times (130)^3} = 90\ MPa$$

$$\sigma_2 = \frac{K_2 \times 32 \times MR}{\pi d^3} = \frac{1{,}90 \times 32 \times (21888\ kNmm)}{\pi \times (160)^3} \approx 104\ MPa$$

$$S_1 = \frac{200\ MPa}{90\ MPa} = 2{,}22$$

$$S_2 = \frac{200\ MPa}{104\ MPa} = 1{,}92$$

Axle(Figure 4.11) stress values are appropriate to EN13103. Fatigue stress concentration factor as a function of r/d and D/d at the bottom of the transition between two cylindrical section(Figure 4.12)

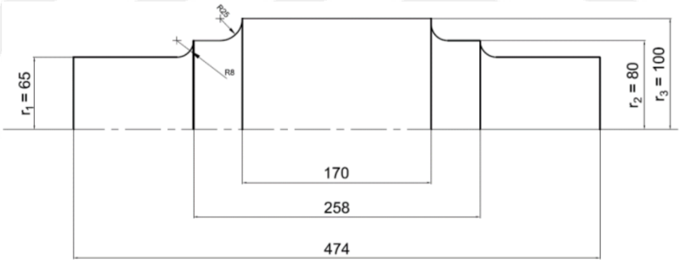

Figure 4.11 : Drawing of the axle

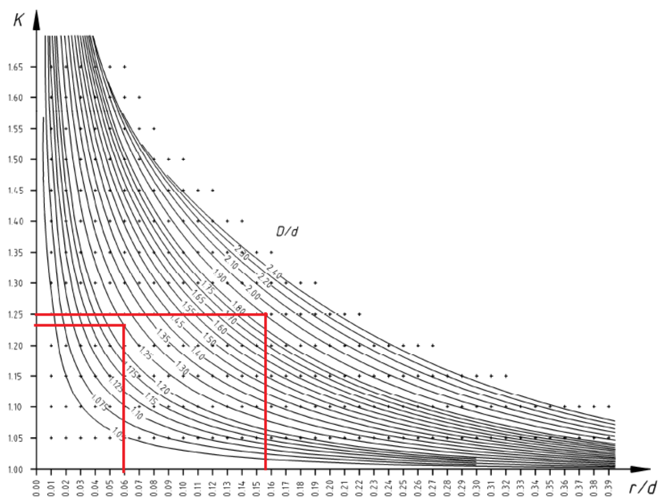

Figure 4.12 : Fatigue stress concentration factor as a function of r/d and D/d at the bottom of the transition between two cylindrical section

4.4 Finite Element Analysis of Bogie Frame

The FEM model for the bogie (Figure 4.13) analysis is created as two parts. First part is created for the steel structure which contains the side frames, bolster and the damping elements. Second part is generated for the axle box. The reference forces from the solution of the first model is used in the second one to complete the bogie analysis.

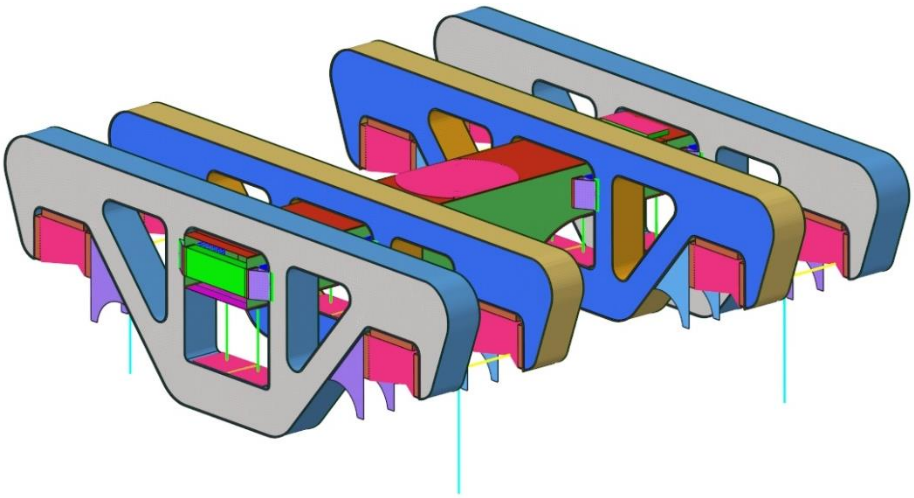

Figure 4.13 : FEM model of the bogie

4.4.1 Elements

Bogie model solved with Abaqus and elements from Abaqus element database are used. Bolster and side frames are constructed by steel sheets. Shell elements are used for modeling them. Pivot, side bearer and axle box (in frame analusis) are modeled with rigid elements. Spring elements used for bogie spring modeling.

The elements used in this analysis are;

- **S3;** 3-node triangular general-purpose shell, finite membrane strains
- **S4R;** 4-node general-purpose shell, reduced integration with hourglass control, finite membrane strains
- **C3D6;** 6-node linear triangular prism, reduced integration with hourglass control
- **C3D8R;** 8-node linear brick, reduced integration with hourglass control

- **Kinematic Coupling;** Kinematic constraint limit the motion of a group of nodes to the rigid body motion defined by a reference node
- **Distributing Coupling;** Distributing constraint, constrains the motion of the coupling nodes to the translation and rotation of the reference node.
- **B33;** 2-node beam element, used to modeling axles.
- **Spring2;** 2-node spring element, used to modeling bogie springs.

4.4.2 Finite Element Model Creation

Bolster and side frames are constructed by steel sheets. Shell elements are used for modeling them. First, bogie geometry which crated with CATIA, imported to Hypermesh (Figure 4.14).

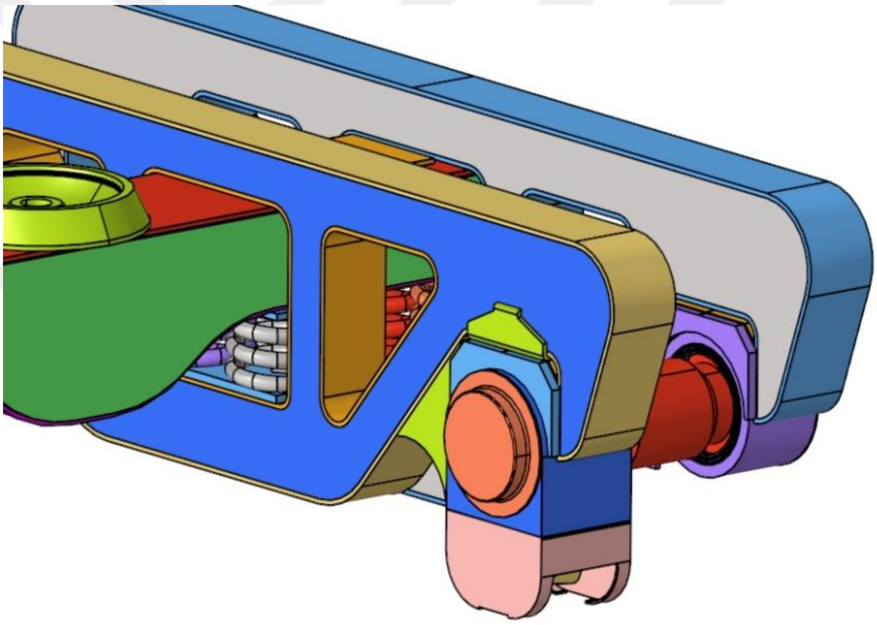

Figure 4.14 : 3D Geometry in Hypermesh

Midsurfaces of sheet metals are created wih midsurface module of Hypermesh (Figure 4.15).

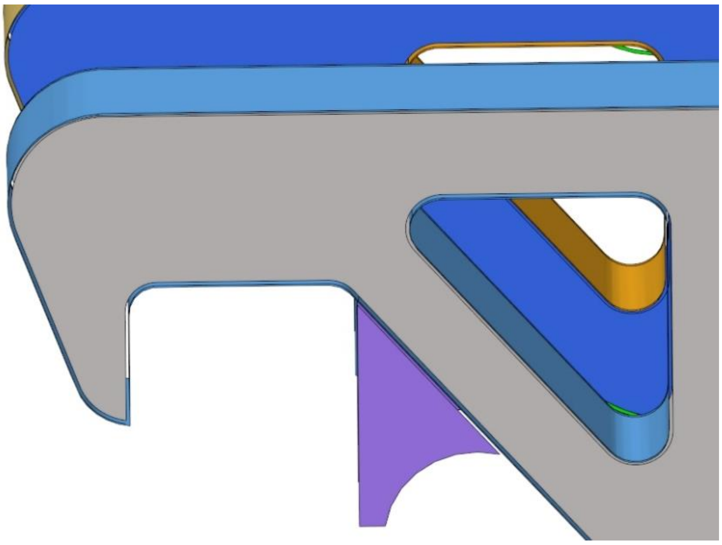

Figure 4.15 : Midsurfaces of solid bodies

The finite element mesh of bogie created with midsurfaces. Characteristic element length of shell elements is 10mm (Figure 4.16).

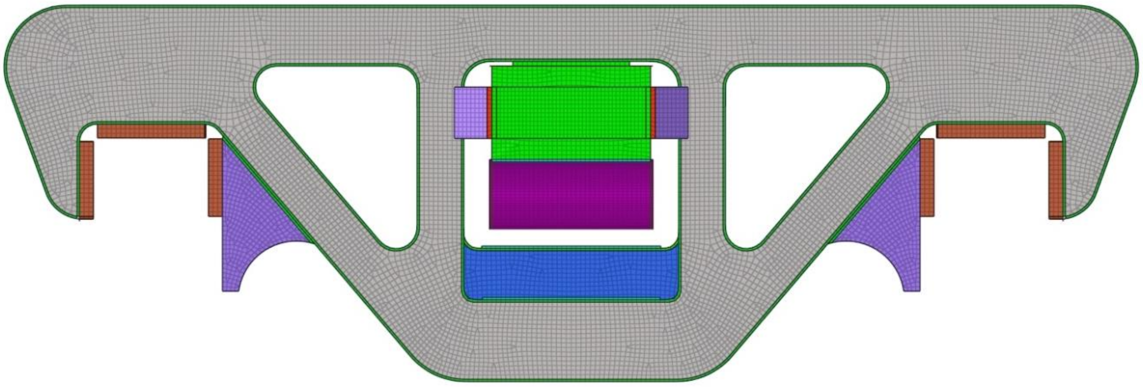

Figure 4.16 : Finite element mesh of bogie

All of the welding of sheet metal elements were done with manuel element creating . Same element types used on creating weld elements. These welding elements have been grouped as a different component (Figure 4.17) in purpose for fatigue analysis.

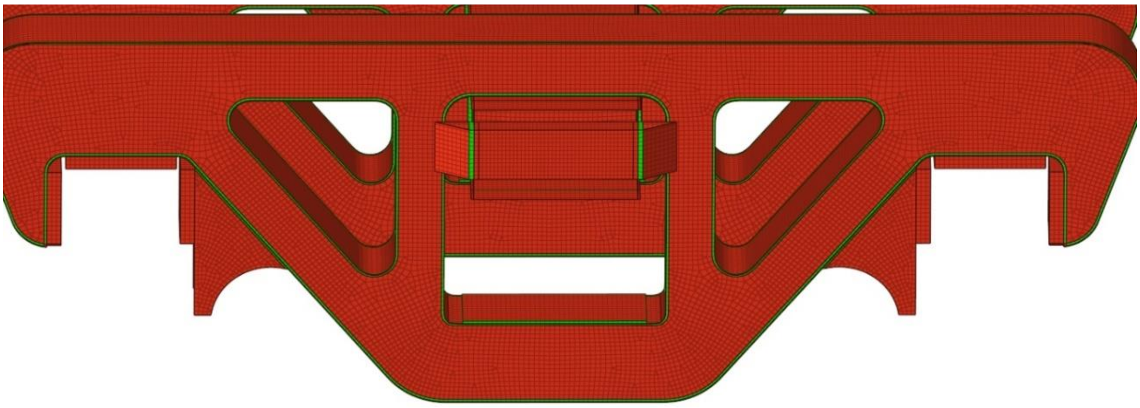

Figure 4.17 : Weld elements (green)

Bogie springs that connected bolster and side frames modeled with SPRING2 elements (Figure 4.18).

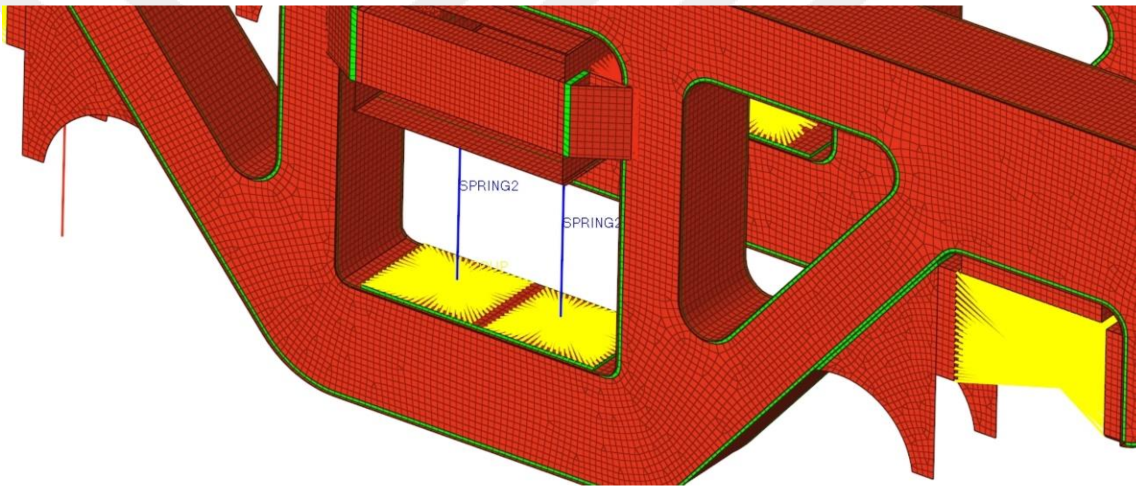

Figure 4.18 : Spring elements (green)

Pivot, wheels and axle boxes modeled as rigid elements with eligible degree of freedom connections (Figure 4.19).

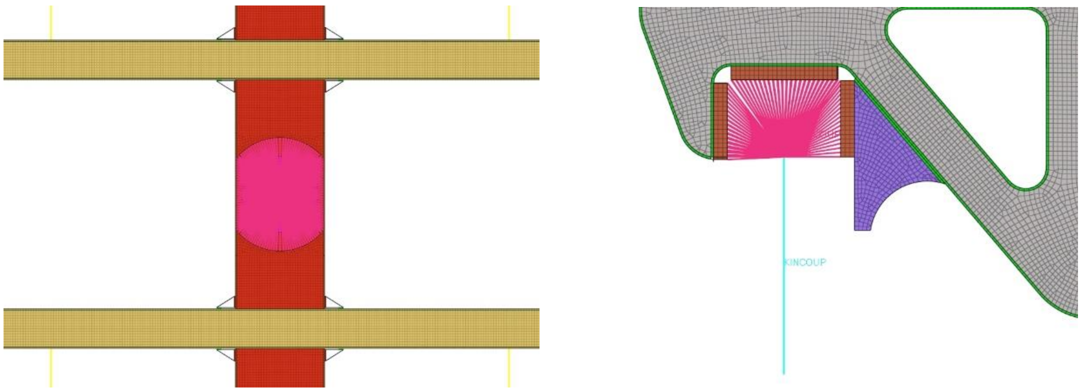

Figure 4.19 : Pivot and axle boxes model as rigid elements

Wheel modeled with rigid element, and axles modeled with beam element(B33). A point mass attached at midpoint of beam. Wheel weigth modeled with this mass on node, for gravity loads in analysis (Figure 4.20).

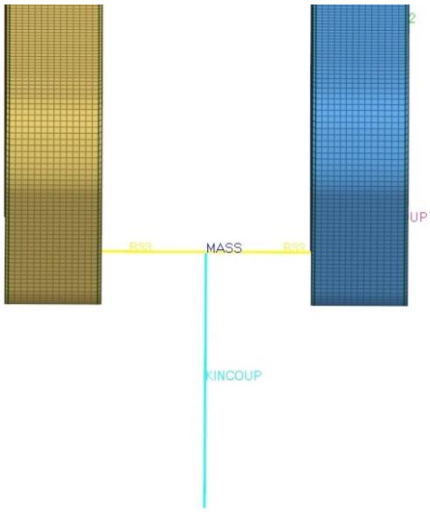

Figure 4.20 : Axle and wheels model as rigid elements

A coupling-nonlinear spring-coupling system has been modelled as the possible contact connection between the frames and the supports.That spring model response when loaded with positive forces on contact direction, and it is irresponsive when loaded negative forces on contact direction.

Boundary conditions applied to wheels, at the node which is connecting to rail (Figure 4.21). That boundary conditions is variable depends on the load cases.

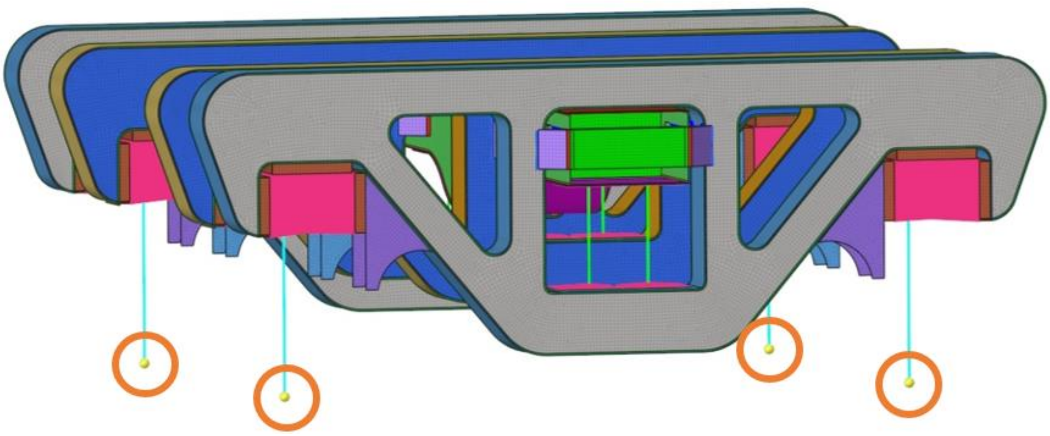

Figure 4.21 : Mesh of bogie and boundary condition nodes of wheels (orange)

4.5 Finite Element Analysis of Inner Axle Box

Second part of model creation is modeling axle box. Inner axle box is part which blocking relative motion of frames and wheelsets. It is consisting 7 parts in finite element model. Inner and outer housing, roller-bearing, the part which connecting inner frame , cover, springs and lock part (Figure 4.22).

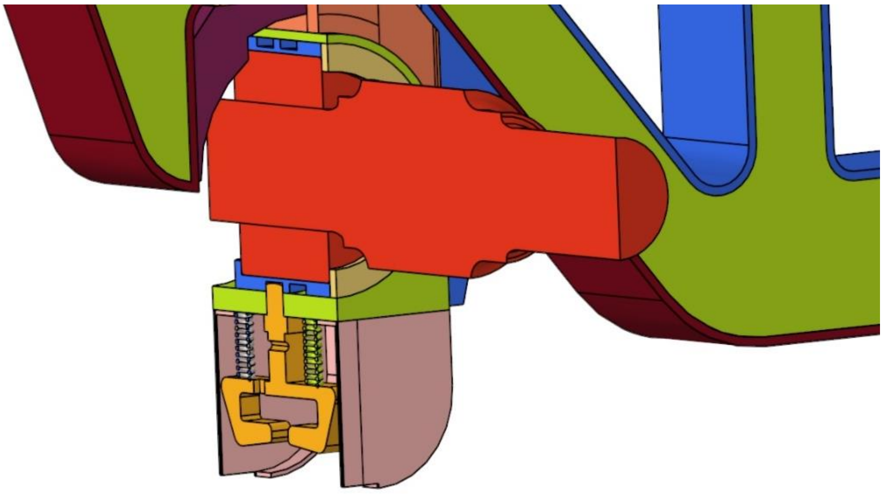

Figure 4.22 : 3D Geometry of inner axle boxes

The axle modeled as a rigid element in that analysis Screws of cover modeled with beam and rigid elements. Springs connected to hex elements of lock part with rigid elements (Figure 4.23).

Finite element model of axle box contains hex-elements mostly. Characteristic element length is 3.21mm.

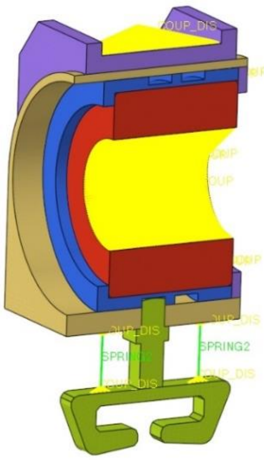

Figure 4.23 : Finite element mesh of inner axle boxes

All axle box elements constituted with 3D elements, Two types of elements are used in modeling, C3D6 for prism elements and C3D8R for hex elements (Figure 4.24).

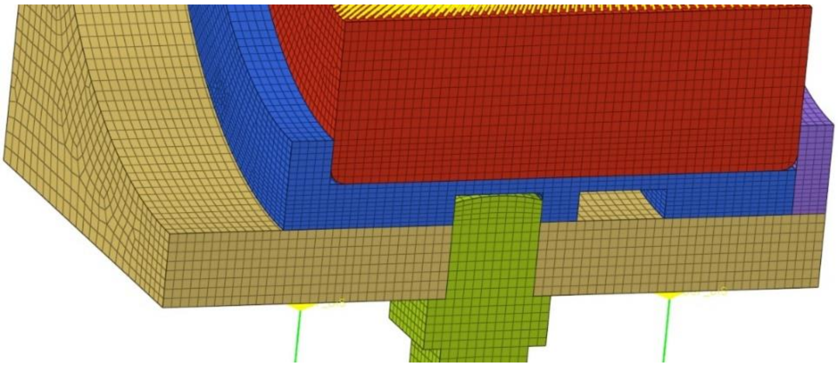

Figure 4.24 : Mesh elements

There is 26 contact surface and 39 contact groups for contact modeling in the analysis (Figure 4.25, Figure 4.26 , Figure 4.27). This surfaces and groups made by manually due to solve more accuracly.

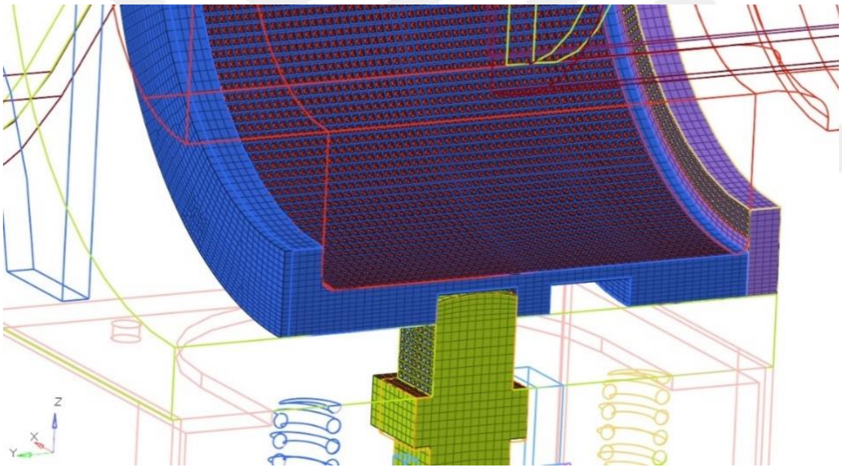

Figure 4.25 : Contact surfaces and geometry

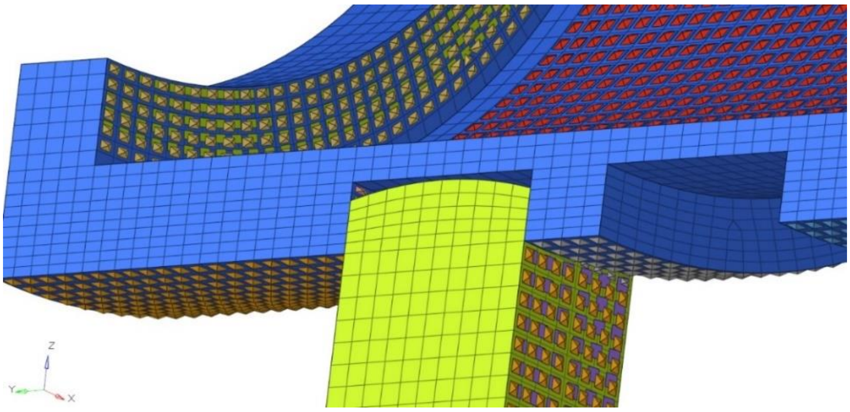

Figure 4.26 : Contact surfaces (below)

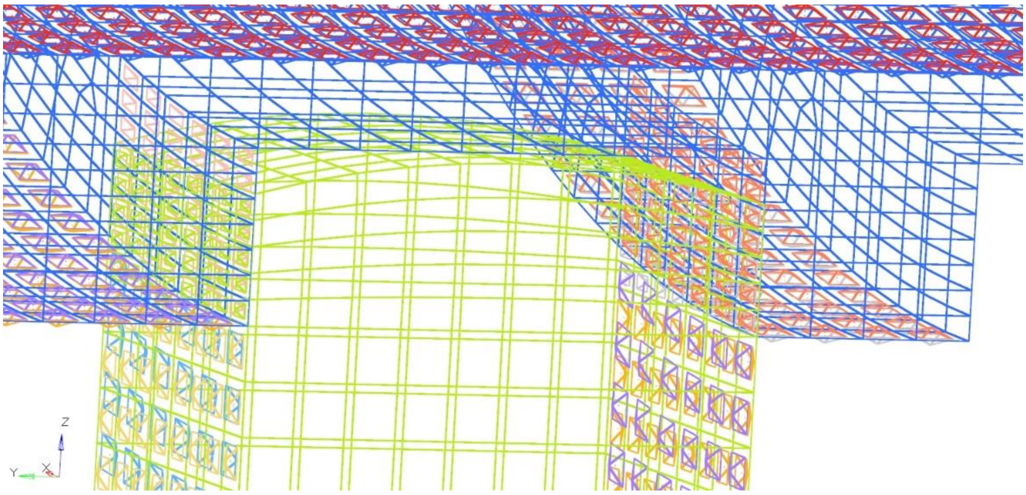

Figure 4.27 : Contact surfaces (lock part)

Screws connects the cover and the inner housing. They are modeled with 1D beam element B33 and connected to other parts with rigid elements (Figure 4.28).

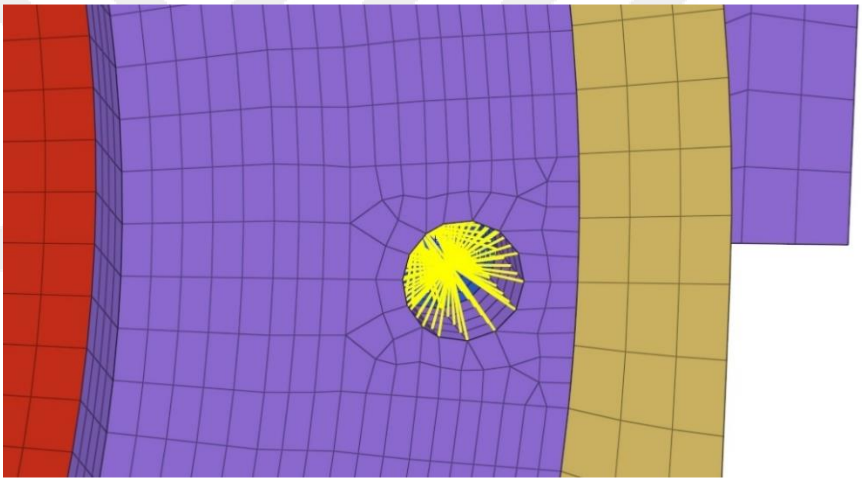

Figure 4.28 : Screw models with beam and rigid elements

The analysis of inner axle solved with x-plane symmetry boundary conditions. Forces used in the analysis recieved from solution of frame analysis, and applied to reference nodes of the model.

4.6 Fatigue Analysis with LIMIT CAE

The fatigue analysis of bogie is solved using LIMIT CAE software. Load cases and cycles calculated with **EN 13749** standart. All weld regions on the bogie modeled manually. At first, the finite element model of bogie with weld element sets, imported to LIMIT (Figure 4.29).

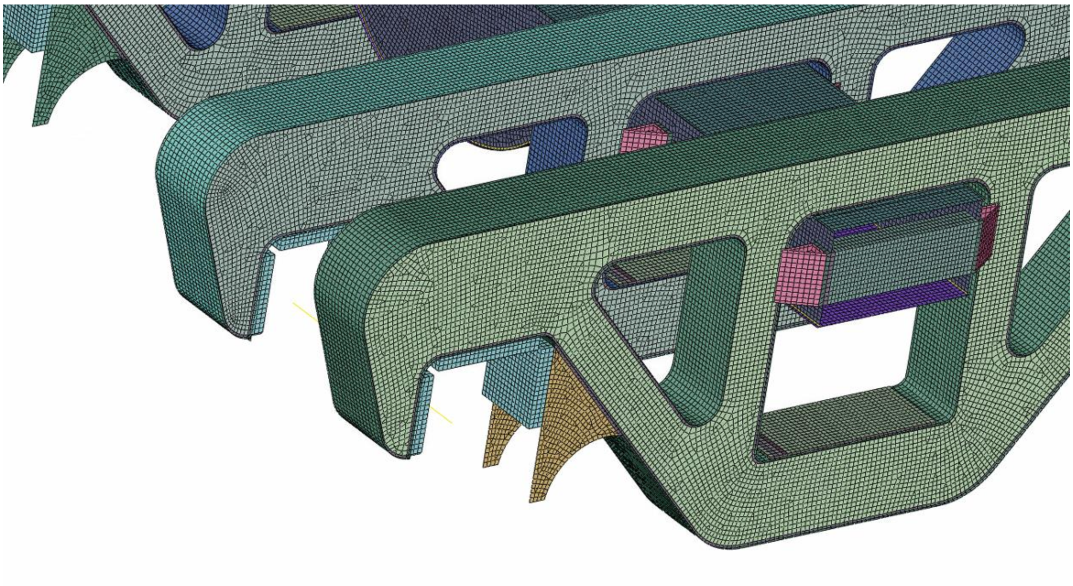

Figure 4.29 : Finite element model of bogie in LIMIT-CAE

Different weld regions modeled according to actual weld action in manufacturing of bogie (Figure 4.30).

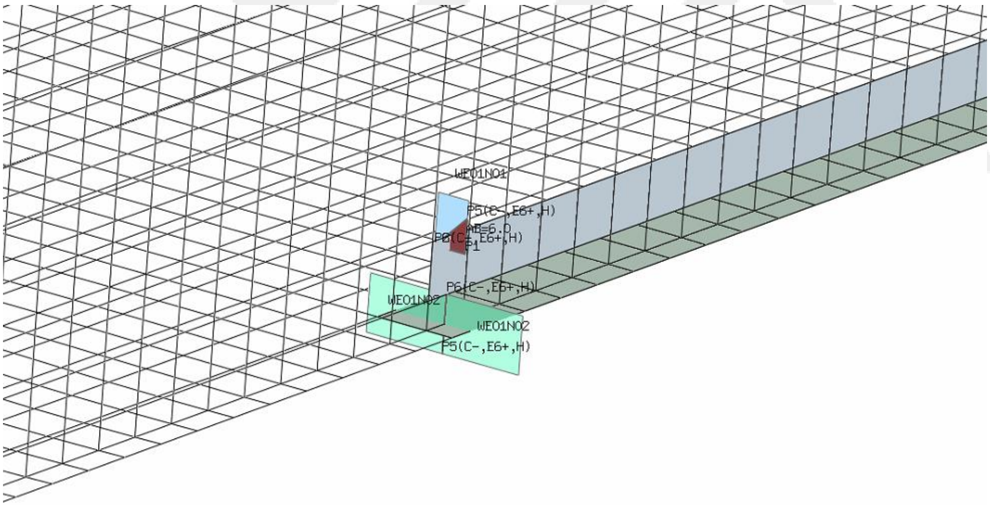

Figure 4.30 : Weld model of a weld region

Weld notch case lines of all weld regions, thickness values and weld details entered as input data in LIMIT weld setup interface. Weld setups defined according to weld type, welding geometry and weld quality. Most of welds of bogie frame are full penetration weld on one side type (Figure 4.31, Figure 4.32). On plates under the bogie springs and nails on the bolster, flange plate welding are used (Figure 4.33). There are in total 31 weld regions and weld setup datas in the model.

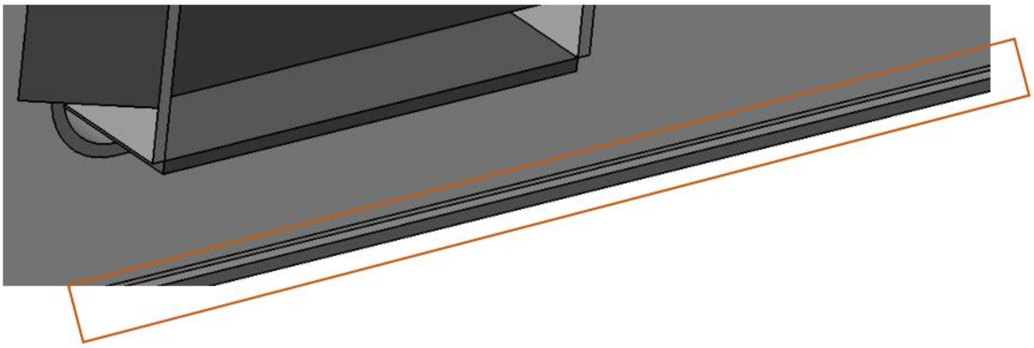

Figure 4.31 : Full penetration weld on one side region

1.3.7	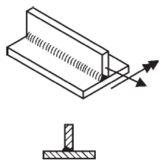	Full penetration weld on one side	Single-bevel weld Single-bevel weld with additional fillet weld Single-bevel weld with backing	10a 1) 10c 1) 10e 1)	Yes	100% NDT-V	CP A	B+
1.3.8						10% NDT-V	CP B and CP C1	B
1.3.9						Visual inspection	CP C2	B-
1.3.10					No	100% NDT-V	CP A	C+
1.3.11						10% NDT-V	CP B and CP C1	C
1.3.12						Visual inspection	CP C2	C-

Figure 4.32 : Notch Case Lines of Full Penetration Weld on One Side

Eligible paralel to weld and perpendicular to weld notch case lines datas selected from **DVS 1612**, and written as an input to the interface. These notch case lines are depending on the weld quality and force direction (Figure 4.32).

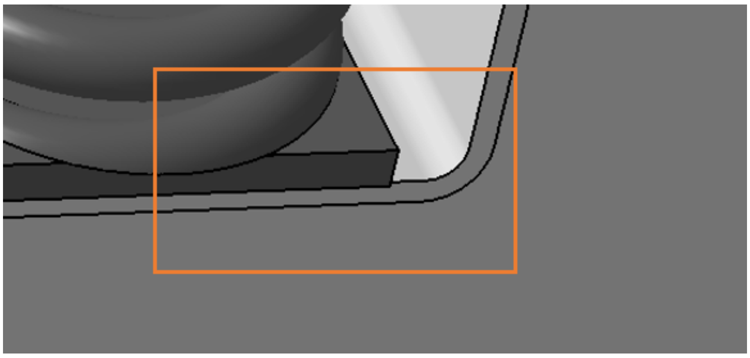

Figure 4.33 : Welds on plates under the bogie springs

Joint and weld type					Type and scope of inspection	Weld performance class according to DIN EN 15085-3	Notch case line	Remarks
Structural detail	Description	Weld type	Weld No. according to DIN EN 15085-3	Post-weld treatment of weld surface				
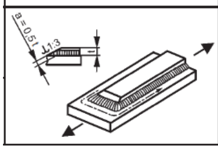	Welded-on flange plate, fillet welds with post-weld treatment and flange plate processed at the front faces	Fillet weld respectively lap seam weld	13e	Yes	10% NDT-S	CP B CP C1	E1+	
					Visual inspection	CP C2	E1	

Figure 4.34 : Notch case lines of welded-on flange plates

Load cases and cycles calculated according to **EN 13749**. The load cases consists of the repetition of cycles based on vertical and transverse forces.

The vertical loads, applied on pivot;

- A static component: $F_{zp} = F_z(1-\alpha)$
- A dynamic component: $F_{zpd} = \pm \beta F_z(1-\alpha)$

The vertical loads, applied on each sidebearer (alternately);

- A quasi-static component: $F_{z1qs} = F_{z1qs} = \pm \alpha F_z$
- A dynamic component: $F_{z1d} = F_{z2d} = \pm \beta F_z$

Transverse loads are applied the pivot;

- A quasi-static component $F_{y1qs} = F_{y2qs} = \pm 0.05F_{z + m*g}$
- A dynamic component $F_{y1qs} = F_{y2qs} = \pm 0.05F_{z + m*g}$

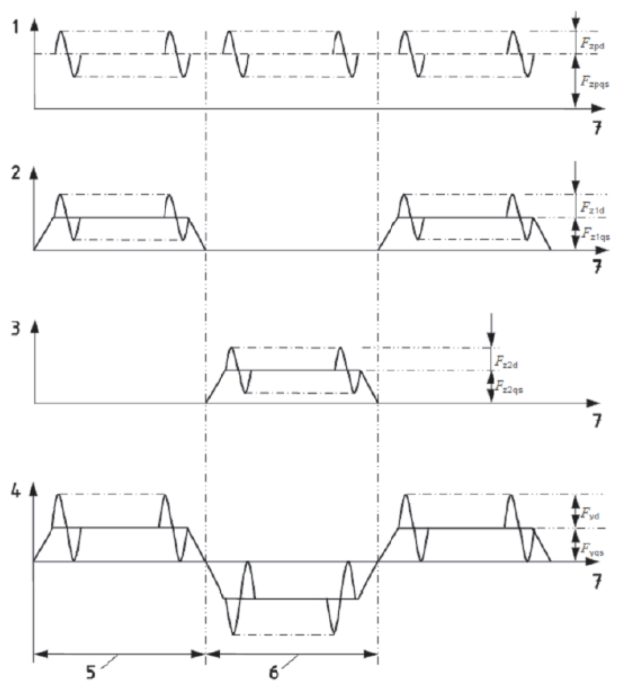

Figure 4.35 : Variation of vertical and transverse forces with respect to time[19]

Cycles in the analysis are consisting 3 parts.; the first part is $6*10^6$ cycle with static, quasi-static and dynamic loads, second part is $2*10^6$ cycle with static, 1.2*quasi-static and 1.2*dynamic loads, and the third part is 1.4*quasi-static and 1.4*dynamic loads (Figure 4.35). Fatigue Dynamic Test Loading Sequence can be seen in Figure 4.36.

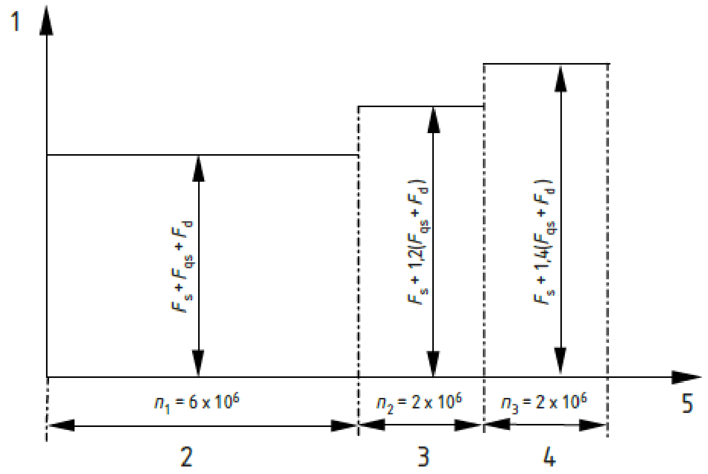

Figure 4.36 : Fatigue dynamic test loading sequence [19]

The notch case lines which imported from **DVS 1612**, are applicable for $2x10^6$ cycles. Load cases from **EN 13749** standart has $10x10^6$ cycles.

For this situation, stress scaling calculation method used in the fatigue analysis. This method is based on the finding of the equivalent stress value(σ_{sc}) from normal stress value(σ_i) with help of slope of fatigue strength curve(m) according to EN1993-1-9 (Figure 4.37). The equivalent stress value is scaled from normal stress values in static analysis with calculation below, for simulating the same fatigue effect with reducing the cycle rate.

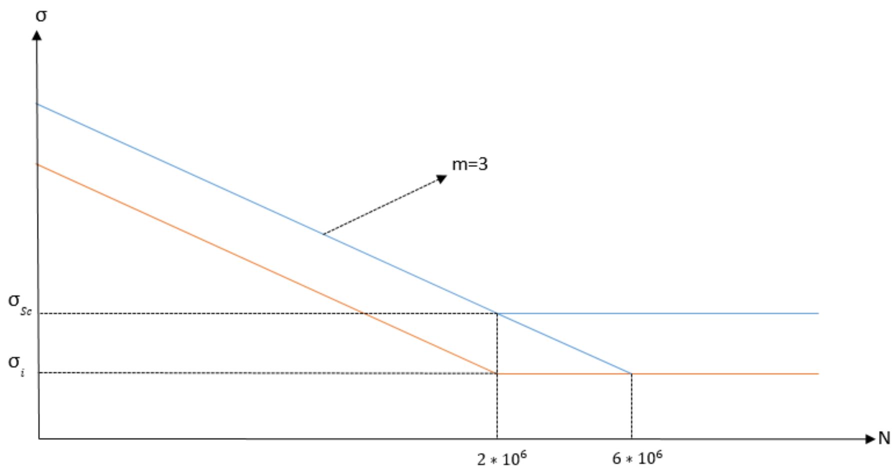

Figure 4.37 : Stress scaling

$$\frac{\sigma_{sc}}{\sigma_i} = \frac{(6 * 10^6)^{1/3}}{(2 * 10^6)^{1/3}}$$

$$F_S = 224kN$$

$F_{qs} = 96kN$

$F_d = 96kN$

$$\frac{224 + (192 * 1.2)}{416} = \frac{(N_1)^{1/3}}{(2 * 10^6)^{1/3}}$$

$$\frac{224 + (192 * 1.4)}{416} = \frac{(N_2)^{1/3}}{(2 * 10^6)^{1/3}}$$

$N_1 + N_2 + 2 * 10^6 = 11.6 * 10^6$cycles

Stress scaling factor;

$$\frac{(11.6 * 10^6)^{1/3}}{(2 * 10^6)^{1/3}} = 1.81$$

Table 4.4 : Fatigue Load Cases

Force	Value	Unit	Coefficients	Value	Unit	Reference to Standards
Fz	400	[kN]	α	0.2	-	EN 13749: 2011, F.3.3.2, Page 41
m^+	4.5	[ton]	β	0.3	-	EN 13749: 2011, F.3.3.2, Page 41
Types of Forces	**Location**	**Types of Components**	**Equation**	**Value**	**Unit**	**Standards**
Vertical Loads	For the Pivot	Static Component - F_{zp}	$F_{zp} = F_z(1-\alpha)$	320	[kN]	EN 13749: 2011, G.6, Page 48
		Dynamic Component - F_{zpd}	$F_{zpd} = \pm \beta F_z(1-\alpha)$	+- 96	[kN]	EN 13749: 2011, G.7, Page 48
	For the Sidebearer	Quasi Static Component - F_{z1qs} or F_{z2qs}	$F_{z1qs} = F_{z2qs} = \pm \alpha F_z$	80.00	[kN]	EN 13749: 2011, G.8, Page 48
		Dynamic Component - F_{y1d} or F_{y2d}	$F_{y1d} = F_{y2d} = \pm \beta Fz$	+- 24	[kN]	EN 13749: 2011, G.9, Page 48
Transverse Loads	Applied to Each Axle	Quasi Static Component - F_{y1qs} or F_{y2qs}	$F_{y1qs} = F_{y2qs} = \pm 0.05F_z + m^+g$	22.21	[kN] [kN]	EN 13749: 2011, G.10, Page 48
		Dynamic Component - F_{y1d} or F_{y2d}	$F_{y1d} = F_{y2d} = \pm 0.05F_z + m^+g$	+- 22.21	[kN] [kN]	EN 13749: 2011, G.11, Page 48

5. RESULTS

5.1 Results of Frame Finite Element Analysis

All 27 load cases results were analyzed with ABAQUS, after the solution of model (Figure 5.1).

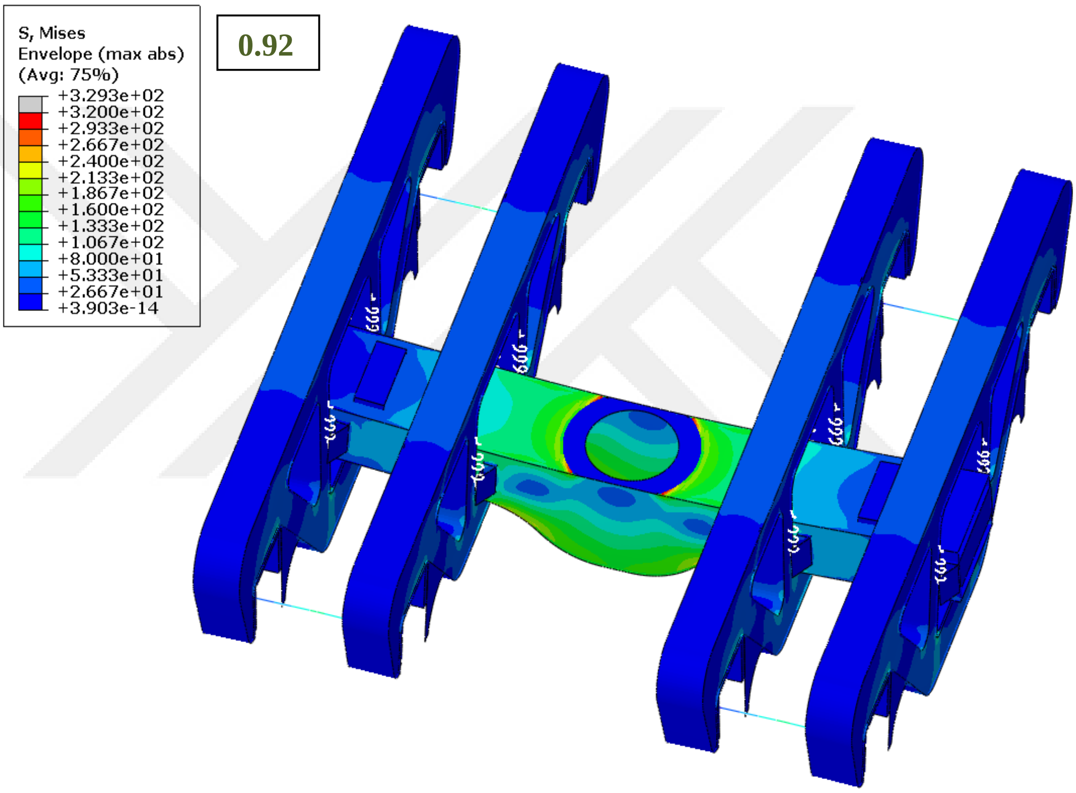

Figure 5.1 : LC01 Von Mises stresses

As a result of the first analyzes, it was observed that some regions had high stress values in some load cases and were at risk. Thereafter, some improvement was made in areas at risk. These improvements responded positive results and eliminated the dangers in these load cases. The final shape of the bogie frame, which is intended to be produced from S355 steel with a yield strength of 355MPa, has no regions exceeding the yield limit value. The 0.92 value is ratio of max stress in analysis and yield stress value of the material.

Improvements made at Bogie;

- In LC01 load case, the bolster has high stress values at the bottom. Subsequently, a more durable form was created by increasing the radius values of the curves at the bottom and the high stresses was eliminated (Figure 5.2).

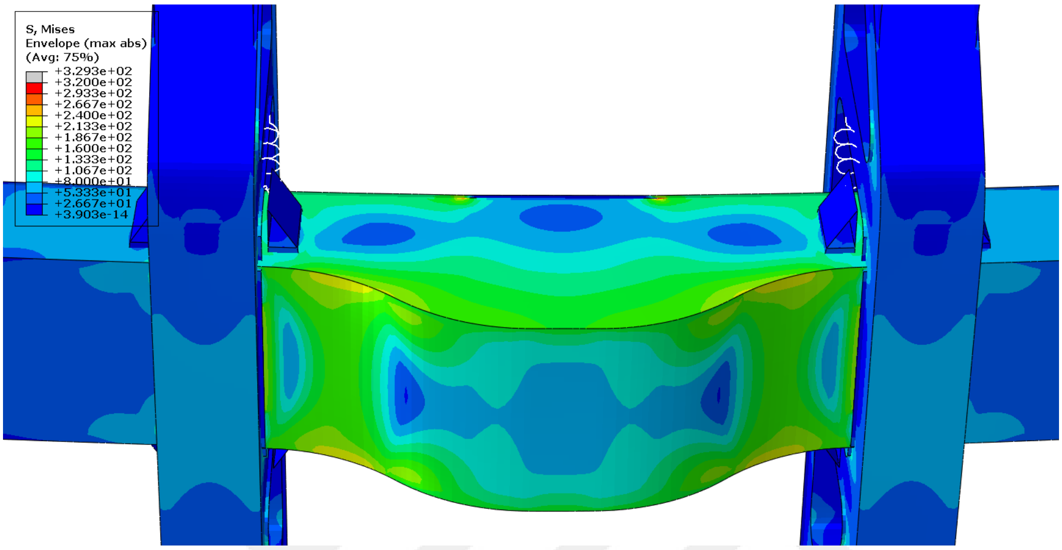

Figure 5.2 : Bottom view of bolster

- In LC06 load case, high bending stress is detected in the inner side frame which carries the whole transverse load. Then, the wall thickness of the plates is increased, With this change, it did not exceed the yield limit even at the most difficult transverse force (Figure 5.3).

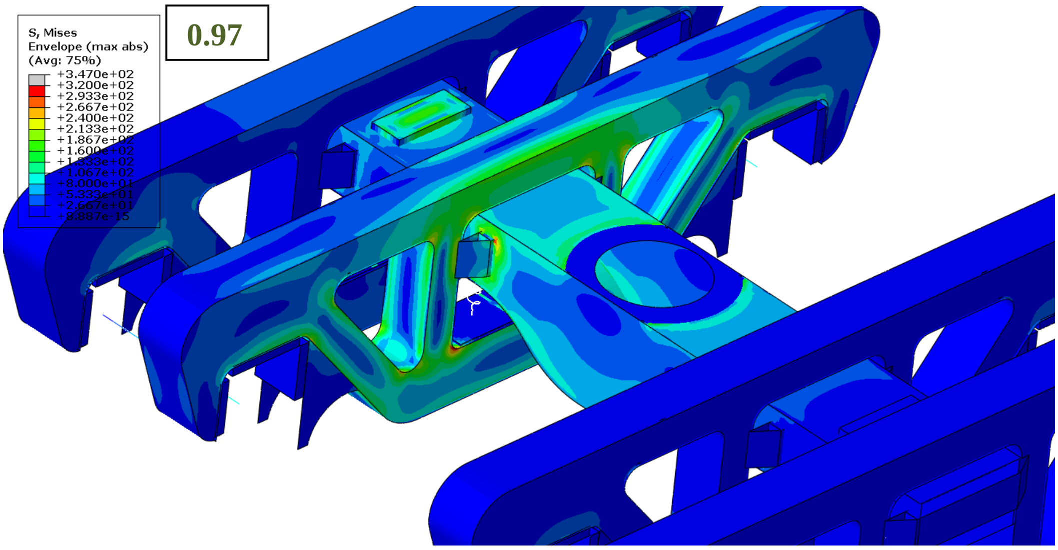

Figure 5.3 : Bogie under transverse force

- In LC06 load case, high bending stress is detected in the inner side frame due to spring plates. Then, the thickness of the plates is reduced at sides of plates. After this change, the stresses at sides of plates are below the yield limit (Figure 5.4).

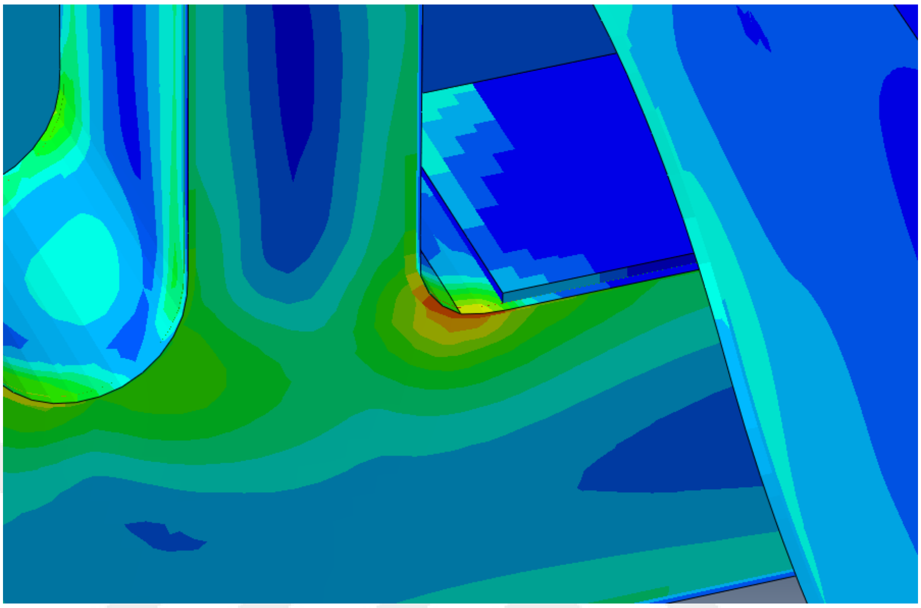

Figure 5.4 Stresses on plates under the springs

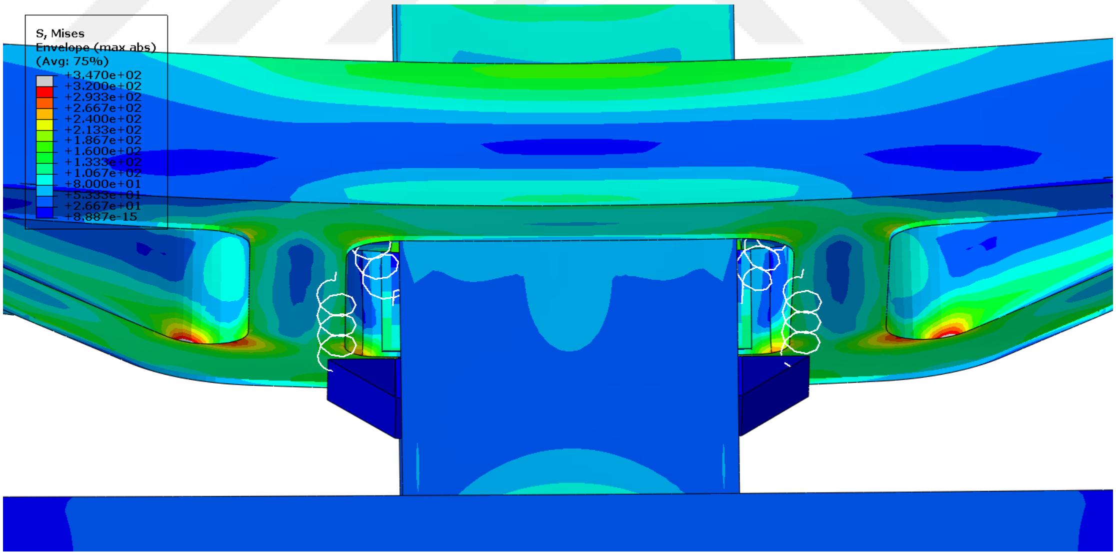

Figure 5.5 : LC06 Von Mises stresses

- In LC08 load case, a very high stress was observed in the nail areas of the bolster. This problem is solved by placing support parts in bolster, between the nails (Figure 5.6).

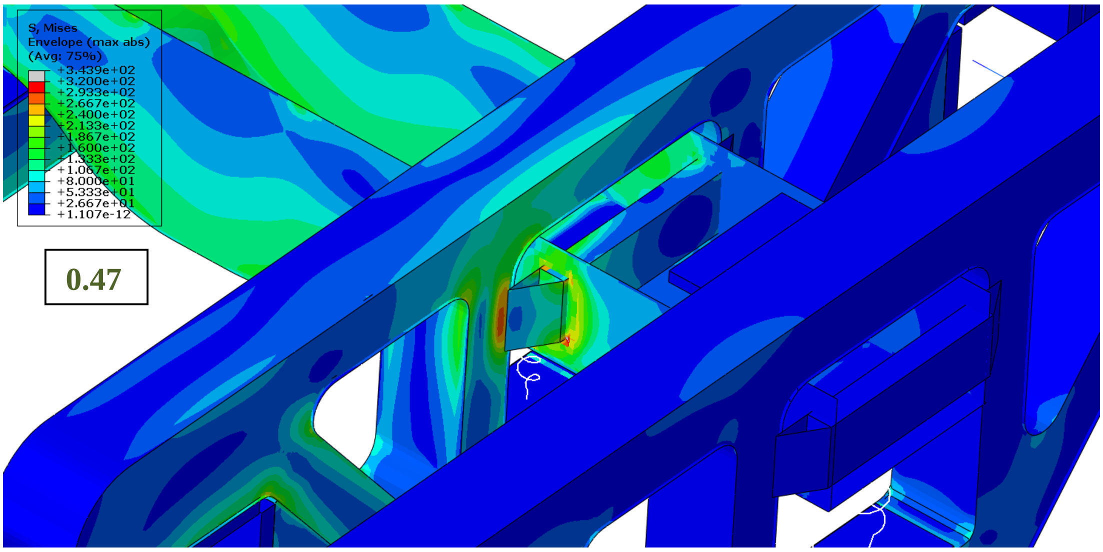

Figure 5.6 : LC08 Von Mises stresses

According all this information, all the stress values in the bogie are below the yield stress limit. Results of all 27 load cases in APPENDIX A.

5.2 Results of Inner Axle Box Finite Element Analysis

Inner axle box analyzed in the LC01 and LC06 load cases which have the highest forces. There is no high stress values in the LC01 load case with the maximum force in the vertical direction (Figure 5.7).

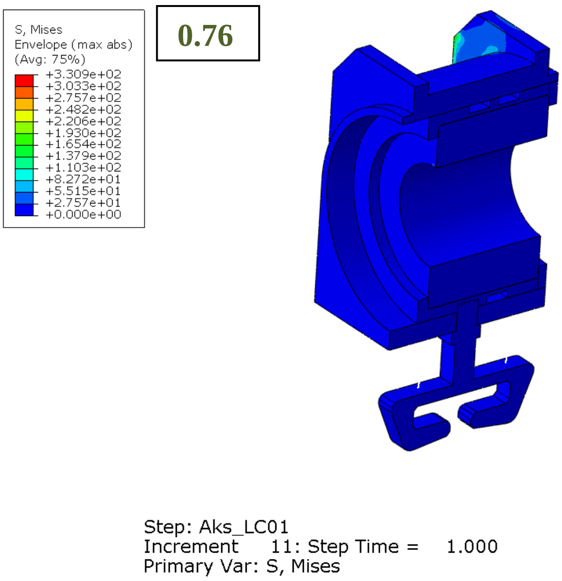

Figure 5.7 : Axle box LC01 Von Mises stresses

In LC06 load case, whole transverse load carried by the locking part (Figure 5.8, Figure 5.9, Figure 5.10). The stress values in the locking part are well below the yield stress limit of the S700 steel in which the axle box is made.

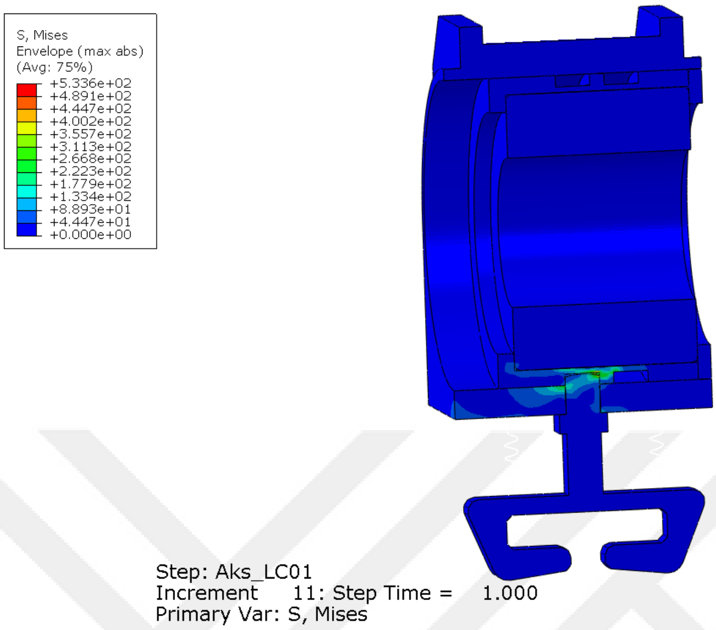

Figure 5.8 : Axle Box LC06 Von Mises stresses

In the results of the analysis, it was found that the lid connected to the screws with inner housing was too much enforced. This problem is solved by mounting the lid on the other side of the inner housing.

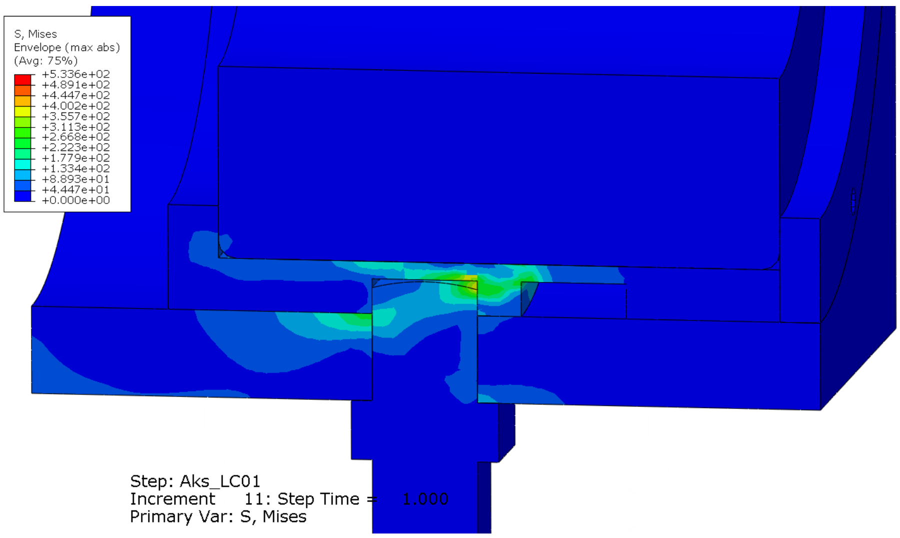

Figure 5.9 : Axle Box LC06 Von Mises stresses

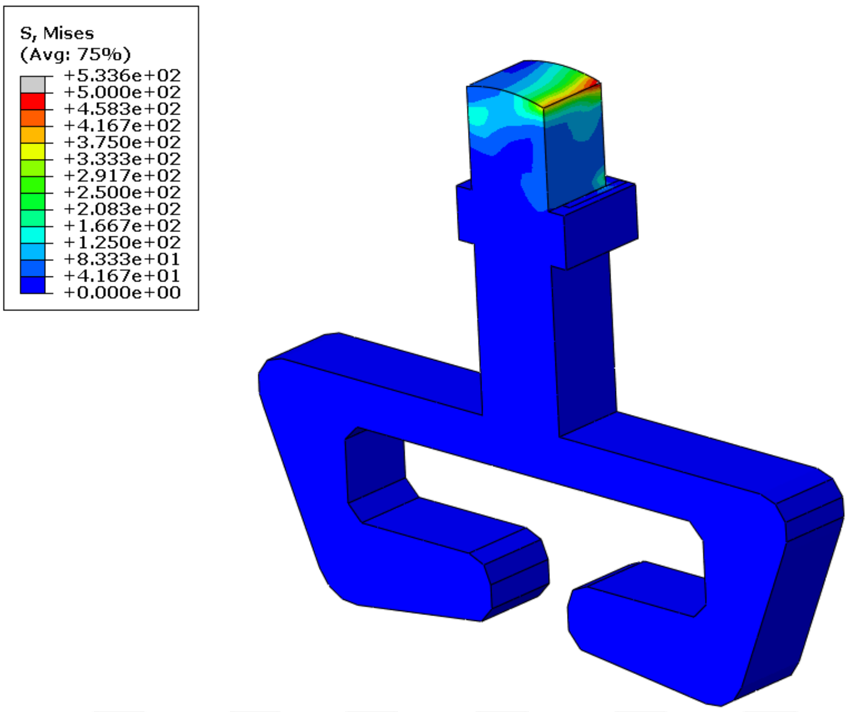

Figure 5.10 : Axle Box LC06 Von Mises stresses

5.3 Results of Fatigue Analysis

The weld fatigue model was analyzed particularly for each weld region (Figure 5.11), considering applicability and geometrical suitability.

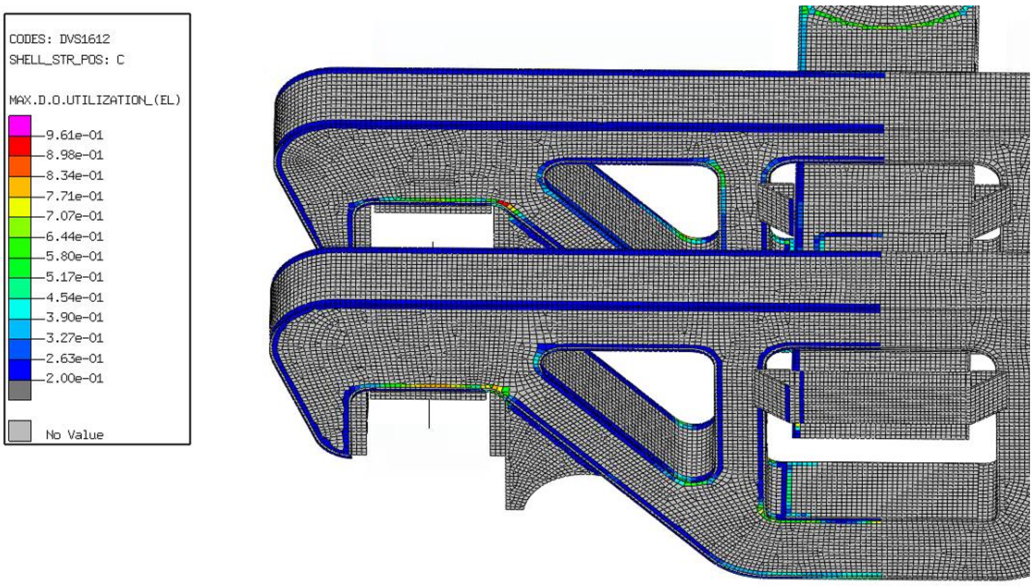

Figure 5.11 : Fatigue analysis of frame

Result of the first analyzes, it was observed that some weld regions were risky, especially spring regions (Figure 5.12).

High bending stress is detected in the inner side frame due to spring plates. Then, the thickness of the plates is reduced at sides of plates. After this change, the stresses at sides of plates are below the yield limit.

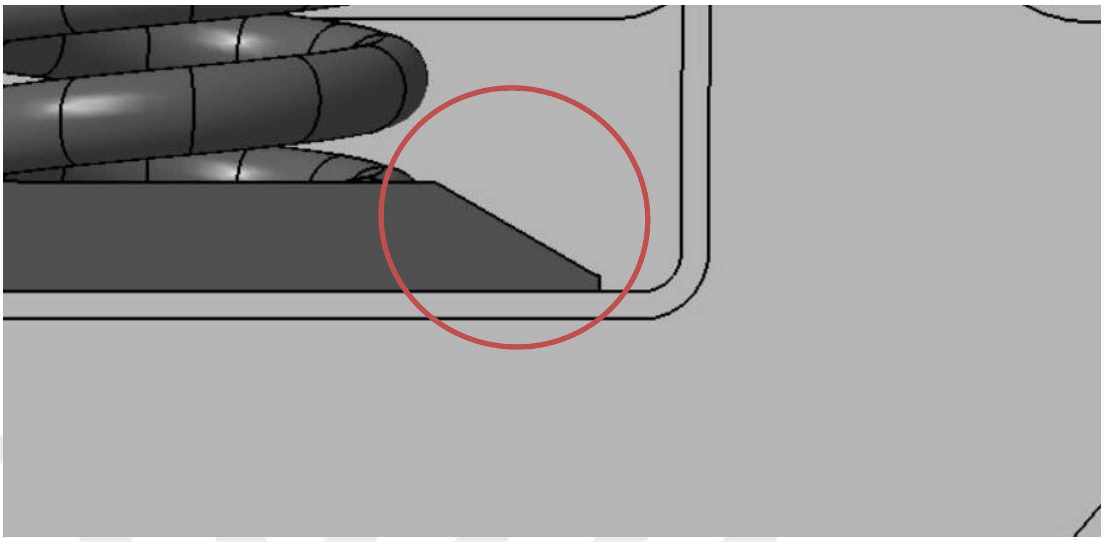

Figure 5.12 Spring plates after improvement.

Some weld regions' weld quality improved with NDT-V (Non-Destructive-Controlling of the Welds) and post-weld treatment of weld surface. With these operations, the notch case lines of the some weld regions is upgraded to "**B**" or "**B+**" value from "**C**" or "**C-**" (Figure 5.13).

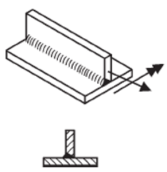	Full penetration weld on one side	Single-bevel weld Single-bevel weld with additional fillet weld Single-bevel weld with backing	10a[1)] 10c[1)] 10e[1)]	Yes	100% NDT-V	CP A	B+
					10% NDT-V	CP B and CP C1	B
					Visual inspection	CP C2	B-
				No	100% NDT-V	CP A	C+
					10% NDT-V	CP B and CP C1	C
					Visual inspection	CP C2	C-

Figure 5.13 : Improve the Weld Quality With NDT-V and Post-Weld Treatment

Thereafter, results of second analysis is succesful, and all weld calculations are under the fatigue damage limit (Figure 5.14, Figure 5.15, Figure 5.16).

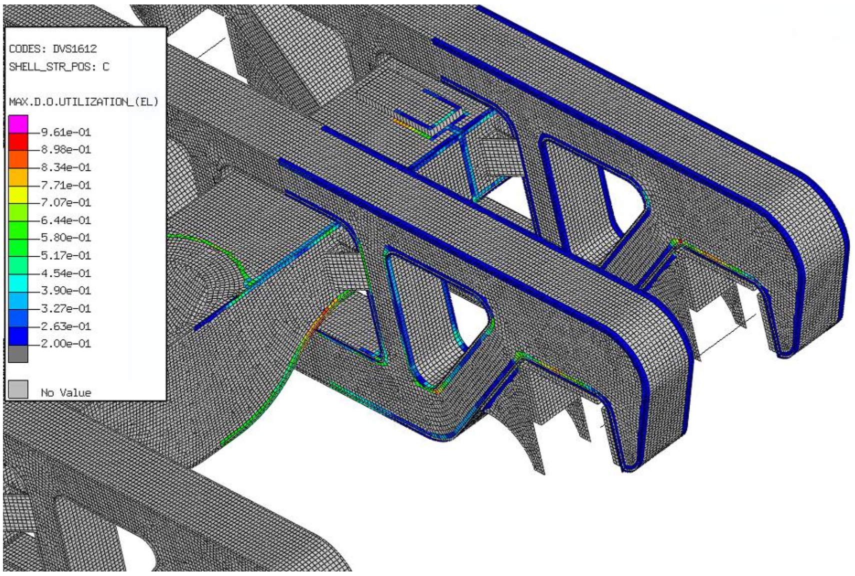

Figure 5.14 : Fatigue analysis of frame

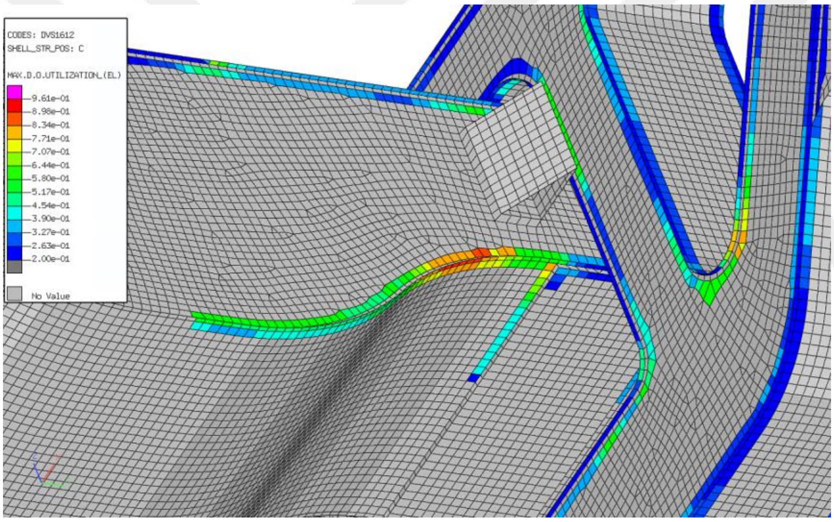

Figure 5.15 : Bolster below welds

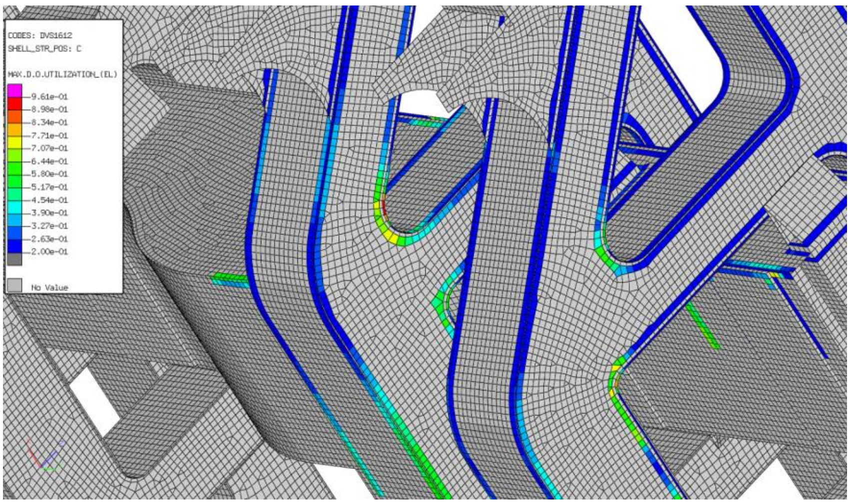

Figure 5.16 : Side frame welds

6. CONCLUSION AND RECOMMENDATIONS

Within the study in this thesis, it is aimed to eliminate the time and energy loss with the design of a bogie which has variable gauge between its wheels. The bogie is appropriate for the working and manufacturing conditions of our country and which is also conforming to the railway system standards. If the necessary conditions are met, this project will make a great contribution to prevent the loss of time and energy loss in the trade route of our country.

With the help of the new design, the change process time on the borderlines will be reduced from days range to hours.

The components of the new concept bogie are designed in accordance with the standards and meet all the requirements in the analytical calculations. The frame of the bogie and the inner axle box were analyzed using the finite element method. After a few structural modeling improvements, it was seen that there was no stress value above the yield stress in all load cases.

The weld fatigue model was analyzed particularly for each weld region, considering applicability and geometrical suitability. After the weld planning of frame, a successful analysis result was obtained.

The new bogie is designed with four side frames and four axles and it is different from bogies currently operating. Therefore, in future studies; a custom made brake system which is accordance with the railway system standards is required.

A simultion of change station can be prepared for analyze the compatibility of the bogie and change stations to be established. After the analyze, a prototype of change station can be manufactured, and the bogie, locking system can be tested on change station.

With a structural optimization process according to the stress distributions of the components, the weight of the bogie can reduce. When doing that optimization project, all finite element analysis static stress results and fatigue analysis results should be considered.

This is a pre-concept project. A prototype of the bogie must be manufactured and must be tested according to standards. With the help of strain-gauges to be used in these tests; stress calculation and comparison of these results with the analytical calculations and the finite element analysis solution will be a good process to verify the modeling. Running analysis and safety assesment can be evaluated with the prototype.

REFERENCES

[1] **Url-1, <**_https://en.wikipedia.org/wiki/Track_gauge_ > date retrieved 23.06.2018.

[2] **Url-2,** <_https://www.flickr.com/photos/scjody_> date retrieved 23.06.2018.

[3] **Khennane, A.** (2006). Introduction to Finite Element Analysis Using MATLAB and Abaqus, CRS Press.

[4] **Reddy, J. N ,** (2006), An Introduction to the Finite Element Method, Mc Graw Hill, USA.

[5] **BS EN 13749** (2011), Railway applications Wheelsets and bogies Method of Specifying the Structural Requirements of Bogie Frames. Retrieved from https://shop.bsigroup.com/ProductDetail/?pid=000000000030270277

[6] **Url-3, <** https://www.railway-technology.com/ date retrieved 03.07.2018.

[7] **Url-4, <**_http://www.railway-technical.com/_ date retrieved 12.08.2018.

[8] **Url-5, <**_http://www.kaykacmakine.com.tr/_ date retrieved 18.08.2018.

[9] **Url-1, <**_https://gurutzpe.com/en/sectors/_ date retrieved 20.08.2018.

[10] **Saeed Moaveni., (**2010), Finite Element Analysis Theory and Application with ANSYS, Pearson.

[11] **BS EN 15827** (2007), Railway Applications Requirements for Bogies and Running Gears. Retrieved from https://shop.bsigroup.com /ProductDetail/?pid =000000000030205141

[12] **BS EN 13103** (2012), Railway Applications Wheelsets and Bogies Non-powered Axles Design Method. Retrieved from https://shop.bsigroup.com /ProductDetail/?pid=000000000030254369

[13] **BS EN 13261** (2009), Railway applications Wheelsets and Bogies Wheelsets Product Requirements. Retrieved from https://shop.bsigroup.com /ProductDetail/ ?pid=000000000030217346

[13] **BS EN 13260** (2009), Railway Applications Wheelsets and Bogies Axles Product Requirements. Retrieved from https://shop.bsigroup.com /ProductDetail/ ?pid=000000000030217343

[15] **BS EN 14363** (2005), Railway Applications Testing and Simulation for the Acceptance of Running characteristics of Railway Vehicles Running Behaviour and Stationary Tests. Retrieved from https://shop. bsigroup.com/ProductDetail/?pid=000000000030077264

[16] **UIC CODE 510-4** (2002), Variable-gauge running gear for 1435mm/1520mm and 1668mm Recommendations for bilateral agreements. Retrieved from https://global.ihs.com/doc_detail.cfm?document_name=UIC%20510-4%20%28E%29&item_s_key=00755505.

[17] **Altair University, Academic Program, (**2015) Practical Aspects of Finite Element Simulation A Study Guide. Retrieved September 10, 2018. Available from https://altairuniversity.com/

[18] **A.F. Hobbacher, (**2016)**,** Recommendations for Fatigue Design of Welded Joints and Components Second Edition, Springer.

[19] **DVS 1612** (2014) Design and endurance strength assessment of welded joints with steels in rail vehicle construction. Retrieved from https://global. ihs.com/doc_detail.cfm?document_name=DIN%20DVS%201612&item _s_key=00737109

APPENDICES

APPENDIX A : Load Case Results of Bogie Frame Finite Element Analysis

A. APPENDIX A

LC01

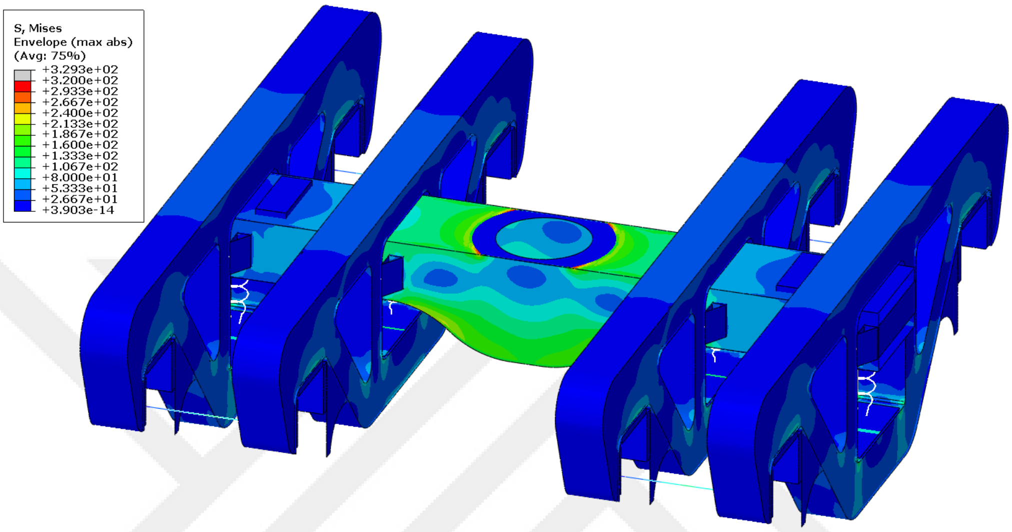

Figure A. 1 : Von Mises Stresses of Load Case 01

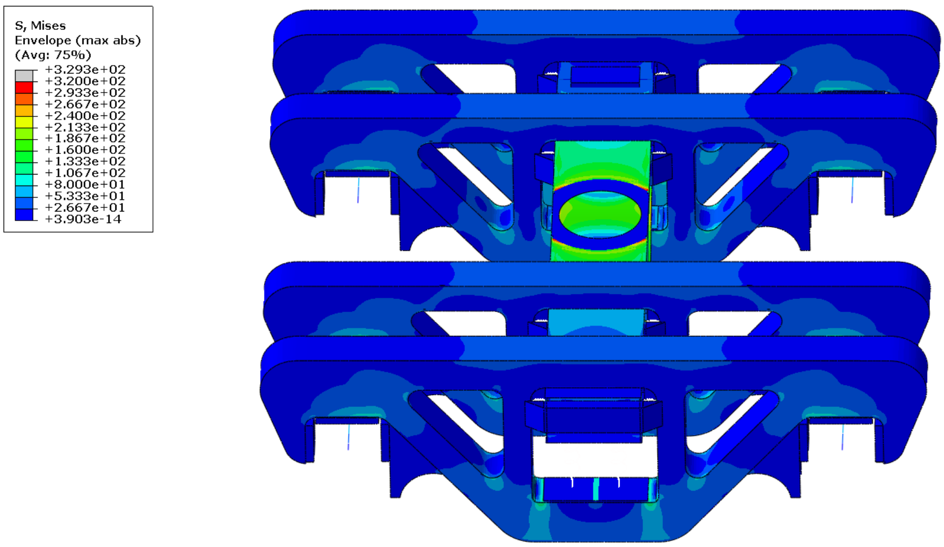

Figure A. 2 : Von Mises Stresses of Load Case 01

LC02

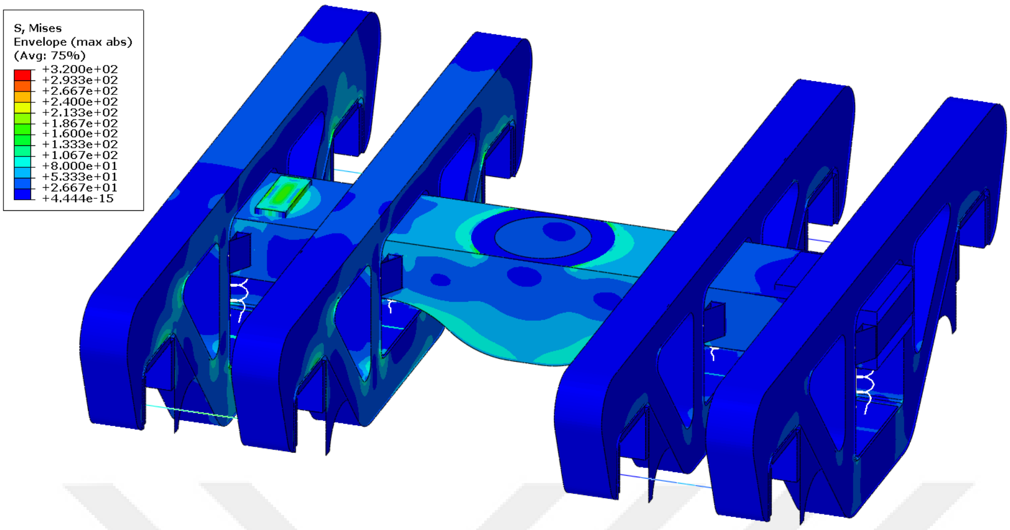

Figure A. 3 : Von Mises Stresses of Load Case 02

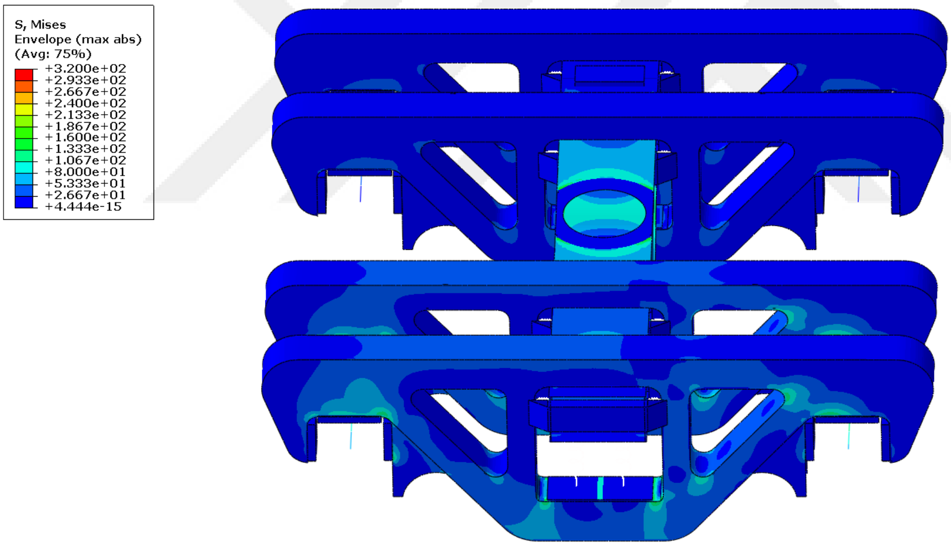

Figure A. 4 : Von Mises Stresses of Load Case 02

LC03

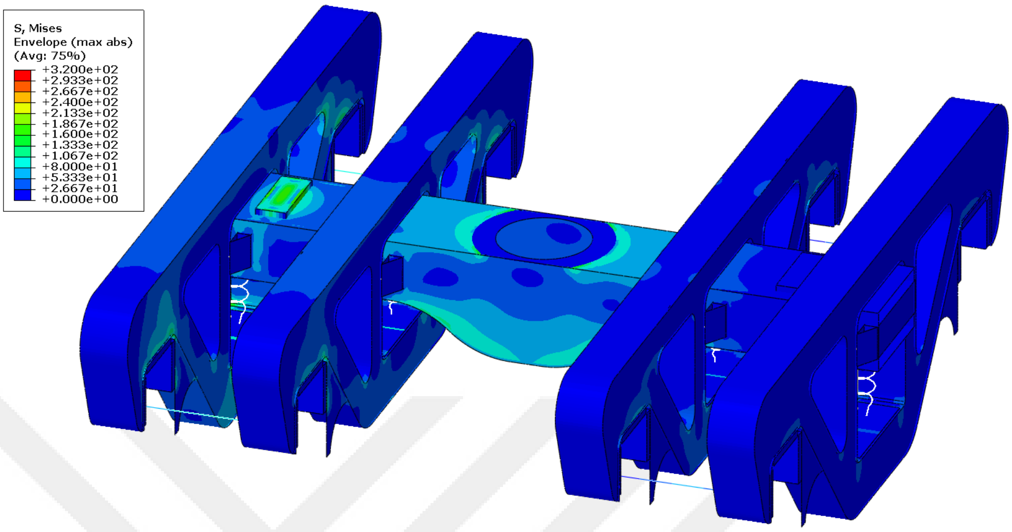

Figure A. 5 : Von Mises Stresses of Load Case 03

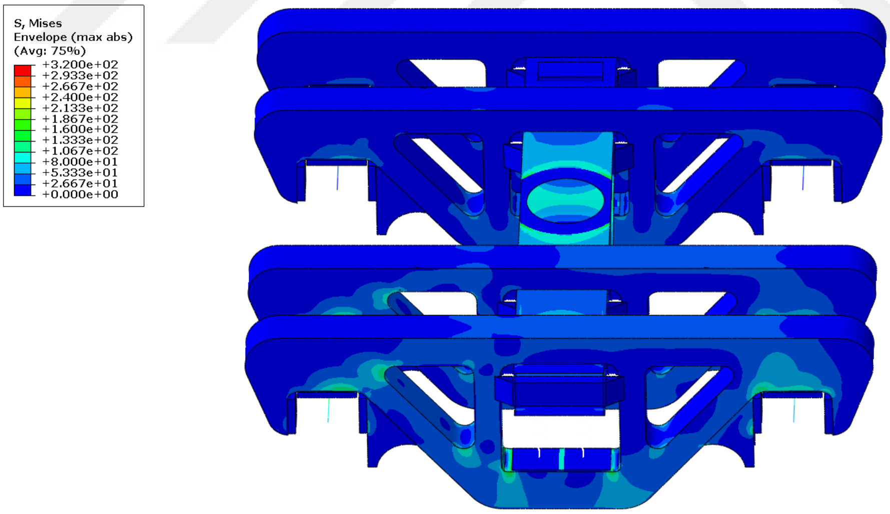

Figure A. 6 : Von Mises Stresses of Load Case 03

LC04

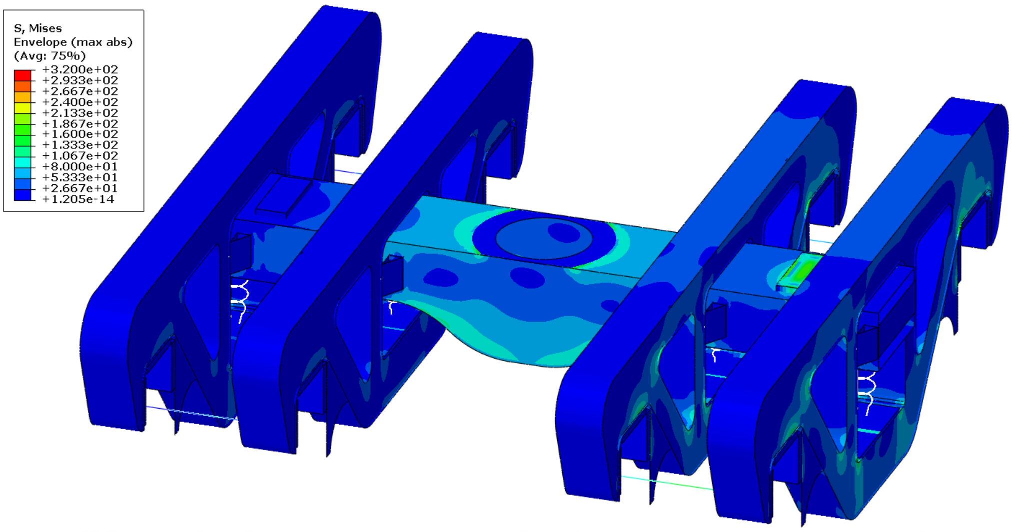

Figure A. 7 : Von Mises Stresses of Load Case 04

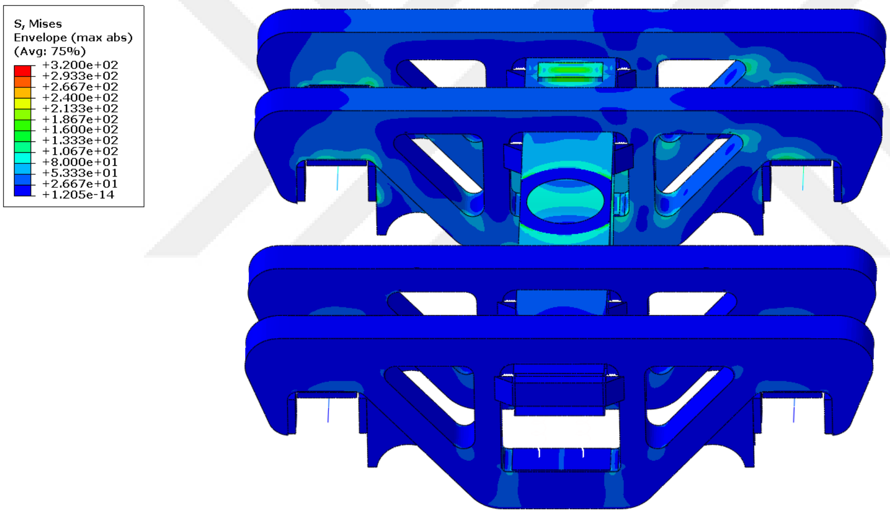

Figure A. 8 : Von Mises Stresses of Load Case 04

LC05

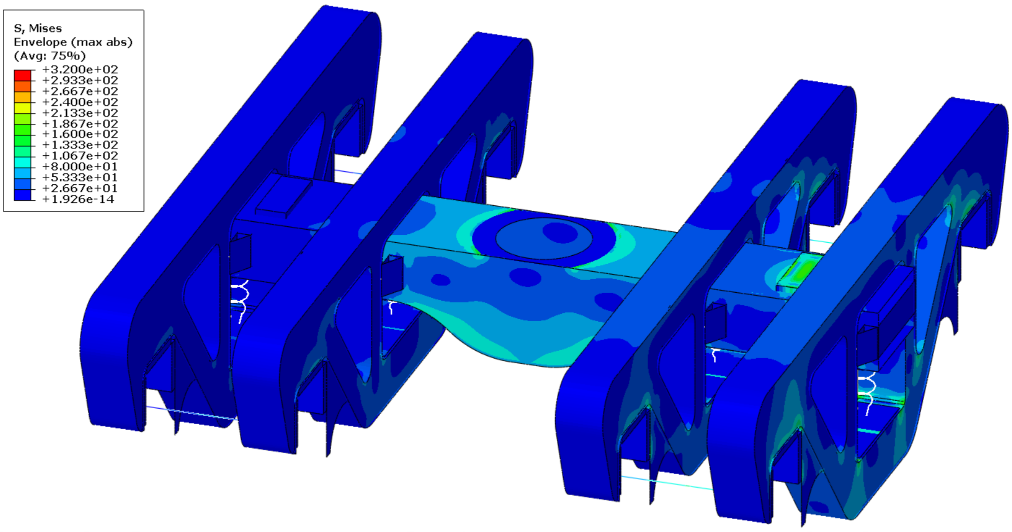

Figure A. 9 : Von Mises Stresses of Load Case 05

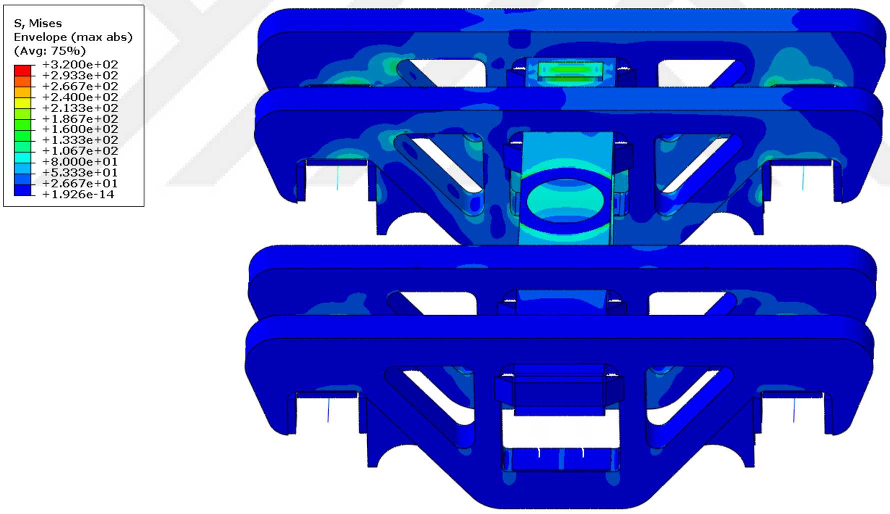

Figure A. 10 : Von Mises Stresses of Load Case 05

LC06

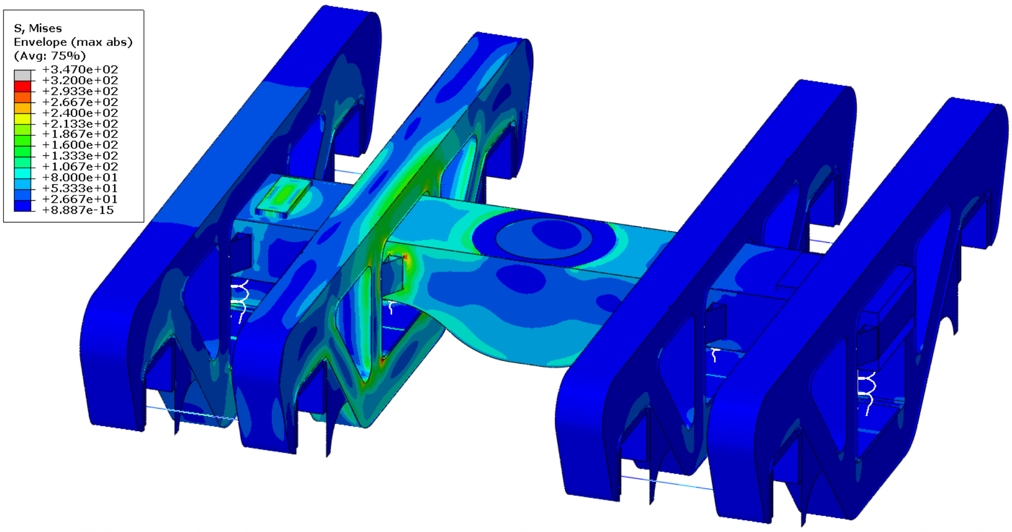

Figure A. 11 : Von Mises Stresses of Load Case 06

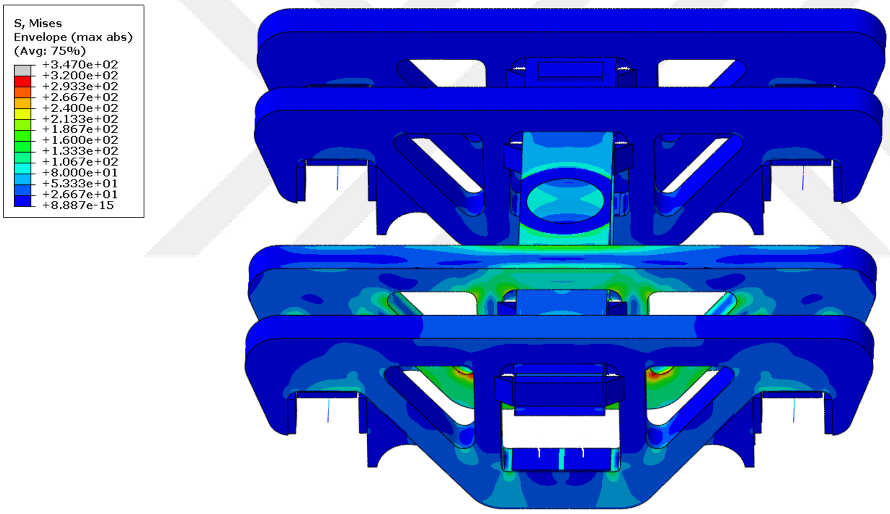

Figure A. 12 : Von Mises Stresses of Load Case 06

LC07

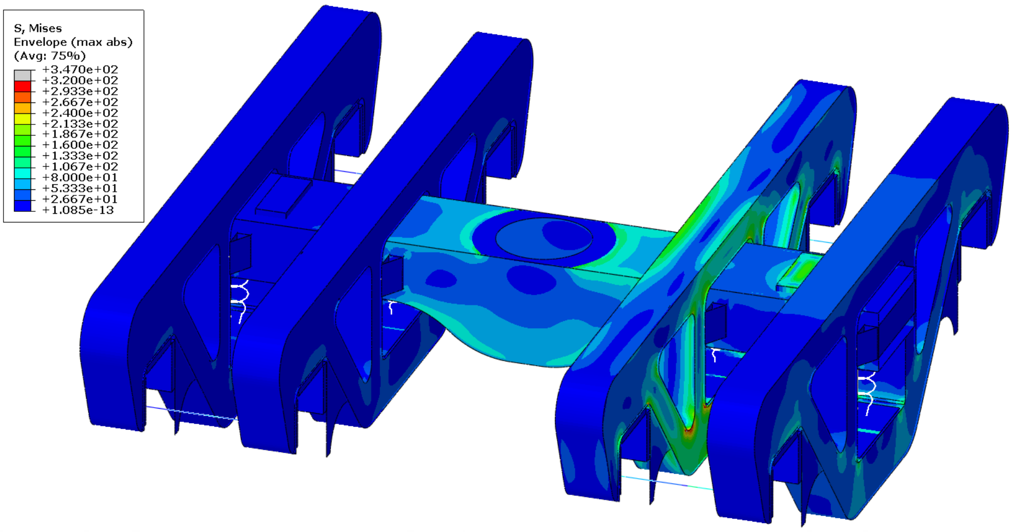

Figure A. 13 : Von Mises Stresses of Load Case 07

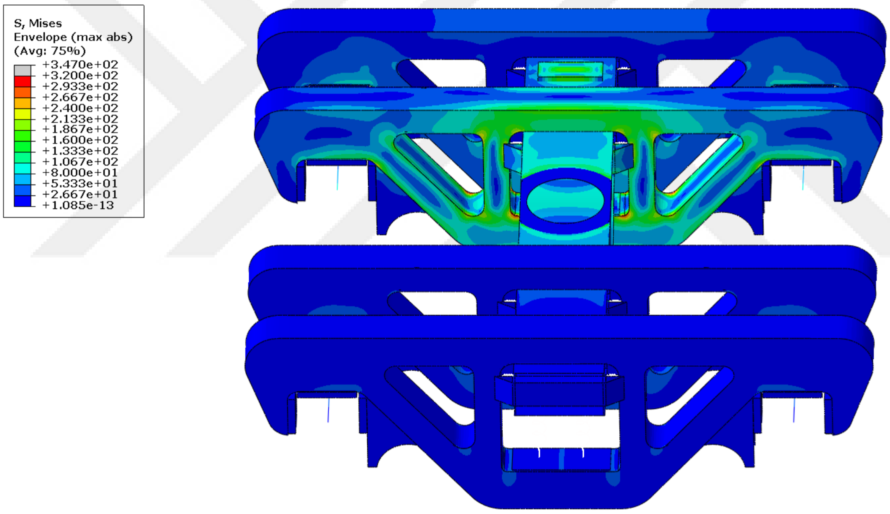

Figure A. 14 : Von Mises Stresses of Load Case 07

LC08

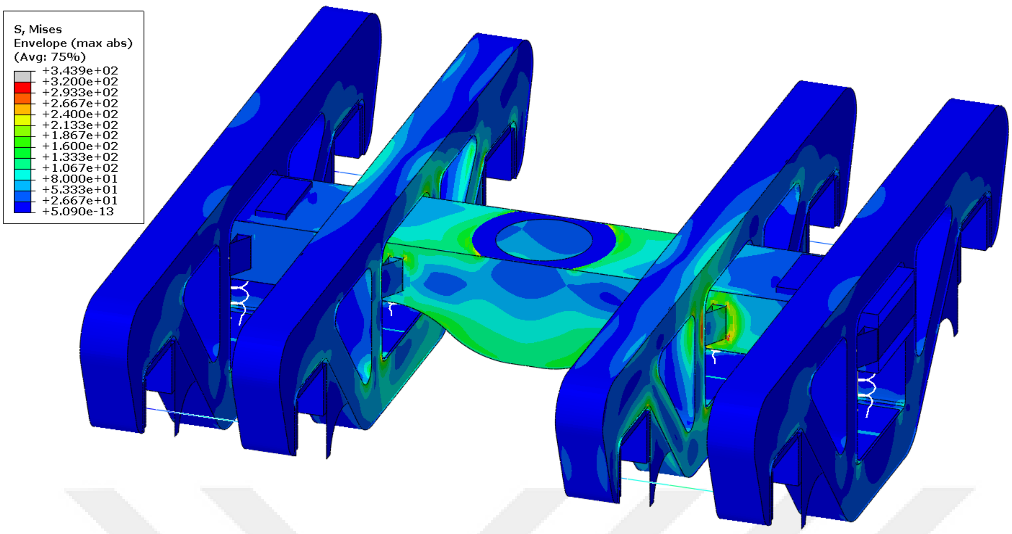

Figure A. 15 : Von Mises Stresses of Load Case 08

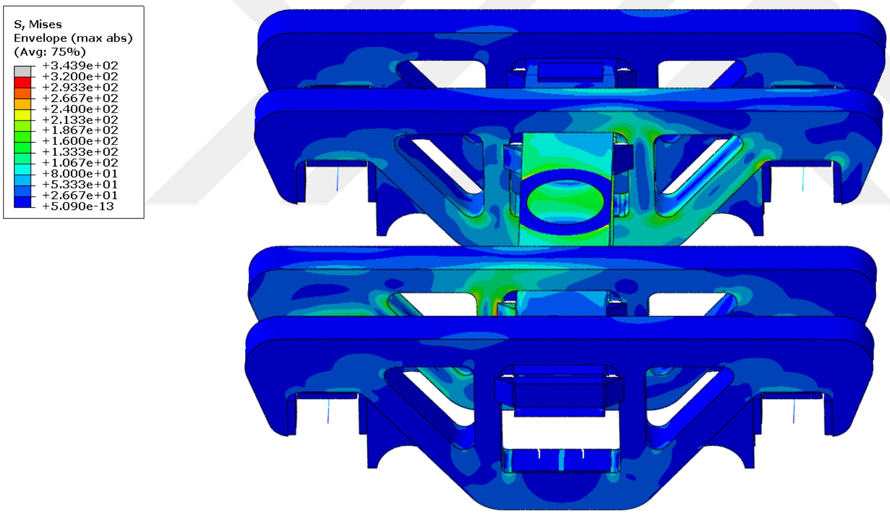

Figure A. 16 : Von Mises Stresses of Load Case 08

LC09

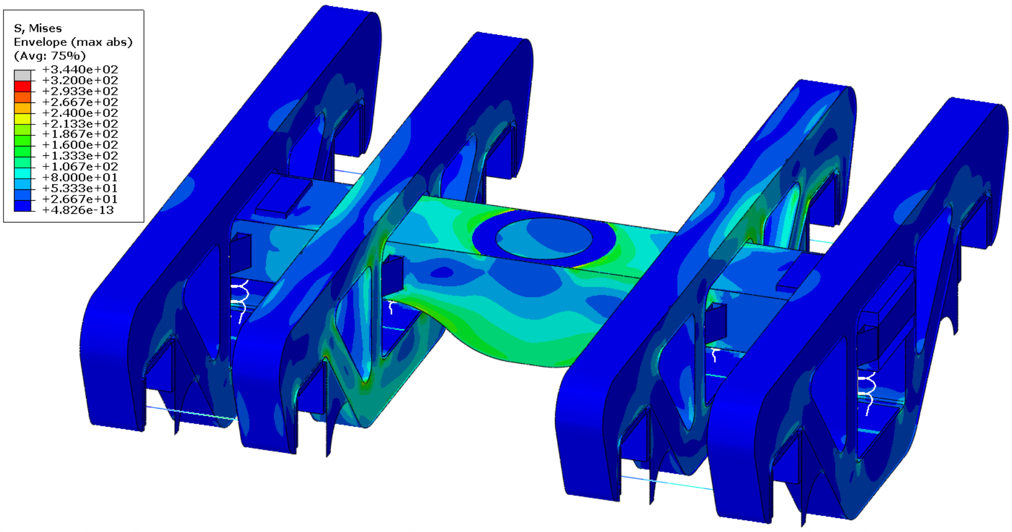

Figure A. 17 : Von Mises Stresses of Load Case 09

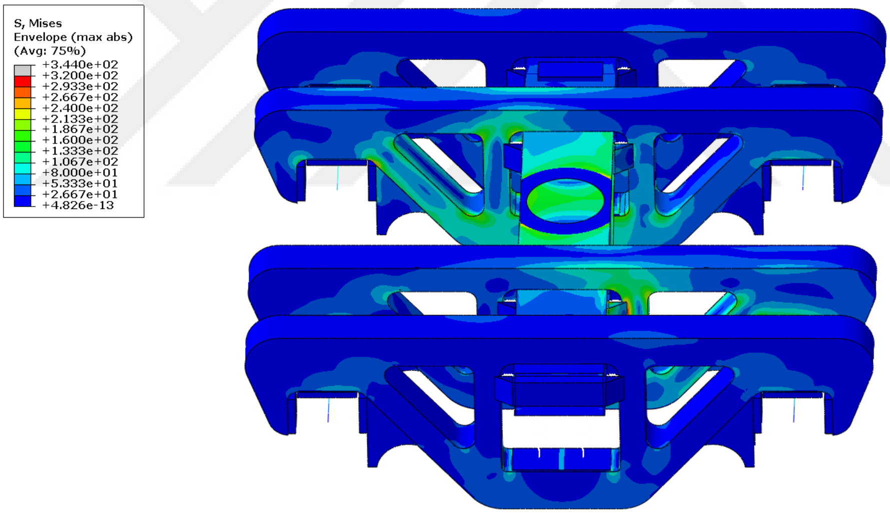

Figure A. 18 : Von Mises Stresses of Load Case 09

LC10

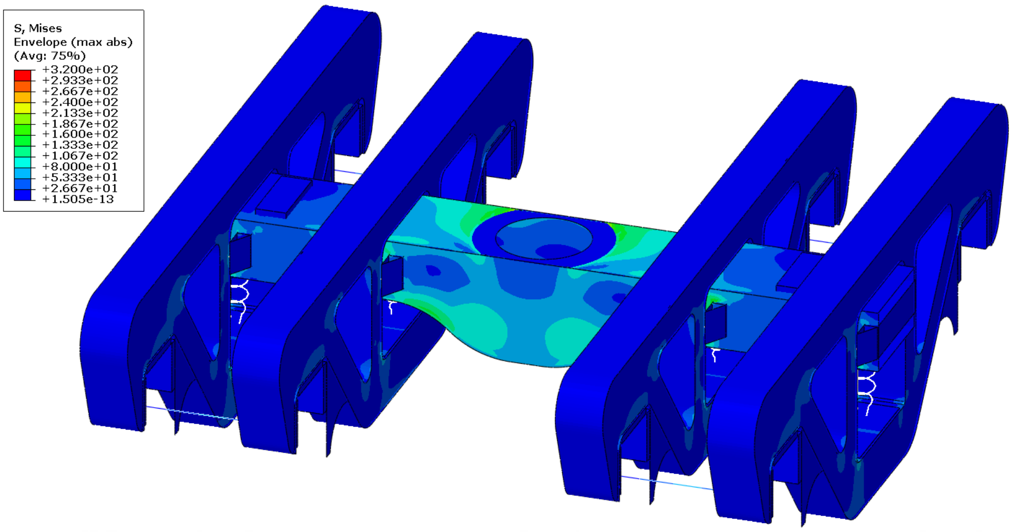

Figure A. 19 : Von Mises Stresses of Load Case 10

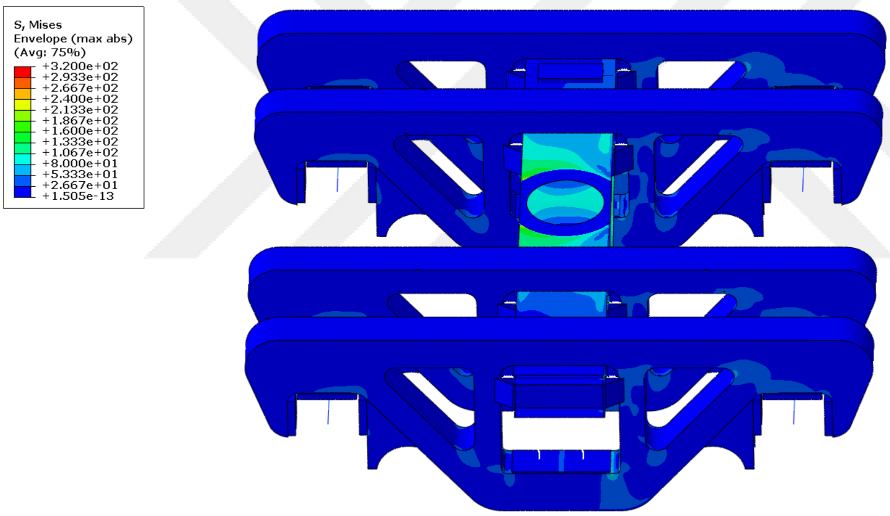

Figure A. 20 : Von Mises Stresses of Load Case 10

LC11

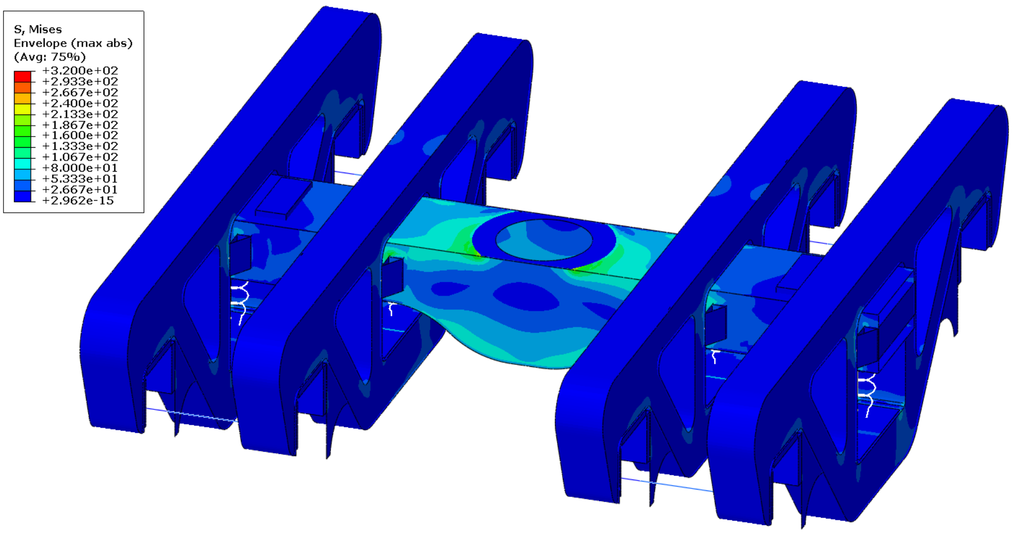

Figure A. 21 : Von Mises Stresses of Load Case 11

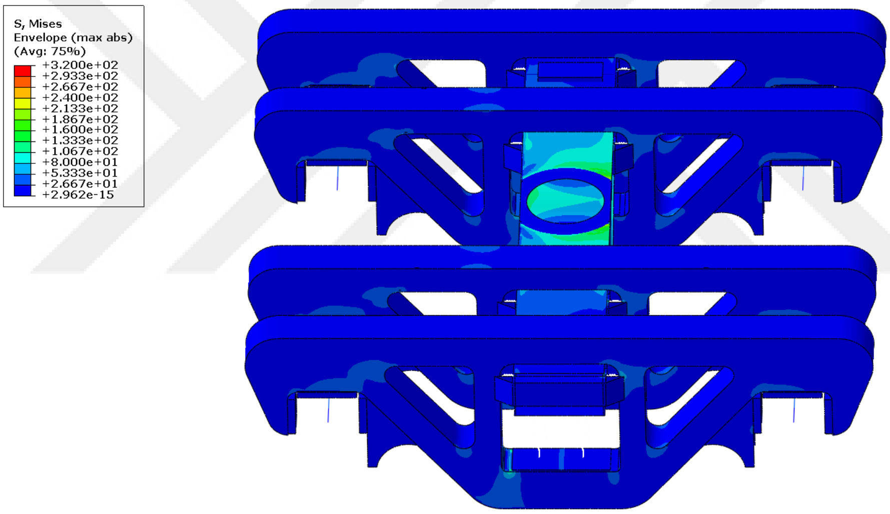

Figure A. 22 : Von Mises Stresses of Load Case 11

LC12

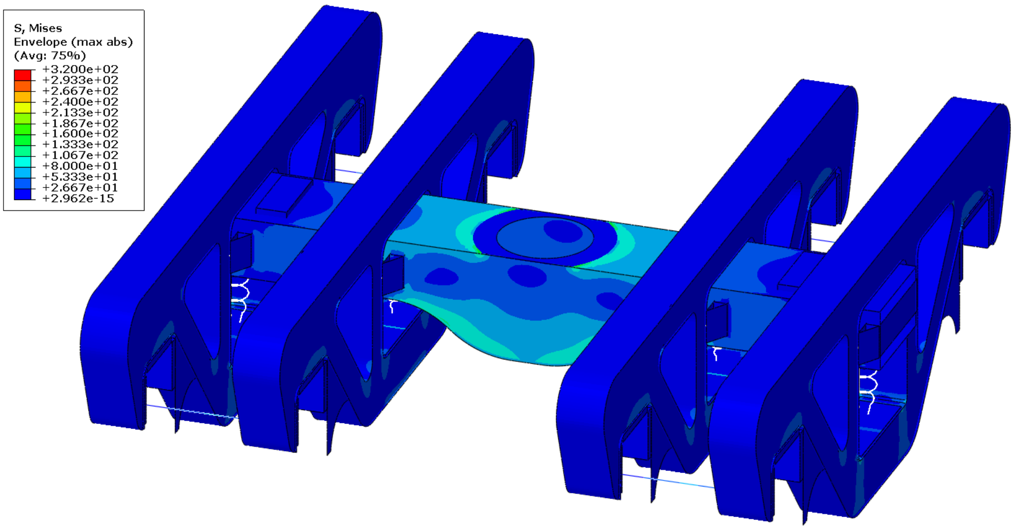

Figure A. 23 : Von Mises Stresses of Load Case 12

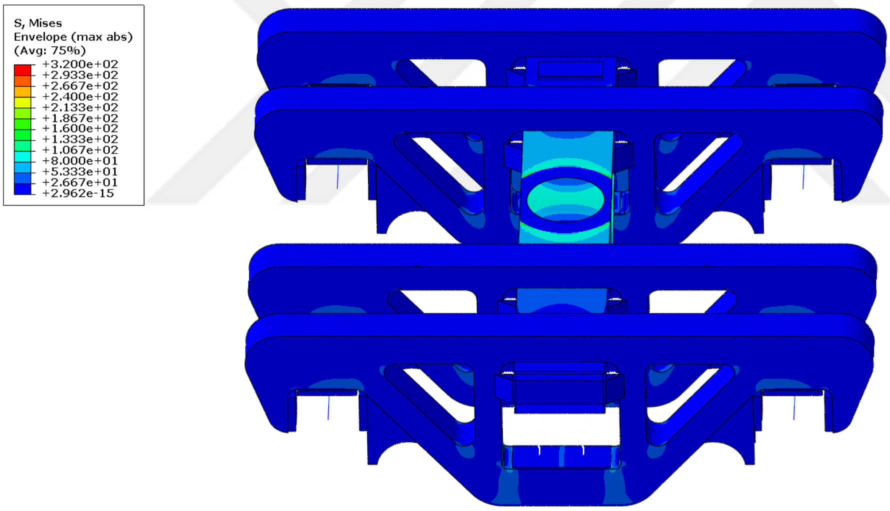

Figure A. 24 : Von Mises Stresses of Load Case 12

LC13

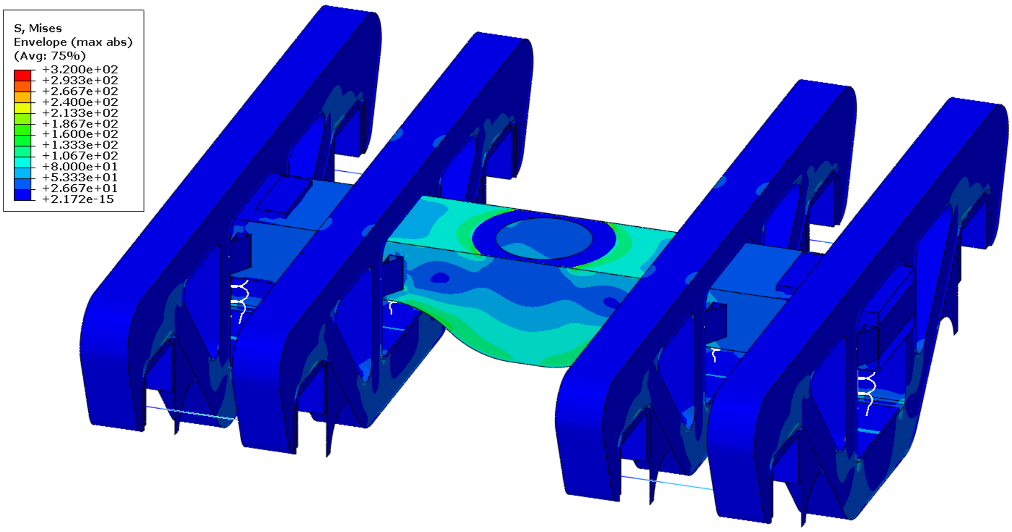

Figure A. 25 : Von Mises Stresses of Load Case 13

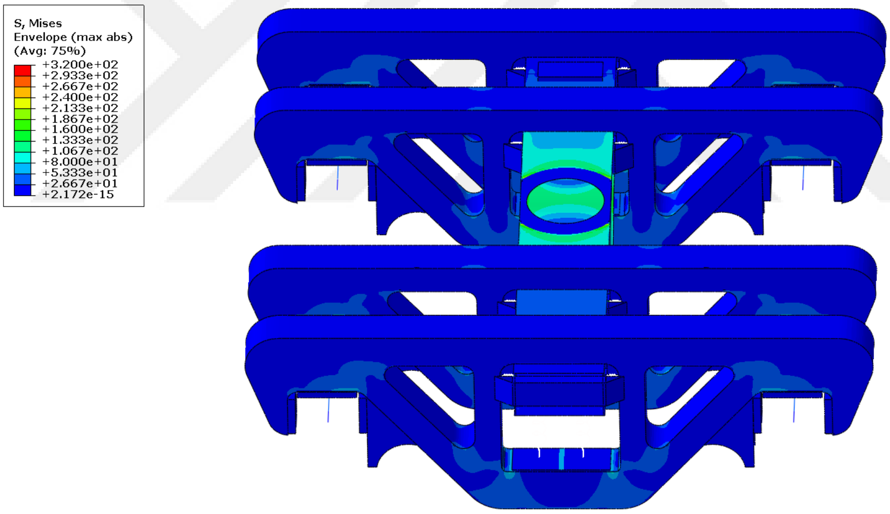

Figure A. 26 : Von Mises Stresses of Load Case 13

LC14

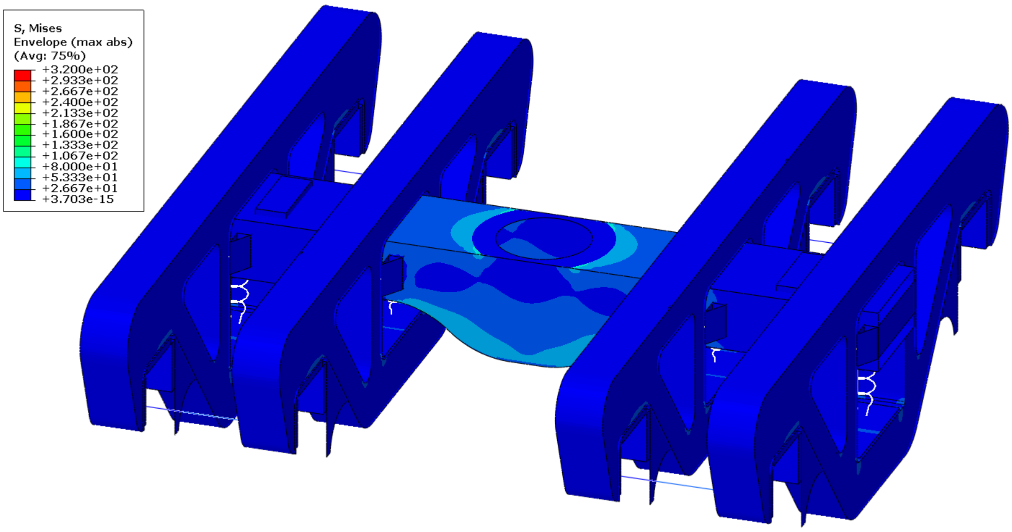

Figure A. 27 : Von Mises Stresses of Load Case 14

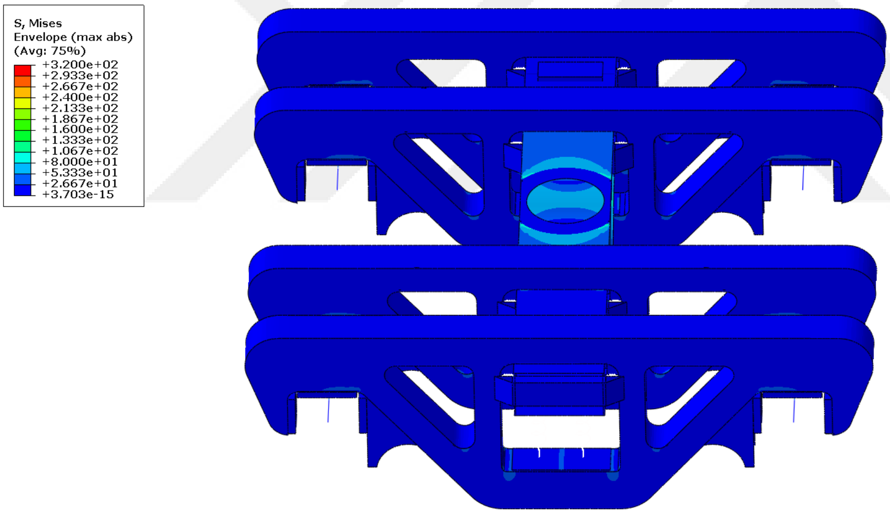

Figure A. 28 : Von Mises Stresses of Load Case 14

LC15

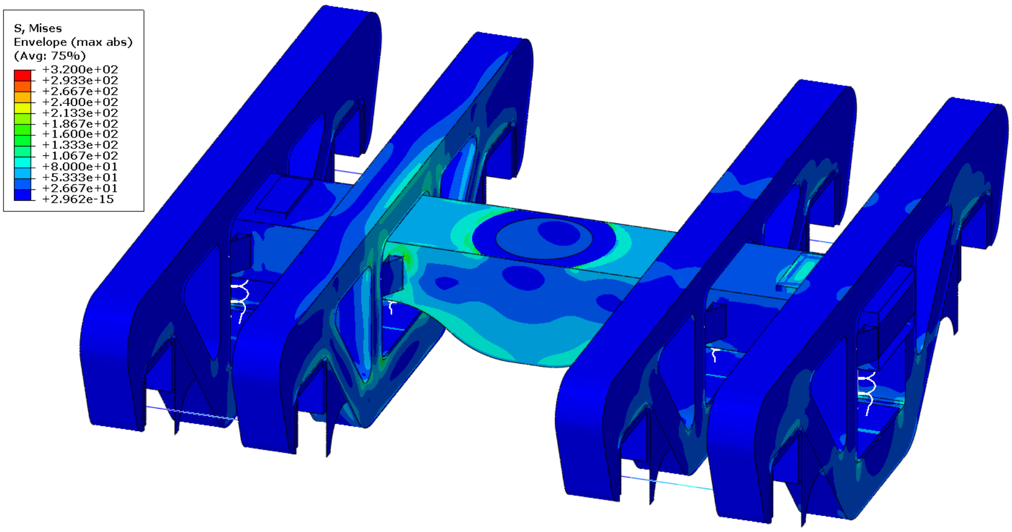

Figure A. 29 : Von Mises Stresses of Load Case 15

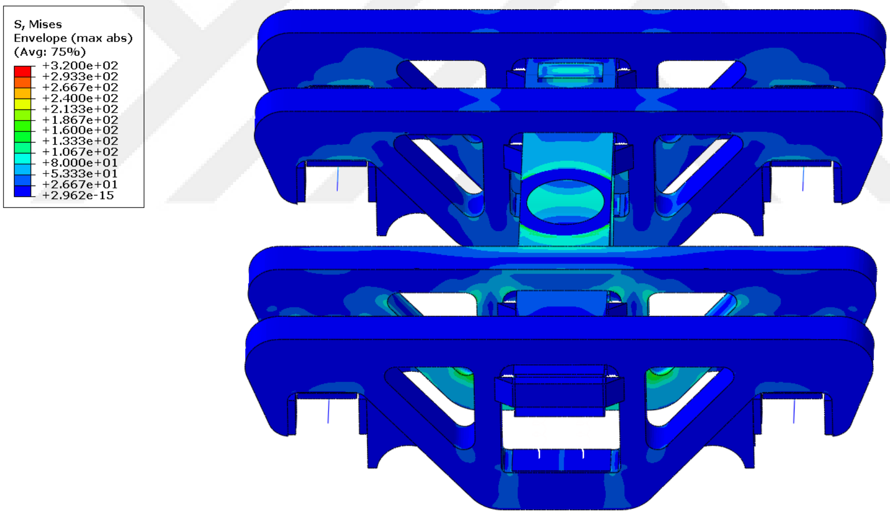

Figure A. 30 : Von Mises Stresses of Load Case 15

LC16

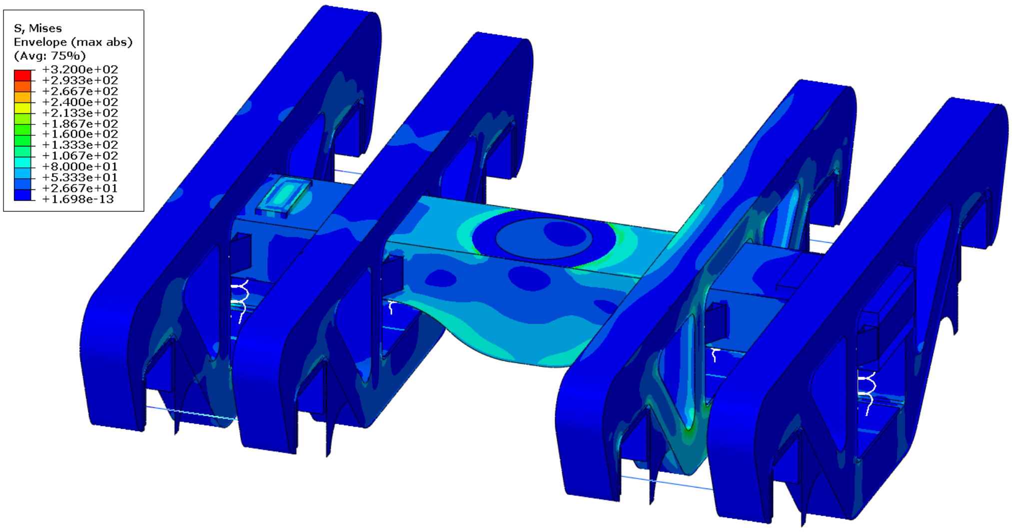

Figure A. 31 : Von Mises Stresses of Load Case 16

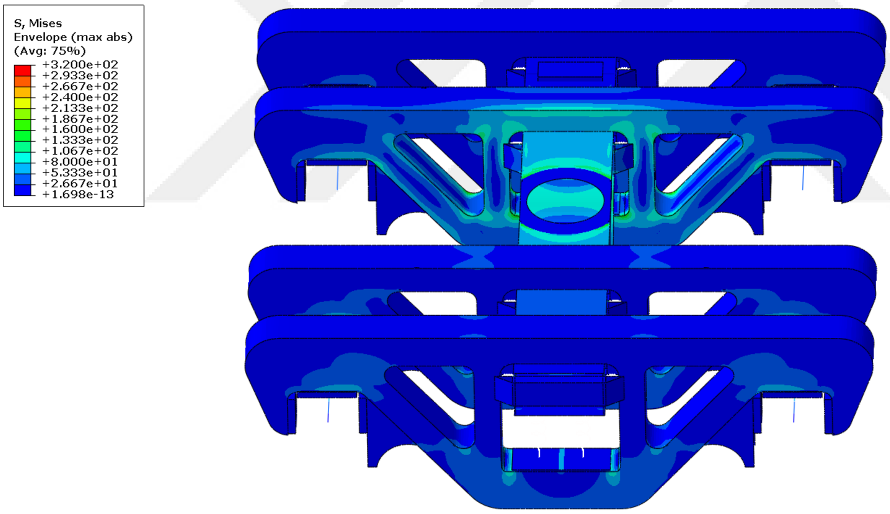

Figure A. 32 : Von Mises Stresses of Load Case 16

LC17

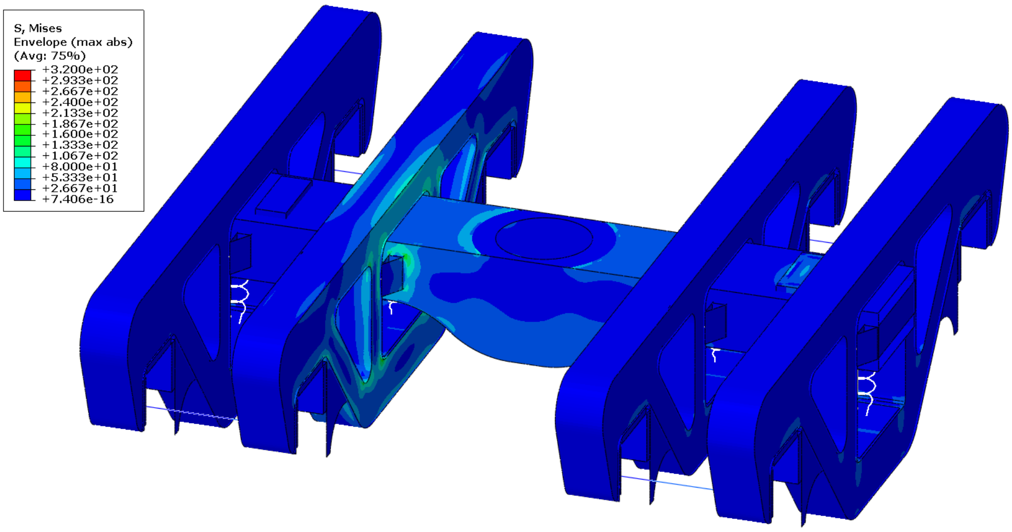

Figure A. 33 : Von Mises Stresses of Load Case 17

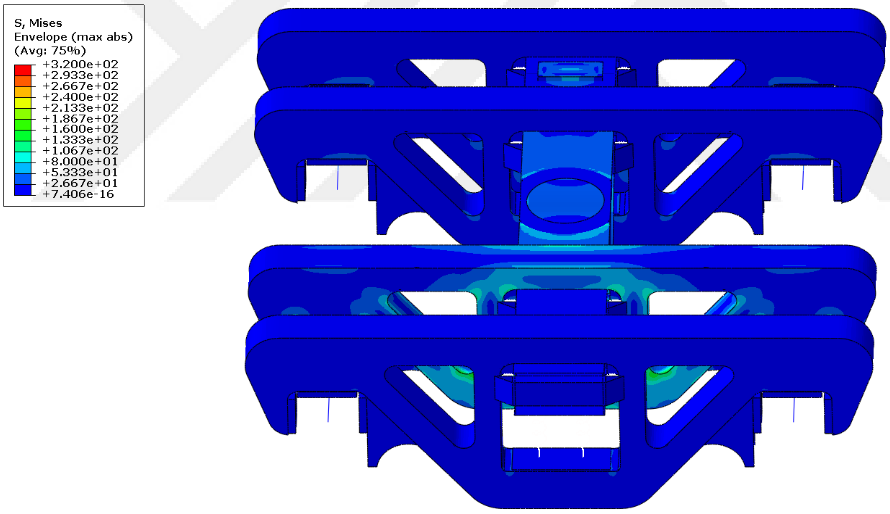

Figure A. 34 : Von Mises Stresses of Load Case 17

LC18

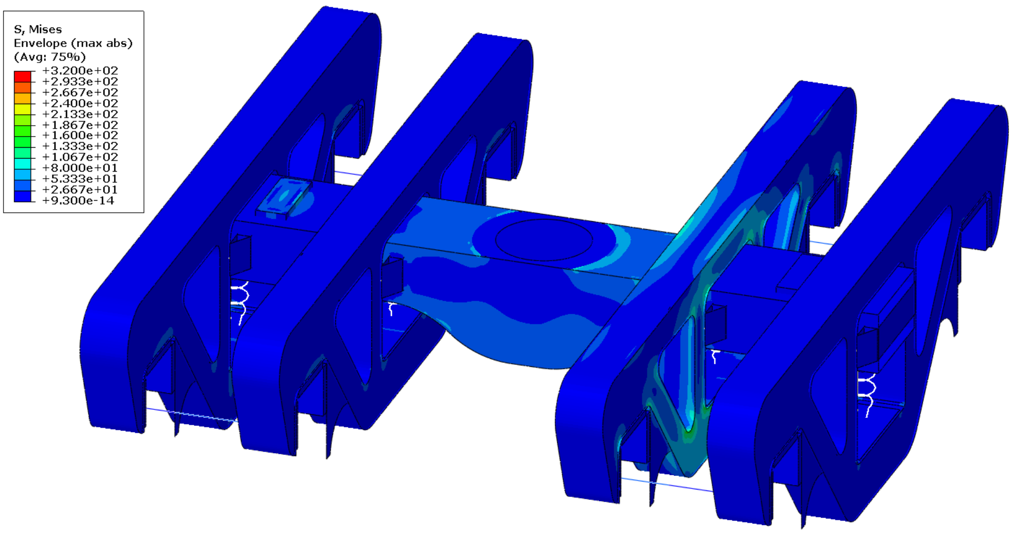

Figure A. 35 : Von Mises Stresses of Load Case 18

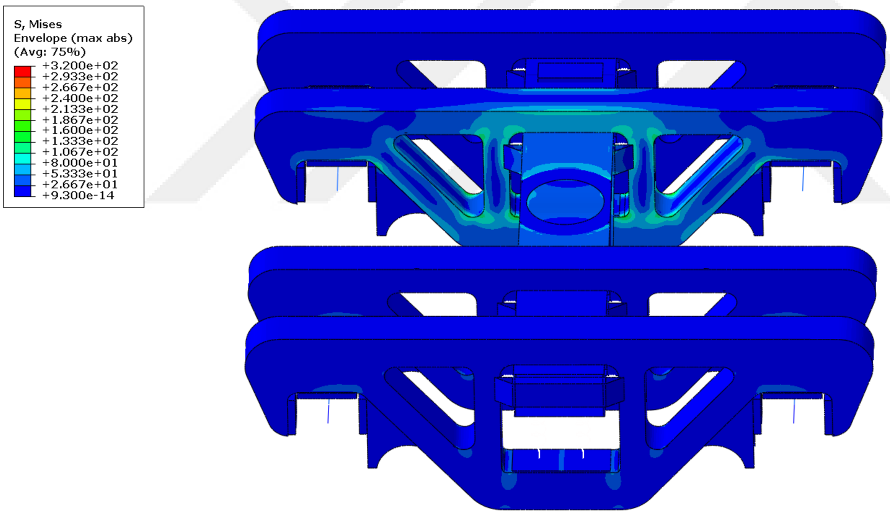

Figure A. 36 : Von Mises Stresses of Load Case 18

LC19

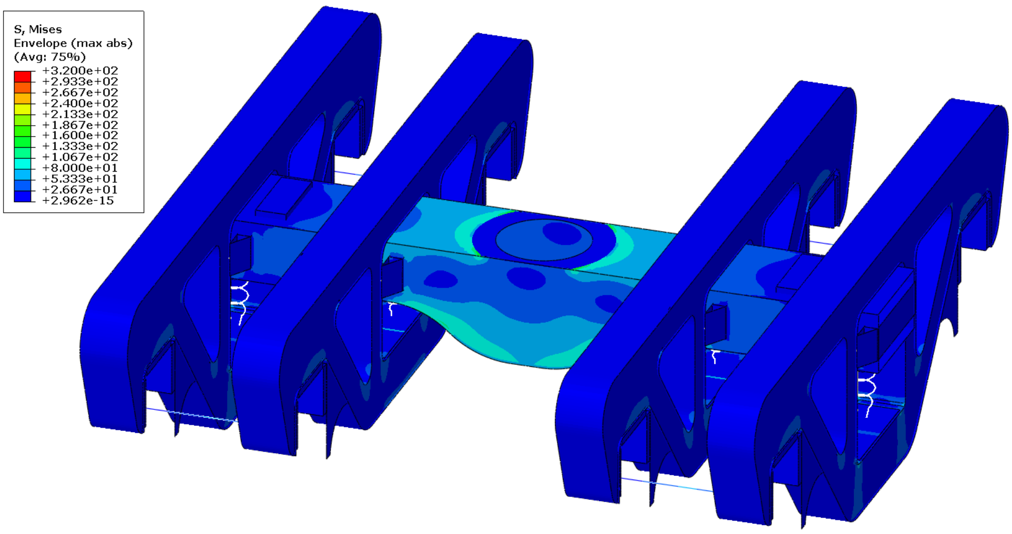

Figure A. 37 : Von Mises Stresses of Load Case 19

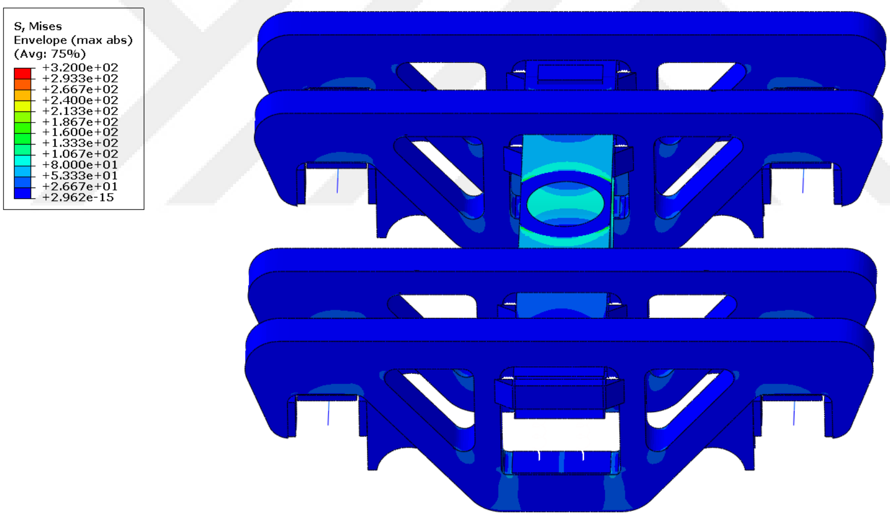

Figure A. 38 : Von Mises Stresses of Load Case 19

LC20

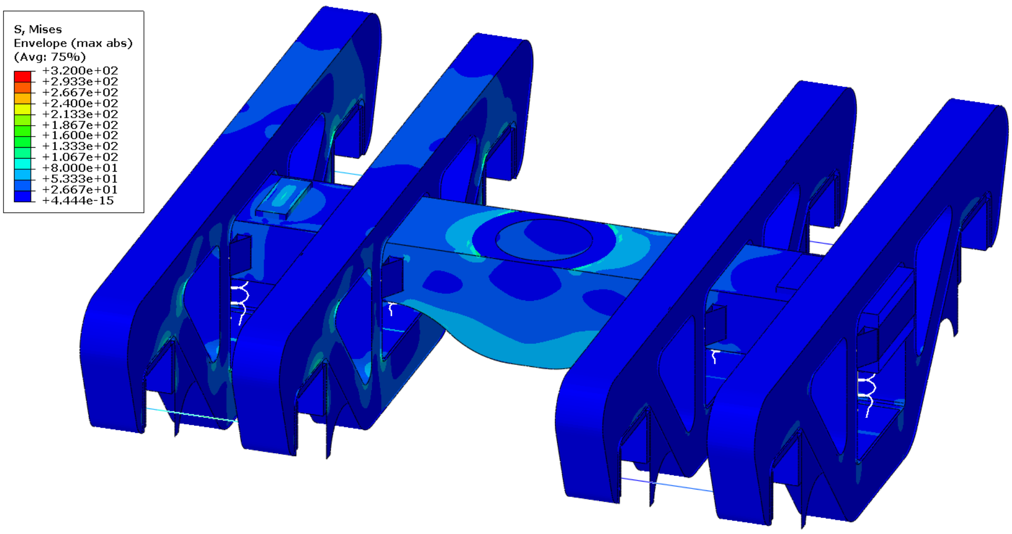

Figure A. 39 : Von Mises Stresses of Load Case 20

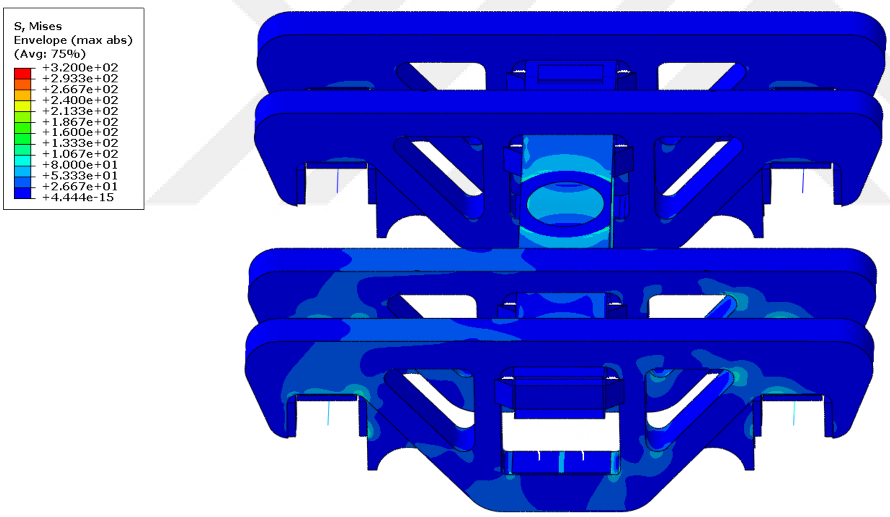

Figure A. 40 : Von Mises Stresses of Load Case 20

LC21

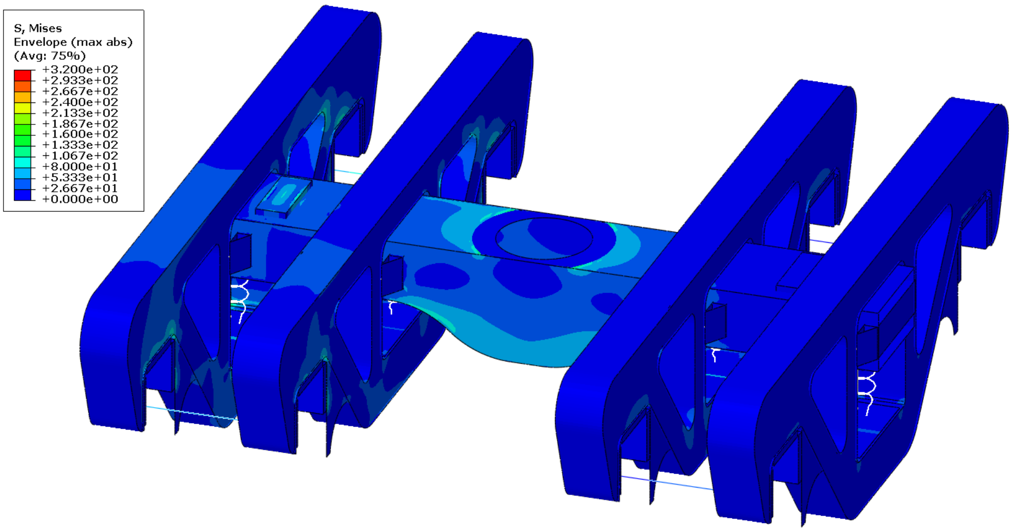

Figure A. 41 : Von Mises Stresses of Load Case 21

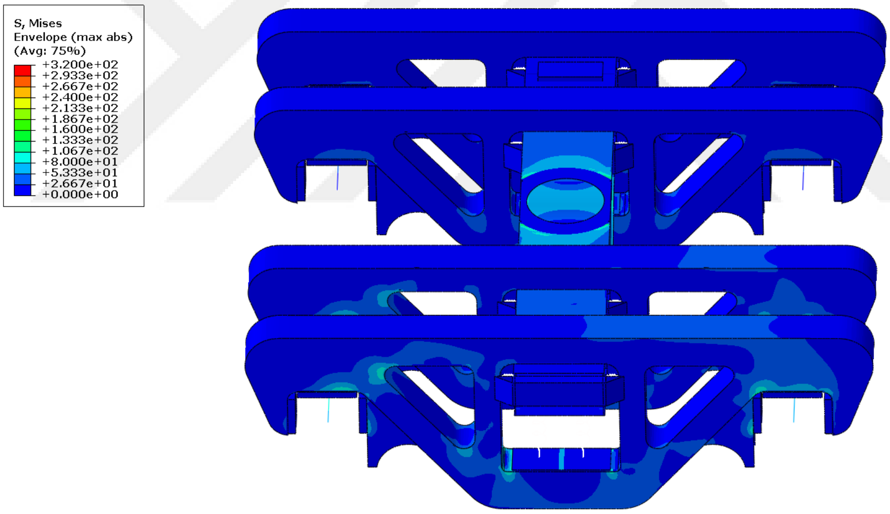

Figure A. 42 : Von Mises Stresses of Load Case 21

LC22

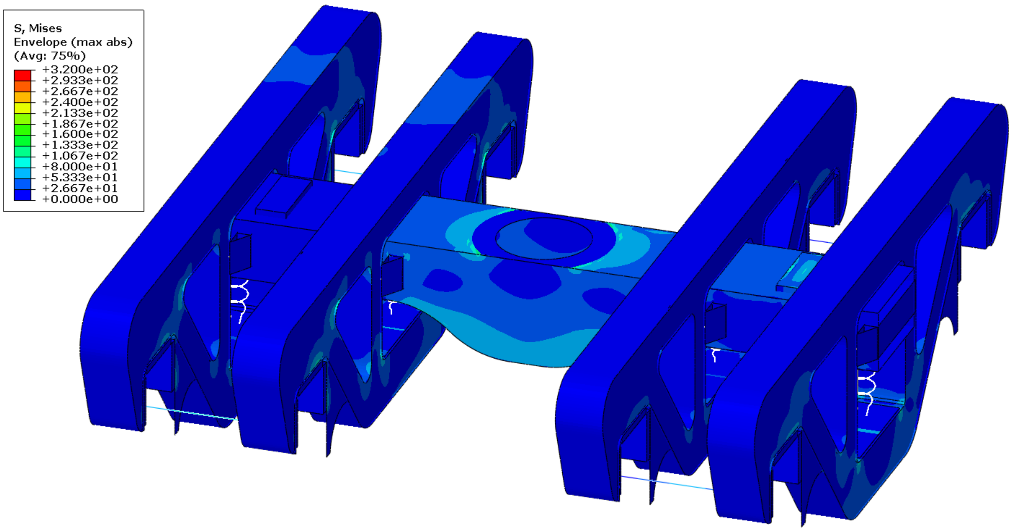

Figure A. 43 : Von Mises Stresses of Load Case 22

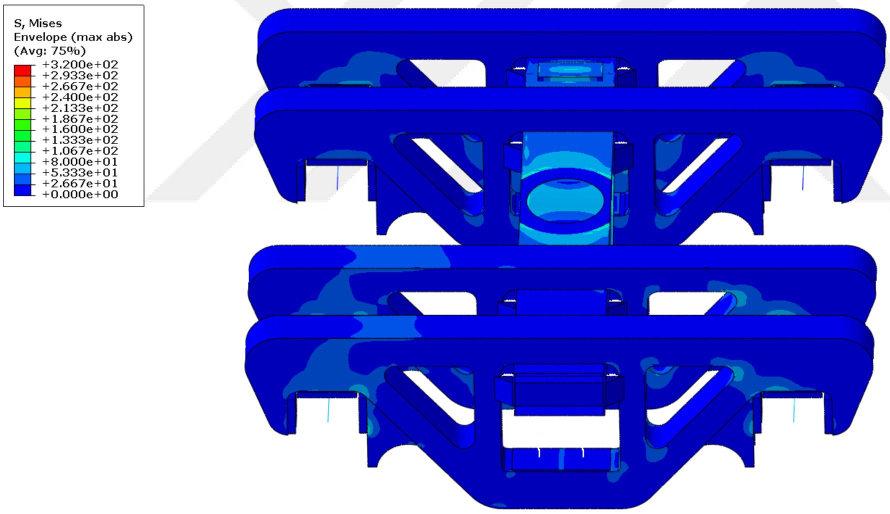

Figure A. 44 : Von Mises Stresses of Load Case 22

LC23

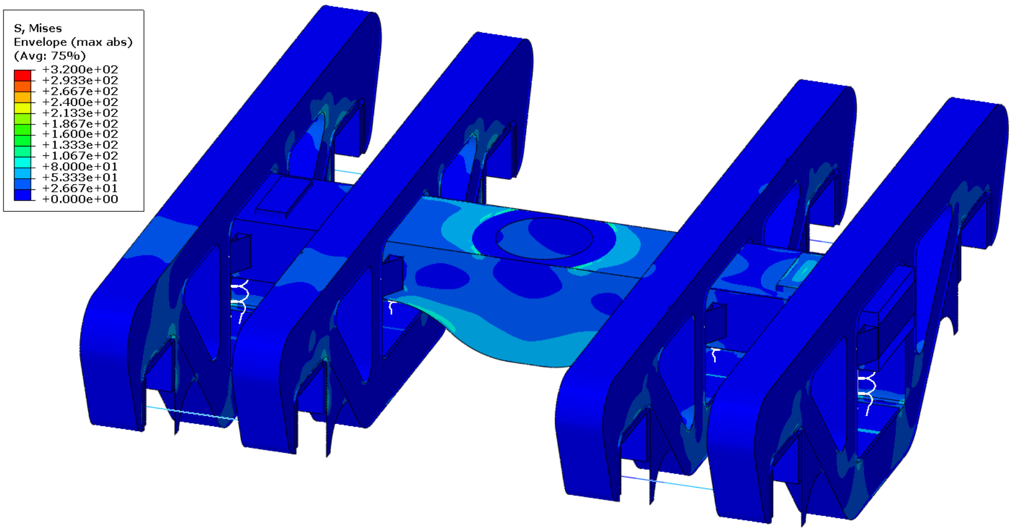

Figure A. 45 : Von Mises Stresses of Load Case 23

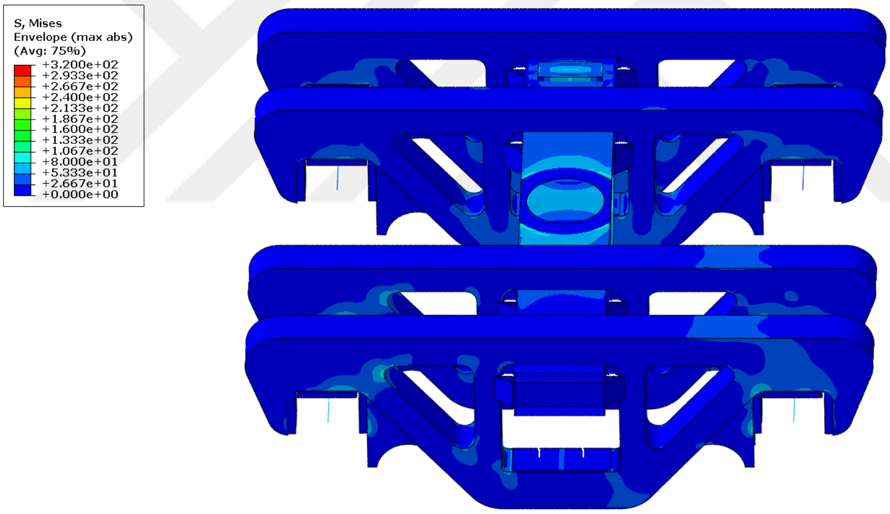

Figure A. 46 : Von Mises Stresses of Load Case 23

LC24

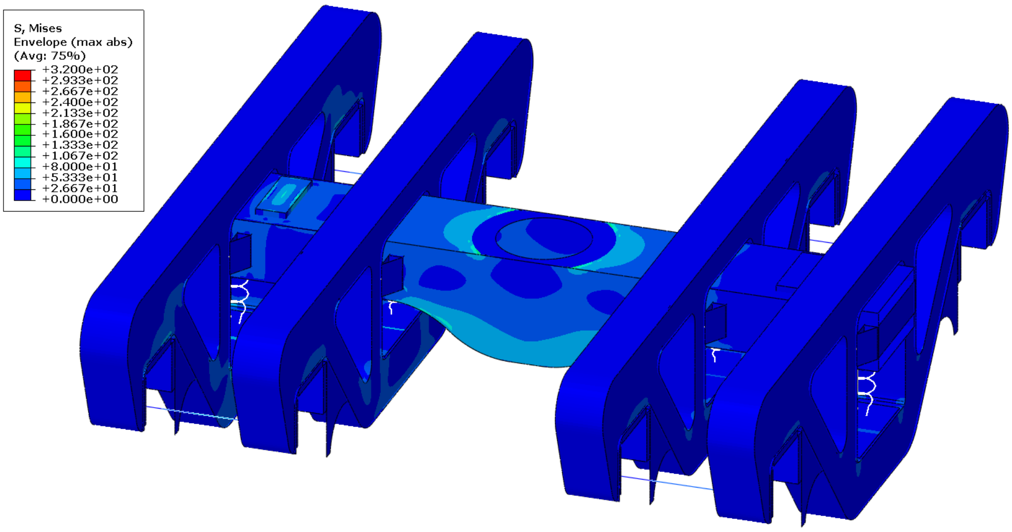

Figure A. 47 : Von Mises Stresses of Load Case 24

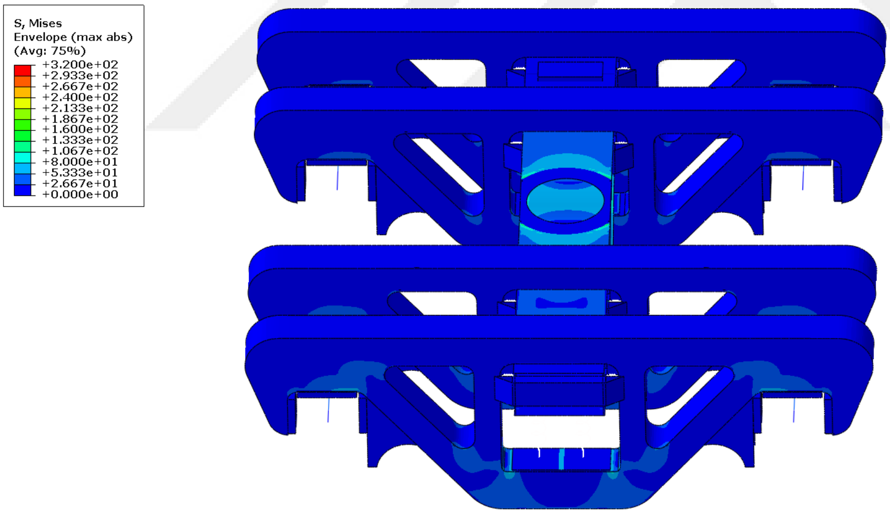

Figure A. 48 : Von Mises Stresses of Load Case 24

LC25

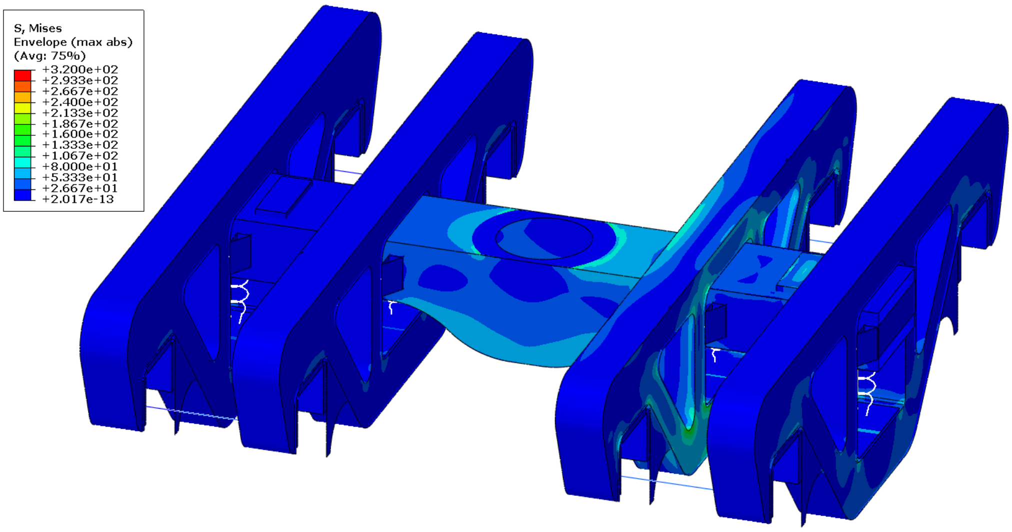

Figure A. 49 : Von Mises Stresses of Load Case 25

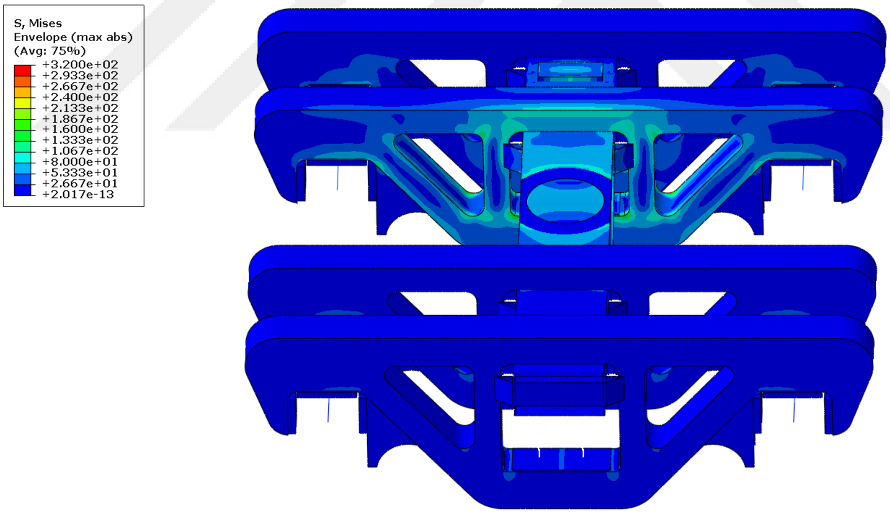

Figure A. 50 : Von Mises Stresses of Load Case 25

LC26

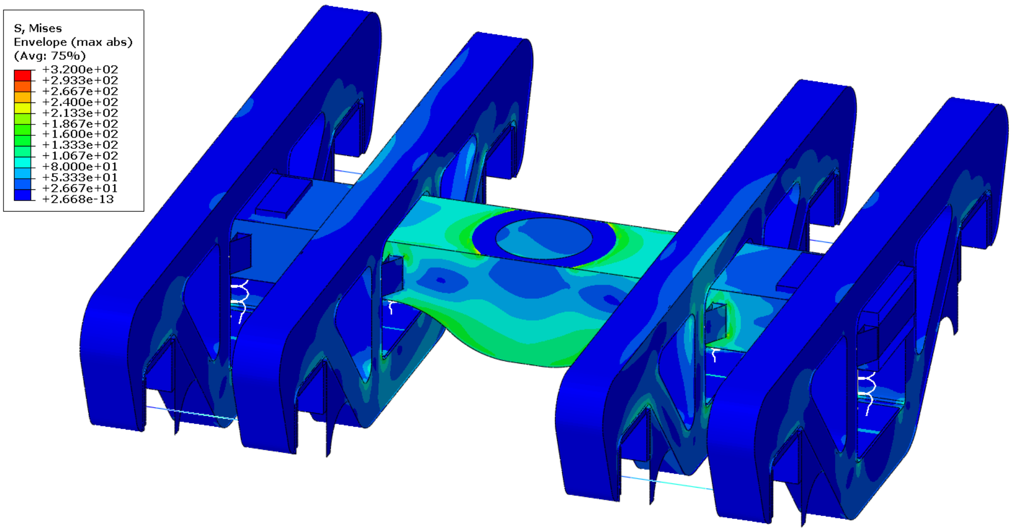

Figure A. 51 : Von Mises Stresses of Load Case 26

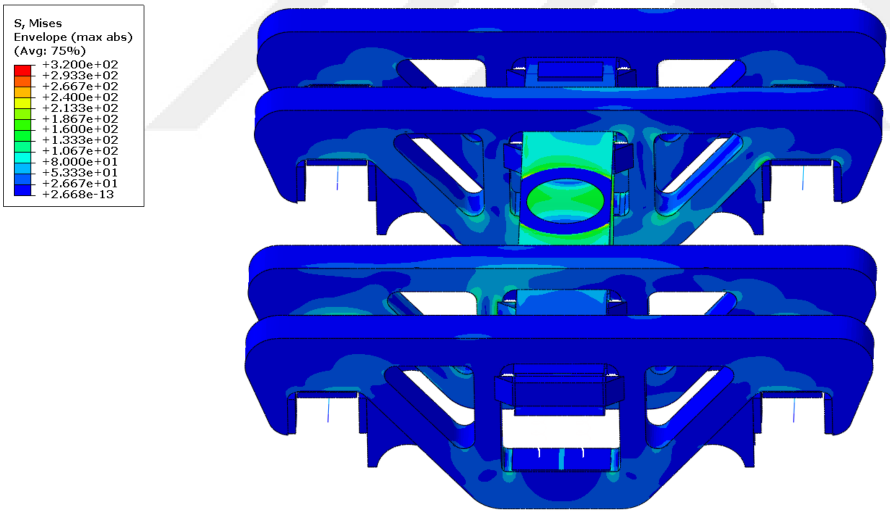

Figure A. 52 : Von Mises Stresses of Load Case 26

LC27

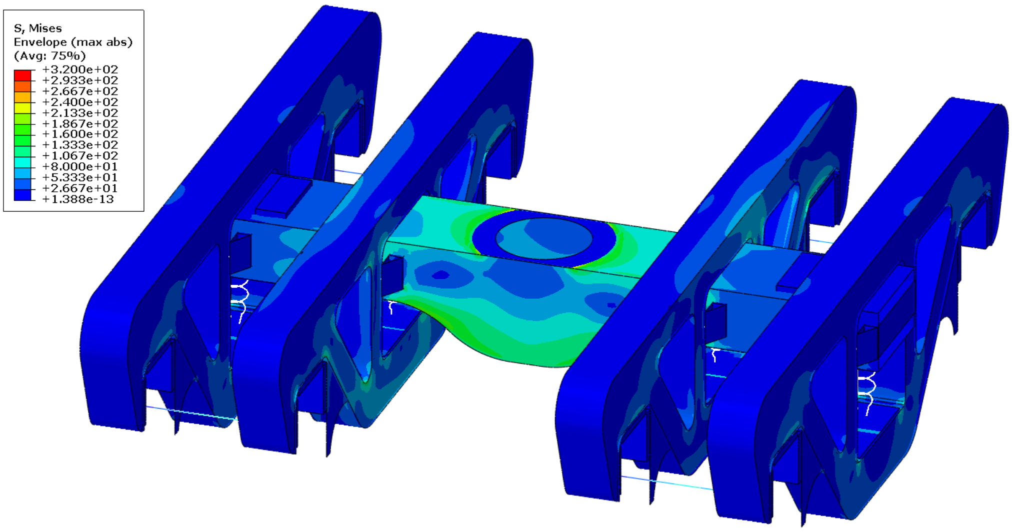

Figure A. 53 : Von Mises Stresses of Load Case 27

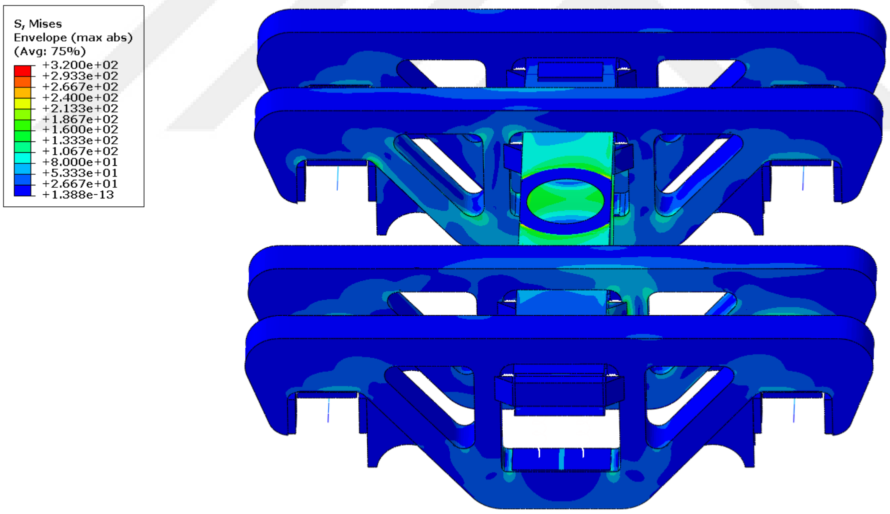

Figure A. 54 : Von Mises Stresses of Load Case 27